IN PURSUIT OF IMPROVING PEAK FLOW PREDICTION IN THE CANADIAN PRAIRIES

A Thesis Submitted to the
College of Graduate and Postdoctoral Studies
In Partial Fulfillment of the Requirements
For the Degree of Doctor of Philosophy
In the Department of Civil, Geological, and Environmental Engineering
University of Saskatchewan
Saskatoon

By

Mohamed Ismaiel Ahmed

PERMISSION TO USE

In presenting this thesis/dissertation in partial fulfillment of the requirements for a Postgraduate degree from the University of Saskatchewan, I agree that the Libraries of this University may make it freely available for inspection. I further agree that permission for copying of this thesis/dissertation in any manner, in whole or in part, for scholarly purposes may be granted by the professors who supervised my thesis/dissertation work or, in their absence, by the Head of the Department or the Dean of the College in which my thesis work was done. It is understood that any copying or publication or use of this thesis/dissertation or parts thereof for financial gain shall not be allowed without my written permission. It is also understood that due recognition shall be given to me and to the University of Saskatchewan in any scholarly use which may be made of any material in my thesis/dissertation.

DISCLAIMER

Reference in this thesis/dissertation to any specific commercial products, process, or service by trade name, trademark, manufacturer, or otherwise, does not constitute or imply its endorsement, recommendation, or favoring by the University of Saskatchewan. The views and opinions of the author expressed herein do not state or reflect those of the University of Saskatchewan and shall not be used for advertising or product endorsement purposes.

Requests for permission to copy or to make other uses of materials in this thesis/dissertation in whole or part should be addressed to:

Head of the Department of Civil, Geological, and Environmental Engineering
57 Campus Dr
University of Saskatchewan
Saskatoon, Saskatchewan S7N 5A9 Canada

OR

Dean
College of Graduate and Postdoctoral Studies
University of Saskatchewan
116 Thorvaldson Building, 110 Science Place
Saskatoon, Saskatchewan S7N 5C9 Canada

Abstract

The prairies were subjected to multiple unprecedented floods over the past decade that caused major damages to agricultural and residential areas. Accurate prediction of the magnitude and timing of floods is important as it is an essential component of flood risk management programs. However, the accuracy of predicting floods and the associated flooding extents have not drawn much attention in the prairies due to difficulties in predicting prairie streamflow in general. Such difficulties are caused, mainly, by the limitations of the currently available modeling approaches in handling the pothole complexities – a dominant feature in prairie watersheds. This thesis focuses on improving the prediction of floods (peak flows), in particular, and the streamflow in general, along with the associated landscape pluvial and nival flooding extents that frequently occur in the complex pothole-dominated environment of the Canadian prairies. This aim is achieved through adapting/developing a set of models that are built and tested for the prairies to contribute to solving the flood prediction problem in the prairies. The first model is a new Hydrological model for the Prairie Region (HYPR), which is proposed as an engineering solution for the prediction of the flood peak in the prairies. HYPR is a modified version of the HBV model, developed by coupling the conceptual HBV model, for hydrological processes representation, and the Probability Distribution Model based RunOFf generation algorithm (PDMROF) for pothole representation. The second model is a novel Prairie Region Inundation MApping model (PRIMA), which is developed as a distributed hydrologic routing model for more accurate and comprehensive storage dynamics simulation and inundation mapping in the prairies. PRIMA uses a set of rules along with Manning's equation (iteratively) to route the water over the landscape. The third model is the Modelisation Environmentale Communautaire (MEC)—Surface and Hydrology (MESH), which is modified by coupling it with PRIMA to improve the non-contributing area and potholes dynamic representation in complex land surface models for better prediction of peak flows and the associated flooding extents. In this model, called MESH-PRIMA, MESH handles the vertical fluxes calculations based on physically based equations and PRIMA routes the water over the landscape and accounts for the effect of potholes on changing the net runoff reaching the stream network.

HYPR shows good simulation of the overall hydrograph and peak flows, on a daily resolution, as indicated by the Nash-Sutcliffe Efficiency (NSE) of 0.72 and NSE for flows over threshold (NSE_{OT}) of 0.78, respectively, averaged over multiple prairie watersheds for the entire

simulation period. Although HYPR's process representation is simple, it shows acceptable simulation of internal hydrologic variables (e.g., accumulated snow on ground) when compared against field measurements. HYPR can be useful when data or computational resources are limited. As for PRIMA, it shows potential for simulating the inundation extents when compared against remote sensing observations of water extents with an accuracy of 85 % averaged over two prairie basins in Saskatchewan, Canada. PRIMA is three to eight times as computationally efficient as the recently developed Wetland DEM Ponding Model (WDPM). The MESH-PRIMA model shows an improved hydrograph and flood simulation on a daily resolution (NSE = 0.55 and NSE_{OT} = 0.60, respectively) compared to the MESH model with its current prairie algorithm (NSE = 0.49 and NSE_{OT} = 0.55, respectively) for the entire simulation period. More importantly, MESH-PRIMA can identify the spatial distribution of water over the landscape and quantify the spatial non-contributing area for different flood events. The proposed models in this thesis can be used for efficient pothole storage dynamics simulation, inundation mapping, streamflow, and peak flow prediction in the prairies. The models can be used for a wide spectrum of hydrologic or hydraulic purposes ranging from limited data, conceptual-lumped-operational mode (e.g., HYPR) to detailed data, physically based research mode (e.g., MESH-PRIMA). These models, especially MESH-PRIMA, improve our understanding of the complexities of the prairie hydrology and the impacts of land depressions on changing the watershed response. More importantly, the methods proposed in MESH-PIMA can be explicitly used in most land-surface schemes within earth system models, allowing for important application in climate change and numerical prediction systems that typically ignore this important prairie phenomenon.

Acknowledgements

I would like to acknowledge and thank several individuals who have directly or indirectly contributed to this thesis. First of all, I would like to acknowledge the efforts that both my supervisors (Dr. Amin Elshorbagy & Dr. Alain Pietroniro) have been doing during my PhD. I would like to give a special thank you to Dr. Amin Elshorbagy for his endless support, both professionally and personally throughout my program. I would like to thank him for the well-organized time frame of my thesis with critical milestones that had contributed to finishing this thesis in time. His dedication and commitment inspire me a lot. I offer my sincere thanks to Dr. Alain Pietroniro for his continued encouragement and support throughout my program. His endless encouragement helped me overcome many difficulties in this program. I was fortunate to be supervised by both. Their advices and insights from scientific and engineering perspective, constructive comments, and critical assessment of my work not only improved this thesis but also improved my technical and writing skills and made me a better researcher. The last year of my program was a tough one due to the COVID-19 pandemic that has been affecting everyone, but I was able to make it through thanks to their encouragement and support.

I would like to extend my gratitude to my thesis committee. I would like to thank the thesis committee members for their valuable comments that improved the work and for suggesting good reading materials that helped in improving my understanding of modelling and research practices. I would like to thank Dr. Saman Razavi for introducing the topic of model sensitivity and uncertainty analysis – in his course – in a well-structured and well-organized way. He motivated and encouraged me during my first term at the U of S, which made that first term here a great experience. I would like to thank Dr. Kerry Mazurek for her useful feedback on my work and for introducing me to the engineering hydraulics in a well-coordinated way both theoretically and practically. I wanted to thank Dr. Karl Lindenschmidt for his advices and insights on the flood hazard and flood risk issues. I would like to thank Dr. Bart Nijssen for his support as the external examiner and his technical insights on the problem of computational efficiency and process representation for model development. I am grateful to Dr. Chris Hawkes for his support as the committee chair.

My appreciation is extended to the Saskatchewan Water Security Agency, especially to Curtis Hallborg, manager of flow forecasting and operations and his team for providing data and information about the Qu'Appelle river basin and for offering me an internship at the Saskatchewan Water Security Agency. I am grateful for that opportunity, which helped me in putting my research into practice and getting to know more about the engineering and water resources management practices in Saskatchewan.

My gratitude is extended to Dr. Kevin Shook (Department of Geography and Planning, University of Saskatchewan), who provided data and technical support to my work. I wanted to thank him for sharing his ideas with me and for introducing me to the open-source software/tools idea, which helped me in improving my research work. Working with him was very interesting and he helped me in enhancing my understanding of prairie hydrology. His open-mindedness, support, and technical insights made it very interesting to model the graveyard of hydrological models - the complex prairie environment. I would like to thank Dr. James Craig (University of Waterloo) for critically reviewing the technical aspects of the HYPR model and for implementing it into the Raven modelling framework. I wanted to thank Dr. Raymond Spiteri and his students (Department of Computer Science, University of Saskatchewan) for their efforts in re-coding PRIMA to support parallel processing on both CPUs and GPUs. A special thank you goes to Dan Princz (Environment and Climate Change Canada) for his support in running and tackling the technical details of the complex land surface MESH model and for his contribution in implementing PRIMA inside MESH. I would like to thank CANSIM lab mates for the times that we had in discussing many research issues that contributed directly or indirectly in improving this work. The funding from the Natural Sciences and Engineering Research Council of Canada (NSERC) strategic network through the Canadian FloodNet research network (Grant number: NETGP451456-13) and the Department of Civil, Geological and Environmental Engineering, University of Saskatchewan is greatly acknowledged.

A great thank you goes to my family for their unconditional support throughout my program and my entire life. I really appreciate the efforts that my wife, Menna Elrashidy, have been doing to support me during my program. Being a wife of a busy overwhelmed PhD student is tough, but Menna was able to handle it. She stood by my side and helped me through discussing issues and suggesting ideas. I am grateful to my lovely little daughter, Saja, for providing the required breaks from research and for motivating me to finish my thesis. I am grateful to my Father, Ismaiel Ahmed, and Mother, Intesar Zahr Eldein, for their great role in supporting and encouraging me in different ways throughout my life. I am also grateful to my two sisters, Heba and Hasnaa for their support and encouragement. I would like to thank my parents-in-law, Tarek Elrashidy and Aml Omar for their encouragement and support.

Finally, Praise is to Allah [God] by Whose grace good deeds are completed.

Dedication

I dedicate this thesis to my family, especially my mother, wife, and daughter. Their love, affection, encouragement, prayers, and doaa' make me able to finish this work and be successful in my life.

In honor of my late father, Ismaiel Ahmed, who always supported me. May Allah (God) grant him a place in Jannah (heaven).

Table of Contents

List of Tables

List of Figures

Chapter 1 Introduction

1.1 Overview and Motivation

The provinces of Manitoba, Saskatchewan, and Alberta in Canada, and the states of Montana, North and South Dakota, and Minnesota, in the United States, are defined as the North American prairies (Figure 1.1). These prairie environments are often referred to as the "graveyard of hydrological models" (D.M. Gray), largely due to the existence of millions of land depressions formed during recent glacial retreat, known as prairie potholes, that add a complex storage regime to the landscape. Also, the relatively cold, dry, and windy environment adds to the challenges of hydrology in these regions. The potholes make the prairie watersheds' response to be complex, non-linear, and hysteretic as they can retain significant amounts of runoff (Shook *et al.*, 2013; Gharari and Razavi, 2018). Cold region processes are dominant in the prairies; blowing snow redistribution and sublimation result in a heterogonous snow depth distribution (Fang et al., 2007). Further, during early spring, snowmelt is the main source of overland flow over frozen soil (Gray and Landine, 1988; Pomeroy *et al.*, 2007). These processes are typical of cold regions and, when coupled with land depressions typical of the North American prairies, increase the hydrological complexities and have been the topic of studies for many decades (Gray, 1970; Pomeroy *et al.*, 1993, 2014; Hayashi *et al.*, 2003; Leibowitz and Vining, 2003).

The presence of numerous land depressions impact the runoff propagation in the praries and follows a fill and spill mechanism (Shaw *et al.*, 2012). This mechanism is challenging and complex (Winter, 1989; Shook and Pomeroy, 2011) because the majority of surface runoff is retained in land depressions and may or may not contribute to the streamflow in the region. Because the land depressions are disconnected from the stream network, they do not necessarily contribute to streamflow under low rainfall or snowmelt events (Martin, 2001; Hayashi *et al.*, 2003). Thus, the majority of the prairie region does not contribute flow to the stream network and therefore, these areas are typically known as non-contributing areas (Figure 1.1), wherein they do not contribute flow to the watershed outlet for events with a magnitude of a 2-year return period or smaller (Godwin and Martin, 1975). However, under wet conditions, these depressions can be connected and contribute to the streamflow. Such a mechanism results in a dynamic non-contributing area that makes the traditional hydrological models inapplicable (Shaw *et al.*, 2012; B. Mekonnen *et al.*, 2016; Zeng *et al.*, 2020). Traditional hydrological models ignore the fact that contributing area is dynamic and assume that the contributing area is static. Further, they ignore the effect of the prairie potholes in retaining significant amounts of runoff, which when combined with the static contributing assumption lead to overestimation in the streamflow. Accordingly, such models cannot accurately simulate prairie streamflow or the dominant control of the potholes on changing the runoff process.

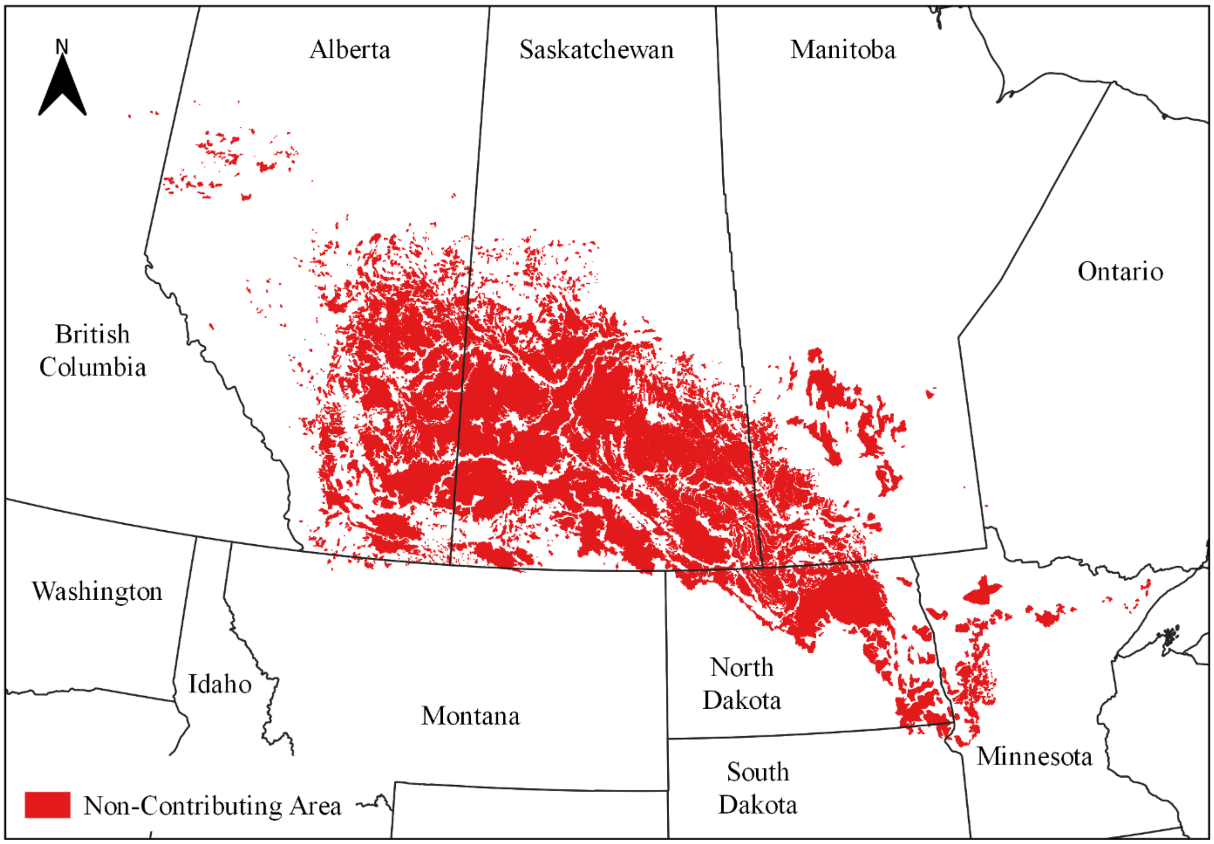

Figure 1.1: A general layout of the extent of the non-contributing areas, as defined by the Prairie Farm Rehabilitation Administration (PFRA), in the North American prairies.

While the cold region processes have been studied extensively and are currently reasonably represented in hydrological models, the complexities of the dynamic connection between prairie potholes still pose a major challenge to the streamflow simulation in the prairies. However, some efforts have been made to study the potholes and their implications on the system response (Godwin and Martin, 1975; Winter and Rosenberry, 1998; Darboux *et al.*, 2001; Leibowitz and Vining, 2003; Antoine *et al.*, 2009; van der Kamp and Hayashi, 2009; Fang *et al.*, 2010; Shook and Pomeroy, 2011; Shaw *et al.*, 2012, 2013; Shook *et al.*, 2013). Other efforts were made to improve the prairie streamflow prediction by including the pothole complexities in different hydrological models (B. Mekonnen *et al.*, 2015, 2016; Evenson *et al.*, 2016; Nasab *et al.*, 2017; Muhammad *et al.*, 2019; Zeng *et al.*, 2020) or land surface models (M. Mekonnen *et al.*, 2014; Hossain, 2018). However, these efforts use either lumped approaches of the potholes or a simple reservoir approach, which cannot be used to accurately simulate the effects of the potholes on the watershed hydrology, and consequently, the streamflow simulation remains challenging and it becomes even more challenging when focusing on predicting floods.

In the past decade, the prairie region has been impacted by many flooding events that caused severe economic and social damages and disrupted essential services. For example, the 2013 flood caused damages that exceeded CAD $1 billion over the prairie region (Brimelow *et al.*, 2014). Predicting floods and the associated flood hazard (e.g., flow magnitude and inundation depth and extent of flood events of particular probabilities) accurately can contribute to the management of the associated flood risk, which is a function of the hazard and its consequences (Apel *et al.*, 2009), on the prairie region. However, extensive review of the literature showed that the problem of prairie flood prediction has not drawn much attention, yet it is proving to be an important problem. Further, flood impact assessment was typically limited to fluvial flooding (Elshorbagy *et al.*, 2017; Bharath and Elshorbagy, 2018) with less attention to pluvial and nival flooding in the prairies. Pluvial (ponding of rainwater) and nival (snowmelt-related) flooding are typical in the prairies during wet conditions as the potholes are filled and water surface expands, causing the surrounding areas to be flooded.

Improving the streamflow simulation, especially peak flow, is very challenging due to the existence of the potholes, the cold regions processes, and the limited number of applicable modeling approaches in the prairies. For engineering design purposes, there is an obvious lack of simple models for peak flow prediction in the prairies. There are no efficient hydraulic models for simulating pothole storage dynamics and surface flooding extent, which are needed for flood insurance, risk assessment, and landuse planning. This hydraulic model can provide an explicit representation of potholes in any hydrologic or earth system model to improve the prairie streamflow simulation. Furthermore, land surface models with proper representation of the pothole complexities and proper peak flow prediction in the prairies are not available. Such models are needed for better understanding and accurate representation of the hydrologic connectivity in the prairies and the spatiotemporal changes of the non-contributing area and the water extents in depressions (pluvial and nival flood hazard), which lead to better management of available water resources, better flood prediction and impact assessment, and more reliable assessment of the impacts of landuse change on the hydrology of the prairies. Such models can be integrated with Regional Climate Models (RCMs), General Circulation Model (GCMs), or Numerical Weather Prediction models (NWP) to provide more accurate simulation of climate projections and better assessment of the impact of climate change on the hydrology of the prairies.

1.2 Challenges Associated with Flood Prediction in the Prairies

1.2.1 Conceptual and Physically Based Hydrological Models

It is known that complex, physically based distributed models have good representation of the different hydrological processes, which leads to an improved streamflow simulation compared to conceptual models (Refsgaard, 1996; Reggiani and Schellekens, 2003). However, this is not always valid as the streamflow simulation of conceptual models can outperform that of physically based models (Ponce and Hawkins, 1996; Booij, 2003; Uhlenbrook, 2003; Te Linde *et al.*, 2008). The use of physically based models is useful when investigating the spatial variability of the watershed properties or when observations of other internal hydrological variables are available (Pokhrel and Gupta, 2011; Smith *et al.*, 2012; Vansteenkiste *et al.*, 2014). However, the available observations are typically limited to streamflow in most watersheds (Jakeman and Hornberger, 1993; Kuczera and Mroczkowski, 1998). Moreover, physically based models have large number of input variables and parameters (Beven, 1989) that increase the computational cost of these models.

Simple conceptual models can simulate the temporal changes efficiently (Hrachowitz and Clark, 2017; Savenije and Hrachowitz, 2017). Conceptual models are known for their simple representation of hydrological processes with small number of input variables, which makes them computationally efficient and robust, and this is useful for flood prediction (Bourdin *et al.*, 2012). Simple conceptual models are valuable when the data or computational resources are limited and the streamflow simulation is of interest as they require small number of input variables and are computationally efficient, which might lead to an accurate simulation of streamflow (Booij, 2003).

Despite of the many advantages that conceptual models have, the development, modification, and usage of hydrologic models in the prairies were limited to physically based models, such as Modelisation Environmentale Communautaire – MESH (M. Mekonnen *et al.*, 2014; Hossain, 2018) and The Cold Regions Hydrological Model platform (CRHM) (Fang *et al.*, 2010; Pomeroy *et al.*, 2010, 2014) or well established semi-distributed models, such as the Soil and Water Assessment Tool (SWAT) (B. Mekonnen *et al.*, 2015, 2016; Nasab *et al.*, 2017; Muhammad *et al.*, 2018, 2019). It is argued that a simple conceptual model that accounts for the pothole behavior has the potential to work well in the prairies, given the demonstrated ability of conceptual models to simulate the streamflow hydrographs around the globe (Lindström *et al.*, 1997; Hamilton *et al.*, 2000; Bruland and Hagen, 2002; Kampf and Richer, 2014; Smith *et al.*, 2014). Simple models, which account for the pothole dynamics are missing. These models can be useful for operational, design, and/or engineering use (Bourdin *et al.*, 2012). A conceptual model can be a good alternative when available data are limited, and the watershed response is the main interest as such a model is computationally efficient and requires a small number of input variables and calibration parameters. This model can provide computationally efficient flood peak predictions and contribute to the efforts and programs of flood risk management in the prairie environment.

1.2.2 Efficient Simulation of Pothole Storage Dynamics

The surface connectivity between potholes has drawn a lot of attention in the past few decades (Godwin and Martin, 1975; Winter, 1989; Winter and Rosenberry, 1998; Darboux *et al.*, 2001; Leibowitz and Vining, 2003; Antoine *et al.*, 2009; Shook and Pomeroy, 2011; Shaw *et al.*, 2012, 2013; Chu *et al.*, 2013; Shook *et al.*, 2013; Huang *et al.*, 2013; M. Mekonnen *et al.*, 2014; B. Mekonnen *et al.*, 2015, 2016; Yang and Chu, 2015; Nasab *et al.*, 2017; Muhammad *et al.*, 2019, 2018). Shook and Pomeroy (2011) and Shook et al. (2013) developed two models to simulate the fill and spill mechanism in the prairies; Wetland Digital Elevation Ponding Model (WDPM) and conceptual Pothole Cascading Model (PCM). The WDPM is a simplified hydraulic DEM-based model that moves water over the landscape. The PCM is a conceptual model that uses a fixed number of reservoirs to represent potholes. In this model, each pothole is represented as a simple reservoir that fills and spills to the surrounding potholes after exceeding its maximum level. These reservoirs might be connected in series as well as in parallel. The WDPM can identify the spatial connectivity between potholes in the prairies, while the PCM does not represent the actual connectivity because it uses conceptual reservoirs. Both models show hysteresis in the relationship between depressional storage and both water-covered area and contributing area.

Chu *et al.* (2013) developed the Puddle-to-Puddle (P2P) conceptual model based on the Puddle Delineation (PD) algorithm (Chu *et al.*, 2010) to simulate the fill and spill mechanism under rainfall and losses events on two artificial (laboratory) pothole dominated surfaces with areas of 7.81 and 0.52 m^2. The PD algorithm was used to delineate the surface, obtain topographic characteristics of prairie potholes (cascading order, surface area, and storage), and flow direction for the non-pothole area from high resolution DEMs. The study area was divided into two units: puddle units and cell units. The puddle units were identified as the puddle area and the fill-spill-merge process can follow the cascading-merging order obtained from the PD algorithm. The cell units were considered as contributing areas with no puddles and the water was routed through cell-to-cell (C2C) routing algorithm, in which the water movement is instantaneous. The P2P model showed potential to simulate the storage dynamics and the spatial extents of the potholes. However, the implementation of this approach on a real basin was not examined.

M. Mekonnen *et al.* (2014) introduced the PDMROF (Probability Distribution Model based RunOFf generation) algorithm and was based on the PDM concept (Moore, 1985, 2007). The PDMROF uses the Pareto distribution function to represent dynamic contributing areas as a percentage of the basin storage volume. The PDM concept showed potential to simulate the prairie streamflow dynamics when implemented within two different models; MESH (M. Mekonnen *et al.*, 2014) and SWAT (B. Mekonnen *et al.*, 2016). However, the PDM concept cannot represent the spatial extents of the potholes, and its ability to replicate the hysteresis in the relationship between the contributing area and the basin storage was not investigated.

The complex characteristics of the prairie potholes contribute to the non-linearity of the relationship between the contributing area and the basin storage (Spence, 2007; Shaw, 2010). Also, potholes create system memory as the watershed response is a function of the history of inputs and outputs (Shook and Pomeroy, 2011). Prairie pothole hydrology is complex (Hayashi *et al.*, 1998; Fang *et al.*, 2010; Pomeroy *et al.*, 2010) and the hydrological response of potholes has to be examined using their actual properties in the study area. The effect of the pothole complexities, using their actual spatial distribution, on the hydrological response of the basin has not drawn much attention. WDPM showed potential to simulate the pothole complexities and their effect on the system response while accounting for their actual spatial distribution (Shook and Pomeroy, 2011; Shook *et al.*, 2013). Other hydraulic models, such as MIKE SHE (DHI, 1998) and HEC-

RAS 5.0.3 model and newer versions (Hydrologic Engineering Center, 2016), can be used to simulate the inundation extent with the presence of the potholes. However, these models are computationally expensive, and they do not have any hydrologic processes representation. More computationally efficient methods use either lumped concepts of the potholes or simple reservoir approach (e.g., M. Mekonnen *et al.*, 2014; B. Mekonnen *et al.*, 2015, 2016; Evenson *et al.*, 2016; Muhammad *et al.*, 2019), which cannot be used to accurately study the effect of the potholes on the hydrologic system behavior of a particular watershed. There is a tradeoff between computational efficiency and process representation. Computationally expensive methods are complex, but they might have good process representation. On the other hand, conceptual type methods are computationally efficient at the cost of process representation. It is important to develop a method/model that is more computationally efficient compared to more complex counterparts and provides improved process representation compared to the conceptual type methods. Hence, there is a need to develop a new computationally efficient model that can simulate the pothole storage dynamics, based on their actual spatial distribution, and the associated surface water extents. This model can explicitly represent the complex prairie pothole dynamics and can be used to understand the effect of the potholes on the runoff production in different prairie watersheds of varying size. In addition, it can be also used as an inundation mapping model for flood risk assessment purposes in the prairie pothole region, and it can potentially be integrated into distributed watershed and land surface models.

1.2.3 Representation of Potholes in Hydrological Models for Streamflow and Flood Prediction

Primarily, there are three approaches that can be employed to deal with the complexity of prairie non-contributing area within watershed models: (1) the non-contributing area is fixed (static), regardless of the hydrological conditions, (2) the entire watershed area is contributing, and (3) dynamic non-contributing area. The first approach excludes the non-contributing area from the watershed and deals with the remaining as the net watershed area (Wen *et al.*, 2011). In contrast, the second approach ignores the fact that the non-contributing area does not contribute to the streamflow and considers the whole watershed as contributing area (Shrestha *et al.*, 2012). The former method assumes that the contributing area is temporally constant, which fails to simulate the variability in the non-contributing area over time and different precipitation events. The second approach leads to overestimation in the streamflow and ignores an essential and complicated hydrological process (prairie pothole fill and spill). The third approach considers the non-contributing area as a dynamic area that varies with time and the watershed hydrological conditions (Shook and Pomeroy, 2011; Shook *et al.*, 2013; M. Mekonnen *et al.*, 2014; B. Mekonnen *et al.*, 2015, 2016). This methodology is suitable to represent the complex non-contributing area and was proven to enhance the streamflow simulation in prairie watersheds (M. Mekonnen *et al.*, 2014; B. Mekonnen *et al.*, 2016; Zeng *et al.*, 2020). However, most of the existing approaches cannot be used to represent the spatial distribution of water over the landscape or investigate the spatial non-contributing area.

Many researchers tried to simulate the prairie runoff under potholes complexities based on DEMs and satellite imageries to simulate the movement of surface water through the actual potholes within the study area, whereas others used statistical distributions to conceptually represent the fill and spill mechanism. The DEMs/imageries-based runoff models include WDPM (Shook and Pomeroy, 2011; Shook *et al.*, 2013), P2P (Chu *et al.*, 2010, 2013), and the pothole component in SWAT (Evenson *et al.*, 2016; Muhammad *et al.*, 2018, 2019). A new explicit modelling of the individual potholes, identified using the available land cover data, was implemeted in the SWAT modelling system to improve the streamflow prediction (Evenson *et al.*, 2016; Muhammad *et al.*, 2019). Potholes that are located near the stream were excluded from the modelling process as they are assumed to contribute to the stream. Each pothole has a separate pond component in SWAT. The ponds along with the land cover, soil, and terrain data were used to identifiy the computational units (HRUs) in the model. Each HRU contributes flow to the pond that is located inside the HRU and when the pond is filled, the whole HRU contributes flow to the downstream HRUs. This methodology is similar to the PCM approach (Shook and Pomeroy, 2011; Shook *et al.*, 2013), and it results in an increased number (thousands) of HRUs compared to the traditional HRUs without ponds, which makes the model computationally ineffecient and incerases the number of model parameters.

The conceptually based runoff model, wherein the pothole characteristics can be drawn from a statistical distribution without the need of high resolution DEM or satellite imagery, is computationally efficient and showed potential to improve the prairie streamflow simulation when implemented into different hydrological models, such as: MESH (M. Mekonnen *et al.*, 2014) and SWAT (B. Mekonnen *et al.*, 2016; Zeng *et al.*, 2020). However, this approach cannot represent the spatial extents or connectivity among the potholes and it had difficulties in replicating the streamflow of some complex prairie watersheds (e.g., Qu'Appelle river basin in Saskatchewan, Canada; Hossain, 2018). Further, the majority of these models do not represent the spatial distribution of water over the watershed and cannot identify the spatial non-contributing area.

Given the limitations of the available runoff generation approaches in the prairies, there is a need to develop a new algorithm that has a proper representation of the pothole complexities and replicates the hysteretic relationship between the contributing area and watershed storage in the prairies. The algorithm needs to be implemented into land surface models to better simulate the complex response of the prairie watersheds while accounting for the hysteretic relationship between contributing area and watershed storage. This prairie-adapted land surface model can yield a better hydrograph and peak flow simulations compared to the models with the existing algorithms in the prairies (e.g., PDMROF). The model is also needed for better understanding of the earth system components and the actual spatiotemporal dynamics of the hydrologic connectivity in the prairie potholes. It should lead to better quantification of the impacts of climate change on the streamflow in the prairies and can help assess the impact of local scale (pothole) pluvial and nival flooding on the surrounding areas, and update the currently used static spatial non-contributing area map.

1.3 Thesis Objectives

To overcome the above-mentioned challenges, the aim of this thesis is mainly to modify/develop models to improve the prediction of streamflow, and in particular peak flow, as well as the associated pothole flooding extents in the complex prairie environment. Existing models and approaches are modified, and new ones are developed to address the research main goal. To achieve this research goal, the following specific objectives are identified:

1. To adapt a simple hydrological model for streamflow, especially peak flow, prediction in the prairies for practical and engineering purposes;
2. To develop a computationally efficient model for simulating the spatial pothole storage dynamics and the associated pothole flooding extents; and
3. To improve the representation of the pothole storage dynamics, spatiotemporal changes of non-contributing areas, pluvial-nival flooding extents over the landscape, and

streamflow simulation in land surface models in the prairies for better simulation of earth system components.

This study contributes towards solving the flood prediction problem in the prairies and develops/modifies a set of models and tools that can be used for efficient pothole storage dynamics simulation, inundation mapping, streamflow, with emphasis on peaks, prediction. The models are proposed such that they can be applied to various watershed scales and using available data. The proposed models use both limited and detailed hydro-meteorological information, and fine or coarse resolution terrain data for inundation mapping and storage dynamics simulation. The models can be used for a wide spectrum of hydrologic or hydraulic purposes, ranging from limited data, conceptual-lumped-operational mode to detailed data, distributed, physically based research mode.

1.4 Thesis outline

This thesis is a manuscript-style thesis and consists of two published and one submitted manuscripts in international peer reviewed journals. ***Chapter 2*** to ***Chapter 4*** are slightly modified versions of journal manuscripts. In ***Chapter 2,*** a new conceptual model for flood prediction in the Canadian prairies is developed. A novel hydraulic model for flow routing and inundation mapping under pothole complexities in prairie watersheds is developed in ***Chapter 3***. The model presented in ***Chapter 3*** is coupled with the MESH land surface model, and the work is presented in ***Chapter 4***, for better simulation of the prairie hydrology and for improved representation of pothole and non-contributing area dynamics. ***Chapter 5*** provides summary, conclusions, and limitations of the research conducted in this thesis, along with the work significance and contributions to solving the flood prediction problem in the prairies. The thesis ends with some suggestions for future research direction at the end of ***Chapter 5***.

1.5 References

Antoine M, Javaux M, Bielders C. 2009. What indicators can capture runoff-relevant connectivity properties of the micro-topography at the plot scale? Advances in Water Resources 32 (8): 1297–1310 DOI: 10.1016/j.advwatres.2009.05.006

Apel H, Aronica GT, Kreibich H, Thieken AH. 2009. Flood risk analyses - How detailed do we need to be? Natural Hazards 49 (1): 79–98 DOI: 10.1007/s11069-008-9277-8

Beven K. 1989. Changing ideas in hydrology - The case of physically-based models. Journal of Hydrology 105 (1–2): 157–172 DOI: 10.1016/0022-1694(89)90101-7

Bharath R, Elshorbagy A. 2018. Flood mapping under uncertainty: a case study in the Canadian prairies. Natural Hazards 94 (2): 537–560 DOI: 10.1007/s11069-018-3401-1

Booij MJ. 2003. Determination and integration of appropriate spatial scales for river basin modelling. Hydrological Processes 17 (13): 2581–2598 DOI: 10.1002/hyp.1268

Bourdin DR, Fleming SW, Stull RB. 2012. Streamflow modelling: A primer on applications, approaches and challenges. Atmosphere - Ocean 50 (4): 507–536 DOI: 10.1080/07055900.2012.734276

Brimelow J, Stewart R, Hanesiak J, Kochtubajda B, Szeto K, Bonsal B. 2014. Characterization and assessment of the devastating natural hazards across the Canadian Prairie Provinces from 2009 to 2011. Natural Hazards 73 (2): 761–785 DOI: 10.1007/s11069-014-1107-6

Bruland O, Hagen JO. 2002. Glacial mass balance of Austre Brøggerbreen (Spitsbergen), 1971-1999, modelled with a precipitation-run-off model. Polar Research 21 (1): 109–121 DOI: 10.1111/j.1751-8369.2002.tb00070.x

Chu X, Yang J, Chi Y, Zhang J. 2013. Dynamic puddle delineation and modeling of puddle-to-puddle filling-spilling-merging-splitting overland flow processes. Water Resources Research 49 (6): 3825–3829 DOI: 10.1002/wrcr.20286

Chu X, Zhang J, Chi Y, Yang J. 2010. An Improved Method for Watershed Delineation and Computation of Surface Depression Storage. Watershed Management 2010: 333–342 DOI: doi:10.1061/41143(394)100

Darboux F, Davy P, Gascuel-Odoux C, Huang C. 2001. Evolution of soil surface roughness and flowpath connectivity in overland flow experiments. In CatenaElsevier; 125–139. DOI: 10.1016/S0341-8162(01)00162-X

DHI. 1998. MIKE SHE Water Movement – User Guide and Technical Reference Manual, Edition 1.1.

Elshorbagy A, Bharath R, Lakhanpal A, Ceola S, Montanari A, Lindenschmidt KE. 2017. Topography-and nightlight-based national flood risk assessment in Canada. Hydrology and Earth System Sciences 21 (4): 2219–2232 DOI: 10.5194/hess-21-2219-2017

Evenson GR, Golden HE, Lane CR, D'Amico E. 2016. An improved representation of geographically isolated wetlands in a watershed-scale hydrologic model. Hydrological Processes 30 (22): 4168–4184 DOI: 10.1002/hyp.10930

Fang X, Minke A, Pomeroy J, Brown T, Westbrook C, Guo X. 2007. A Review of Canadian Prairie Hydrology : Principles , Modelling and Response to Land Use and Drainage Change A Review of Canadian Prairie Hydrology: Principles , Modelling and Response to Land Use and Drainage Change. Review Literature And Arts Of The Americas (July)

Fang X, Pomeroy JW, Westbrook CJ, Guo X, Minke AG, Brown T. 2010. Prediction of snowmelt derived streamflow in a wetland dominated prairie basin. Hydrology and Earth System Sciences 14 (6): 991–1006 DOI: 10.5194/hess-14-991-2010

Gharari S, Razavi S. 2018. A review and synthesis of hysteresis in hydrology and hydrological modeling: Memory, path-dependency, or missing physics? Journal of Hydrology 566 (June): 500–519 DOI: 10.1016/j.jhydrol.2018.06.037

Godwin RB, Martin FRJ. 1975. Calculation of gross and effective drainage areas for the Prairie Provinces. In Canadian Hydrology Symposium - 1975 Proceedings, 11-14 August 1975, Winnipeg, Manitoba. Associate Committee on Hydrology, National Research Council of Canada; 219–223.

Gray DM. 1970. Handbook on the Principles of Hydrology: with special emphasis directed to Canadian conditions in the discussions, applications and presentation of data. New York: Water Information Center, Inc.

Gray DM, Landine PG. 1988. An energy-budget snowmelt model for the Canadian Prairies. Canadian Journal of Earth Sciences 25 (8): 1292–1303 DOI: 10.1139/e88-124

Hamilton AS, Hutchinson DG, Moore RD. 2000. Estimating Winter Streamflow Using Conceptual Streamflow Model. Journal of Cold Regions Engineering 14 (4): 158–175 DOI: 10.1061/(ASCE)0887-381X(2000)14:4(158)

Hayashi M, Van Der Kamp G, Rudolph DL. 1998. Water and solute transfer between a prairie wetland and adjacent uplands, 2. Chloride cycle. Journal of Hydrology 207 (1–2): 56–67 DOI: 10.1016/S0022-1694(98)00099-7

Hayashi M, Van Der Kamp G, Schmidt R. 2003. Focused infiltration of snowmelt water in partially frozen soil under small depressions. Journal of Hydrology 270 (3–4): 214–229 DOI: 10.1016/S0022-1694(02)00287-1

Hossain K. 2018. Towards a Systems Modelling Approach for a Large-Scale Canadian Prairie Watershed. Master's Thesis. Dept. of Civil, Geological and Environmental Engineering, University of Saskatchewan.

Hrachowitz M, Clark M. 2017. HESS Opinions: The complementary merits of top-down and bottom-up modelling philosophies in hydrology. Hydrology and Earth System Sciences Discussions (January): 1–22 DOI: 10.5194/hess-2017-36

Huang S, Young C, Abdul-Aziz OI, Dahal D, Feng M, Liu S. 2013. Simulating the water budget of a Prairie Potholes complex from LiDAR and hydrological models in North Dakota, USA. Hydrological Sciences Journal 58 (7): 1434–1444 DOI: 10.1080/02626667.2013.831419

Hydrologic Engineering Center. 2016. HEC-RAS, River Analysis System, Hydraulic Reference Manual. Version 5.0. Davis, California. Available at: http://www.hec.usace.army.mil/software/hec-ras/documentation/HEC-RAS 5.0 2D Modeling Users Manual.pdf

Jakeman AJ, Hornberger GM. 1993. How much complexity is warranted in a rainfall-runoff model? Water Resources Research 29 (8): 2637–2649 DOI: 10.1029/93WR00877 van der Kamp G, Hayashi M. 2009. Groundwater-wetland ecosystem interaction in the semiarid glaciated plains of North America. Hydrogeology Journal 17 (1): 203–214 DOI: 10.1007/s10040-008-0367-1

Kampf SK, Richer EE. 2014. Estimating source regions for snowmelt runoff in a Rocky Mountain basin: Tests of a data-based conceptual modeling approach. Hydrological Processes 28 (4): 2237–2250 DOI: 10.1002/hyp.9751

Kuczera G, Mroczkowski M. 1998. Assessment of hydrologic parameter uncertainty and the worth of multiresponse data. Water Resources Research 34 (6): 1481–1489 DOI: 10.1029/98WR00496

Leibowitz SG, Vining KC. 2003. Temporal connectivity in a prairie pothole complex. Wetlands 23 (1): 13–25 DOI: 10.1672/0277-5212(2003)023[0013:TCIAPP]2.0.CO;2

Te Linde AH, Aerts JCJH, Hurkmans RTWL, Eberle M. 2008. Comparing model performance of two rainfall-runoff models in the Rhine basin using different atmospheric forcing data sets. Hydrology and Earth System Sciences 12 (3): 943–957 DOI: 10.5194/hess-12-943-2008

Lindström G, Johansson B, Persson M, Gardelin M, Bergström S. 1997. Development and test of the distributed HBV-96 hydrological model. Journal of Hydrology 201 (1–4): 272–288 DOI: 10.1016/S0022-1694(97)00041-3

Martin FRJ. 2001. Addendum No. 8 to Hydrology Report #104, Agriculture and Agri-Food Canada PFRA Technical Service: Regina, Saskatchewan, 109 pp. PFRA Hydrology Division, 1983, The Determination of Gross and Effective Drainage areas in the Prairie Provinces, Hydrology Repo.

Mekonnen BA, Mazurek KA, Putz G. 2016. Incorporating landscape depression heterogeneity into the Soil and Water Assessment Tool (SWAT) using a probability distribution. Hydrological Processes 30 (13): 2373–2389 DOI: 10.1002/hyp.10800

Mekonnen BA, Nazemi A, Mazurek KA, Elshorbagy A, Putz G. 2015. Hybrid modelling approach to prairie hydrology: fusing data-driven and process-based hydrological models. Hydrological Sciences Journal 60 (9): 1473–1489 DOI: 10.1080/02626667.2014.935778

Mekonnen MA, Wheater HS, Ireson AM, Spence C, Davison B, Pietroniro A. 2014. Towards an improved land surface scheme for prairie landscapes. Journal of Hydrology 511: 105–116 DOI: 10.1016/j.jhydrol.2014.01.020

Moore RJ. 1985. The probability-distributed principle and runoff production at point and basin scales. Hydrological Sciences Journal 30 (2): 273–297 DOI: 10.1080/02626668509490989

Moore RJ. 2007. The PDM rainfall-runoff model. Hydrology and Earth System Sciences 11 (1): 483–499 DOI: 10.5194/hess-11-483-2007

Muhammad A, Evenson GR, Stadnyk TA, Boluwade A, Jha SK, Coulibaly P. 2018. Assessing the importance of potholes in the Canadian Prairie Region under future climate change scenarios. Water (Switzerland) 10 (11): 1–19 DOI: 10.3390/w10111657

Muhammad A, Evenson GR, Stadnyk TA, Boluwade A, Jha SK, Coulibaly P. 2019. Impact of model structure on the accuracy of hydrological modeling of a Canadian Prairie watershed. Journal of Hydrology: Regional Studies 21 (December 2018): 40–56 DOI: 10.1016/j.ejrh.2018.11.005

Nasab MT, Singh V, Chu X. 2017. SWAT modeling for depression-dominated areas: How do depressions manipulate hydrologic modeling? Water (Switzerland) 9 (1) DOI: 10.3390/w9010058

Pokhrel P, Gupta H V. 2011. On the ability to infer spatial catchment variability using streamflow hydrographs. Water Resources Research 47 (8) DOI: 10.1029/2010WR009873

Pomeroy J, Fang X, Westbrook C, Minke A, Guo X, Brown T. 2010. Prairie Hydrological Model Study Final Report

Pomeroy JW, Gray DM, Brown T, Hedstrom NR, Quinton WL, Granger RJ, Carey SK. 2007. The cold regions hydrological model: A platform for basing process representation and model structure on physical evidence. Hydrological Processes 21 (19): 2650–2667 DOI: 10.1002/hyp.6787

Pomeroy JW, Gray DM, Landine PG. 1993. The Prairie Blowing Snow Model: characteristics, validation, operation. Journal of Hydrology 144 (1–4): 165–192 DOI: 10.1016/0022-1694(93)90171-5

Pomeroy JW, Shook K, Fang X, Dumanski S, Westbrook C, Brown T. 2014. Improving and Testing the Prairie Hydrological Model at Smith Creek Research Basin Available at: http://www.usask.ca/hydrology/reports/CHRpt14_PHM_SCRB.pdf

Ponce VM, Hawkins RH. 1996. Runoff Curve Number: Has It Reached Maturity? Journal of Hydrologic Engineering 1 (1): 11–19 DOI: 10.1061/(ASCE)1084-0699(1996)1:1(11)

Refsgaard JC. 1996. Terminology, Modelling Protocol And Classification of Hydrological Model Codes. Chapter 2 in Distributed Hydrological Modelling., Abbott MB, Refsgaard JC (eds).Springer Netherlands: Dordrecht; 17–39. DOI: 10.1007/978-94-009-0257-2_2

Reggiani P, Schellekens J. 2003. Modelling of hydrological responses: the representative elementary watershed approach as an alternative blueprint for watershed modelling. Hydrological Processes 17 (18): 3785–3789 DOI: 10.1002/hyp.5167

Savenije HHG, Hrachowitz M. 2017. HESS Opinions 'catchments as meta-organisms - A new blueprint for hydrological modelling'. Hydrology and Earth System Sciences 21 (2): 1107–1116 DOI: 10.5194/hess-21-1107-2017

Shaw DA. 2010. The influence of contributing area on the hydrology of the prairie pothole region of North America. PhD thesis, Department of Geography, University of Saskatchewan.

Shaw DA, Pietroniro A, Martz LW. 2013. Topographic analysis for the prairie pothole region of Western Canada. Hydrological Processes 27 (22): 3105–3114 DOI: 10.1002/hyp.9409

Shaw DA, Vanderkamp G, Conly FM, Pietroniro A, Martz L. 2012. The Fill-Spill Hydrology of Prairie Wetland Complexes during Drought and Deluge. Hydrological Processes 26 (20): 3147–3156 DOI: 10.1002/hyp.8390

Shook K, Pomeroy JW, Spence C, Boychuk L. 2013. Storage dynamics simulations in prairie wetland hydrology models: Evaluation and parameterization. Hydrological Processes 27 (13): 1875–1889 DOI: 10.1002/hyp.9867

Shook KR, Pomeroy JW. 2011. Memory effects of depressional storage in Northern Prairie hydrology. Hydrological Processes 25 (25): 3890–3898 DOI: 10.1002/hyp.8381

Shrestha RR, Dibike YB, Prowse TD. 2012. Modeling Climate Change Impacts on Hydrology and Nutrient Loading in the Upper Assiniboine Catchment. Journal of the American Water Resources Association 48 (1): 74–89 DOI: 10.1111/j.1752-1688.2011.00592.x

Smith MB, Koren V, Zhang Z, Zhang Y, Reed SM, Cui Z, Moreda F, Cosgrove BA, Mizukami N, Anderson EA. 2012. Results of the DMIP 2 Oklahoma experiments. Journal of Hydrology 418–419: 17–48 DOI: 10.1016/j.jhydrol.2011.08.056

Smith T, Marshall L, McGlynn B. 2014. Calibrating hydrologic models in flow-corrected time. Water Resources Research 50 (1): 748–753 DOI: 10.1002/2013WR014635

Spence C. 2007. On the relation between dynamic storage and runoff: A discussion on thresholds, efficiency, and function. Water Resources Research 43 (12) DOI: 10.1029/2006WR005645

Uhlenbrook S. 2003. An empirical approach for delineating spatial units with the same dominating runoff generation processes. Physics and Chemistry of the Earth, Parts A/B/C 28 (6–7): 297–303 DOI: 10.1016/S1474-7065(03)00041-X

Vansteenkiste T, Tavakoli M, Van Steenbergen N, De Smedt F, Batelaan O, Pereira F, Willems P. 2014. Intercomparison of five lumped and distributed models for catchment runoff and extreme flow simulation. Journal of Hydrology 511: 335–349 DOI: https://doi.org/10.1016/j.jhydrol.2014.01.050

Wen L, Lin CA, Wu Z, Lu G, Pomeroy J, Zhu Y. 2011. Reconstructing sixty year (1950-2009) daily soil moisture over the Canadian Prairies using the Variable Infiltration Capacity model. Canadian Water Resources Journal / Revue canadienne des ressources hydriques 36 (1): 83–102 DOI: 10.4296/cwrj3601083

Winter TC. 1989. Hydrologic studies of potholes in the northern prairies. (Ames, ed.). Northern Prairie Wetlands. Iowa: Iowa State University Press.

Winter TC, Rosenberry DO. 1998. Hydrology of Prairie Pothole Wetlands during Drought and Deluge: A 17-Year Study of the Cottonwood Lake Wetland Complex in North Dakota in the Perspective of Longer Term Measured and Proxy Hydrological Records. Climatic Change 40 (2): 189–209 DOI: 10.1023/A:1005448416571

Yang J, Chu X. 2015. A new modeling approach for simulating microtopography-dominated, discontinuous overland flow on infiltrating surfaces. Advances in Water Resources 78: 80–93 DOI: 10.1016/j.advwatres.2015.02.004

Zeng L, Shao J, Chu X. 2020. Improved hydrologic modeling for depression-dominated areas. Journal of Hydrology 590 (July): 125269 DOI: 10.1016/j.jhydrol.2020.125269

Chapter 2 Toward Simple Modeling Practices in the Complex Canadian Prairie Watersheds

This chapter is a slightly modified version of the published article (Ahmed *et al.*, 2020a), modified to make it consistent with the format and body of the thesis. This chapter is the final accepted draft of the paper prior to copyediting or other production activities by the journal.

Citation: Ahmed MI, Elshorbagy A, Pietroniro A. 2020a. Toward Simple Modeling Practices in the Complex Canadian Prairie Watersheds. Journal of Hydrologic Engineering 25 (6): 04020024 DOI: 10.1061/(ASCE)HE.1943-5584.0001922. With permission from ASCE. The permission of reproduction is presented in Appendix A.1.

Authors Contributions and The Contribution of This Chapter to The Overall Study

The following are the contributions from the different authors of this (chapter) published manuscript. M. I. Ahmed contributed to the conceptualization, methodology, software, validation, formal analysis, investigation, data curation, writing - original draft, and visualization. A. Elshorbagy contributed to the conceptualization, methodology, writing - review & editing, supervision, and funding acquisition. A. Pietroniro contributed to the writing - review & editing, and supervision.

This chapter fills an important gap in operational hydrology by proposing the HYdrological model for Prairie Region. This model can be used to simulate the hydrograph and peak flows of complex prairie watersheds. HYPR covers the first objective of this thesis and contributes to solving the flood prediction problem from engineering and design perspective.

2.1 Abstract

The prairie region in Canada has been characterized as "a graveyard of the hydrological models" due to its challenging cold regions processes and the complex landscape with numerous land depressions that influence runoff pathways. Efforts were made at the small basin scale to propose new algorithms and/or modify existing physically based hydrological models in order to achieve some semblance of a coherent mathematical runoff modelling system. To date, there has been very little research on modifying conceptual bucket-type models to include the lateral pothole flow complexities for peak flow estimation. In this study, the conceptual HBV-light model is modified to work in the prairies by incorporating a conceptual lateral flow component to represent

the pothole storage complexities. The modification of the HBV-light model resulted in a HYdrological model for Prairie Region (HYPR) that can be used for prairie streamflow simulation. The traditional HBV-light and HYPR conceptual models are tested on different pothole-dominated watersheds within the Qu'Appelle River Basin in Saskatchewan, Canada. The incorporation of a pothole storage-modelling component in HYPR results in a better streamflow simulation than that of HBV-light. Also, a new approach is proposed in this study to better identify the proper calibration period to arrive at a successful streamflow simulation. Although HYPR's processes representation is simplified, the model shows potential for simulating the overall hydrograph and peak flows. HYPR shows strengths as a possible tool for operational and flood prediction purposes in the prairies, especially when data are limited.

2.2 Graphical Abstract

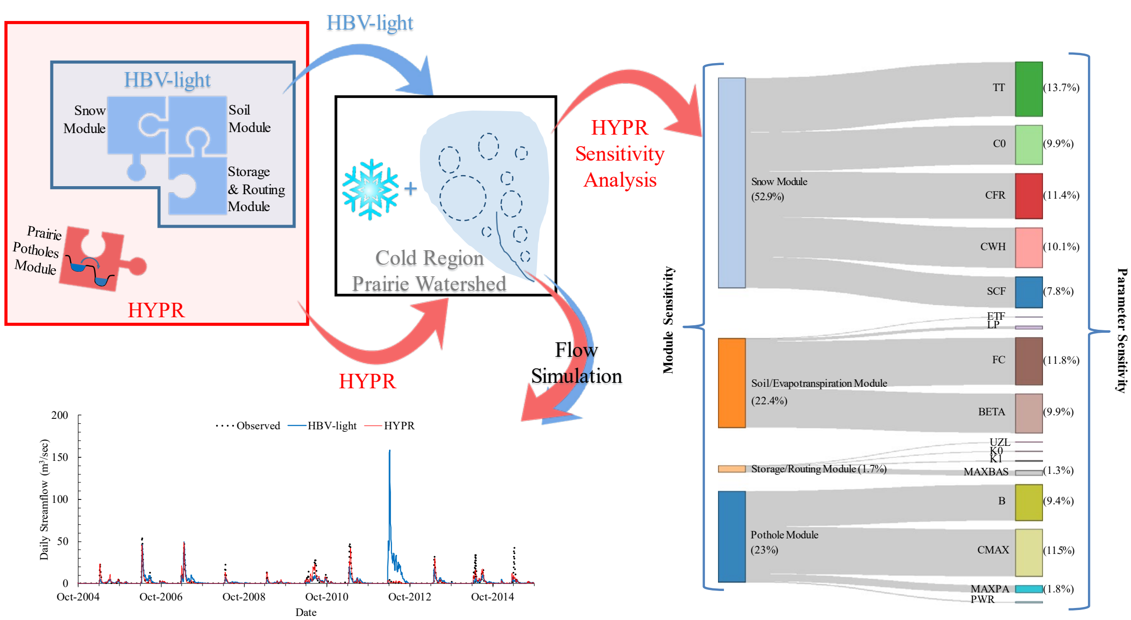

2.3 Introduction

The North American Prairie region contains major areas of the Canadian provinces of Manitoba, Saskatchewan, and Alberta, and the American states of Montana, North and South Dakota, Minnesota, and Iowa. These prairies are characterized by millions of land depressions of glacial origin (Zhang *et al.*, 2009; Anteau *et al.*, 2016), referred to as prairie potholes. The potholes are hydrologically complex with regard to their landscape (Winter, 1989; Shook and Pomeroy, 2011), as they can retain a significant amount of surface runoff (van der Kamp and Hayashi, 2009). Due to the presence of these numerous land depressions, the runoff production in the prairies follows a fill and spill mechanism (Shaw *et al.*, 2012), resulting in disconnected stream networks that do not contribute to the river system under low snowmelt or rainfall events (Martin, 2001; Hayashi *et al.*, 2003). However, under severe rain/snowmelt events, small potholes are filled, the surface area is expanded and many potholes might merge to form a larger pond and might be connected to the stream network (Shook and Pomeroy, 2011). This dynamic connectivity between potholes results in a dynamic contributing area, which makes traditional hydrological models that assume a static contributing area invalid (Shaw *et al.*, 2012).

The Canadian prairies are characterized by low precipitation, of which around 30 % falls as snow during winters (Gray and Landine, 1988; Akinremi *et al.*, 1999). During early spring, snowmelt over frozen soils is the main source of overland flow and accounts for more than 80 % of the annual surface runoff (Gray and Landine, 1988). In summer, the evapotranspiration and infiltration rates are high, and limit the surface runoff to occur only during/after heavy rainfall events (Hayashi *et al.*, 1998; van der Kamp and Hayashi, 2009). Blowing snow redistributes snow from the open, exposed areas to sheltered areas and land depressions. During the redistribution, sublimation of snow occurs and reduces snow accumulation at the end of the winter (Pomeroy *et al.*, 1993). These processes are typical of cold regions and, when coupled with land depressions that are typical of the North American prairies, increase hydrological complexities and they have been the topic of studies for many decades.

Traditional hydrological models that do not account for pothole complexities fail in the prairies, including the state-of-the-art physically based ones. Hence, researchers made considerable efforts to simulate the runoff process in the prairies either by proposing new modelling approaches (Shook and Pomeroy, 2011; Chu *et al.*, 2013), or by modifying well-established models, such as the Soil and Water Assessment Tool (SWAT) (B. Mekonnen *et al.*, 2016; Muhammad *et al.*, 2019), Modelisation Environmentale Communautaire – MESH (M. Mekonnen *et al.*, 2014; Hossain, 2018), and The Cold Regions Hydrological Model (CRHM) (Fang *et al.*, 2010). However, there was limited or no effort/intention to improve conceptual hydrological models for the same purpose.

Researchers argue that conceptual models/approaches do not have the potential to work in the prairies because the representation of the complex prairie hydrological processes is either simplified or missing (Gray *et al.*, 1989). Gray and Landine (1988) concluded that the energy balance method is more suitable than the simple degree-day method for the open grassland prairie snow cover. However, the processes that occur when snowpack starts to melt are more complex than what is being represented by the energy balance approach and more discretization of the snowpack depth is needed to accurately model the snow-related processes. Thus, the degree-day approach might be more suitable than the energy balance method at the catchment scale (Seibert, 1999). Further, the SWAT model that uses the degree-day approach to handle snow-related processes showed potential for simulating the prairie streamflow, when accounting for pothole complexities (B. Mekonnen *et al.*, 2015, 2016; Muhammad *et al.*, 2019).

Some researchers argue that complex physically based distributed models can simulate the observed streamflow better than simple conceptual models (Refsgaard, 1996; Reggiani and Schellekens, 2003), while others argue against this and conclude that complex models do not lead to better results (Ponce and Hawkins, 1996; Booij, 2003; Uhlenbrook, 2003; Te Linde *et al.*, 2008). Distributed physically based models are valuable when either the study involves spatial scenarios or there are observed data related to the hydrological variables at the local interior locations within the watershed (Pokhrel and Gupta, 2011; Smith *et al.*, 2012). However, there are scarce data regarding the hydrological variables and the available data are limited to the observed streamflow in the majority of the watersheds (Jakeman and Hornberger, 1993; Kuczera and Mroczkowski, 1998). Thus, the spatial representation of physical processes and inputs in the physically based models, are not being efficiently used, because the model performance is judged on the output streamflow only. Furthermore, physically based distributed models have their own modelling problems, such as nonlinearity, scale, equifinality, and a large number of input data and parameters (Beven, 2001).

The lumped models show potential for capturing the watershed response (streamflow) at its outlet (Reed *et al.*, 2004; Smith *et al.*, 2012). Conceptual model's parameters are effective and can model the temporal variation efficiently (Hrachowitz and Clark, 2017; Savenije and Hrachowitz, 2017). The simplistic representation of the processes in the conceptual models leads to a low computational cost and a more robust model, which is useful in specific operational contexts (e.g., floods) (Bourdin *et al.*, 2012). To some extent, conceptual models can be thought to be physically based as they maintain the mass balance and can represent the energy balance in a simplified way (Hrachowitz and Clark, 2017). A conceptual model can be a good alternative when the data are limited, and the watershed response is the main interest. It is advised that the selection criteria of model type should be based on the availability of the forcing data, watershed scale, driving processes, and application of the model. This can result in using a more simplified and accurate model for watershed streamflow simulation (Booij, 2003).

While streamflow simulation in the prairies is challenging, capturing the peak flows (floods) is even more challenging for the hydrological models. The prairie region has witnessed multiple floods over the past decade. The 2013 flood event had major impacts on the prairies, causing damages of over CAD $1 billion dollars. Further, more than 5 million hectares of western prairie agricultural land did not produce crops due to the 2011 flood event (Brimelow *et al.*, 2014). It is important to have a hydrologic model that can predict floods accurately, especially in highly populated and agricultural areas, to help in reducing flood risks. Despite the importance of peak flow simulation, the majority of the studies, in the prairies, focused on capturing the general trend of the hydrograph with less attention to the accuracy in peak flow simulation (e.g., M. Mekonnen *et al.*, 2014; B. Mekonnen *et al.*, 2016; Muhammad *et al.*, 2019).

A model that can predict prairie floods accurately, within a timely manner (short execution/run time) and without the need for expensive computational resources, fills an important gap in operational hydrology in this region. Since researches have used conceptual models to reproduce the streamflow in cold regions for many decades, and the physically based models have been found to fail unless a conceptual algorithm is incorporated to represent prairie surface runoff complexities, the incorporation of a conceptual runoff algorithm for prairie pothole complexity within a conceptual model may be beneficial from flood perspective. By proposing this model, we can provide computationally efficient flood-peak predictions and contribute to the reduction of the associated flood risks in the prairie environment.

The main objective of this study is to move toward simple and successful conceptual modelling practices by proposing a conceptual water balance approach, while still accounting for potholes complexities, focusing on peak flows, in the prairies. This study argues that the flexible structure of the conceptual model can yield a better hydrograph and peak flow simulation in the prairies using only two forcing variables and very limited physiographic information. A new conceptual HYdrological model for Prairie Region (HYPR) is proposed in this study by adding a pothole storage component to the HBV-light model (Seibert, 2005; Seibert and Vis, 2012). This study demonstrates the essential need of capturing the potholes dynamics in order to arrive at a successful streamflow simulation in the prairies. A secondary objective of this study is to propose a new approach that can help in identifying the proper period for model calibration to arrive at a successful streamflow simulation.

2.4 Methodology

The streamflow simulation capability of the conceptual HBV-light model (Seibert, 2005; Seibert and Vis, 2012) along with a modified version of the same model, which is referred to as the HYPR model, developed in this study, is tested on different pothole-dominated watersheds. Further simulations were conducted to test the performance of the HYPR model in different calibration periods, assess the sensitivity and uncertainty of model parameters and output, and assess the validity of HYPR in simulating the snow water equivalent. A detailed methodology is presented below.

2.4.1 Hydrological Models

2.4.1.1 HBV Model

Hydrologiska Byråns Vattenbalansavdelning (HBV-97) model (Lindström *et al.*, 1997) is a conceptual rainfall-runoff model that uses the concept of cascading buckets along with different empirical and conceptual equations to represent the hydrological processes. The HBV-light model (Seibert, 2005; Seibert and Vis, 2012) was developed to provide a simple and easy version of the HBV-97 model for research and education. The equations and concepts are the same in both versions, however, many functions from the HBV-97 model have not been incorporated in the HBV-light model (e.g., precipitation correction relative to altitude and precipitation interception) to make it easy to implement. Most of the unimplemented algorithms in the HBV-light model have minor/negligible effects on the hydrological processes in the prairies because the prairies are known for their relatively flat terrain and cropland/grassland cover, which makes the HBV-light model more suitable.

The HBV-light model has four different modules to handle the internal processes and the streamflow simulation that include a snow module, soil module, storage module, and routing module. The snow module handles the snow processes including precipitation phase, snow accumulation, snowmelt, refreezing of the meltwater into the snowpack, and losses from the snowpack (e.g., sublimation). The rainfall and/or meltwater is incorporated into the soil module that estimates the infiltrated and excess water amounts, the soil moisture storage, and evapotranspiration. The excess water is stored in the storage module as surface water storage and groundwater storage. The stored water in the storage module is routed to the watershed outlet via the routing module. The snowmelt is a function of the snowpack depth and is computed using the degree-day method. The actual summertime evapotranspiration and excess water that is released from the soil module are calculated based on the storage in the soil module. The runoff depth is calculated using a linear reservoir approach and is transformed to streamflow using a triangular transformation function that routes the runoff to the watershed outlet (Seibert, 2005; Seibert and Vis, 2012).

2.4.1.2 The Modified HBV Model (HYPR) for the Prairies

The HBV-light model was modified to work in the prairies by incorporating the Probability Distribution Model-based RunOFf generation (PDMROF, M. Mekonnen *et al.*, 2014) conceptual algorithm. The PDMROF uses the Pareto distribution function to represent dynamic contributing areas as a percentage of the basin water storage. In the PDMROF algorithm, the unit (basin or sub-basin) is assumed to consist of spatially distributed storage units with varying sizes. The storage of the unit is described by the critical/spilling depth that varies with time. In the unit, potholes with depth less than or equal to the critical/spilling depth are full and contribute to the streamflow (in the spilling stage). Whereas, the remaining potholes with depth more than the critical/spilling depth are not full yet and do not contribute to the streamflow (in the filling stage).

The modification of the lumped HBV-light model resulted in a new conceptual HYdrological model for Prairie Region (HYPR, Figure 2.1). The HYPR model's parameter that controls the recharge to the groundwater bucket was fixed at a very low value (close to zero) to reflect the prairie conditions as the groundwater flow has a negligible effect on the prairie streamflow, mostly due to low hydraulic conductivity (van der Kamp and Hayashi, 2009; Fang *et al.*, 2010). HYPR required further modifications to handle the evaporation losses from the potholes since these have never been parametrized in the HBV system. In the generic PDMROF algorithm (pothole storage module), S_{max} represents the total available storage in all represented potholes (M. Mekonnen *et al.*, 2014). Intuitively, if the storage within the pothole storage module equals S_{max}, all potholes within the basin are full. Thus, the percent ponded area of the basin is proportional to S_{max} value. The relationship between the ponded surface area and the water depth was proven to vary according to a power relation for individual ponds (Hayashi and Van Der Kamp, 2000). Hence, for simplicity, the percent ponded area of the basin, at a daily time step t, is assumed to follow the power relation suggested by Hayashi and Van Der Kamp (2000) and equals to the following:

$$Ponded\ Area_t = \left(\frac{S_{PSM_t}}{S_{max}}\right)^{2/PWR} \times MAXPA \qquad (2.1)$$

where, S_{PSM_t} is the storage of the Pothole Storage Module at a daily time step *t*, *PWR* is the power that controls the relationship between the area and depth, and *MAXPA* is the percent of watershed area occupied by ponded water when all potholes are 100 % full.

The total evaporation from the basin is a combination of evapotranspiration from the soil module and evaporation from the pothole storage module. The total evaporative flux, at a daily time step *t*, follows the following equation:

$$T_{evap_t} = (Ponded\ Area_t \times PE_t) + [(1 - Ponded\ Area_t\ ) \times AET_t)] \qquad (2.2)$$

where, PE_t is the potential evapotranspiration, and AET_t is the actual evapotranspiration, at a daily time step t, and both are calculated using the HBV-light model's approach. The daily PE_t is a function of the average monthly potential evapotranspiration (PE_m), which can be obtained using different approaches/equations such as Hargreaves equation or Penman-Monteith method. The PE_t is expressed in the HBV system as follows:

$$PE_t = \left(1 + ETF \times (T_t - T_m)\right) \times PE_m \qquad (2.3)$$

where, *ETF* is the temperature anomaly correction of potential evapotranspiration, T_t is the average daily temperature, and T_m is the average monthly temperature. The actual evapotranspiration is a function of soil moisture (*SM*) and is expressed in the HBV system as follows:

$$AET_t = \begin{cases} PE_t & SM > LP \\ PE_t \times (SM/LP\ ) & SM \leq LP \end{cases} \qquad (2.4)$$

where, *LP* is the limit for potential evapotranspiration. Finally, at each time step, the contributing area is calculated via the pothole storage module and is used in the calculation of direct runoff contributing to streamflow. Table 2.1 shows a summary and a description of HYPR parameters and their ranges. Both HBV-light and HYPR models run in a lumped mode and require only daily total precipitation, mean daily temperature, and long-term evapotranspiration data.

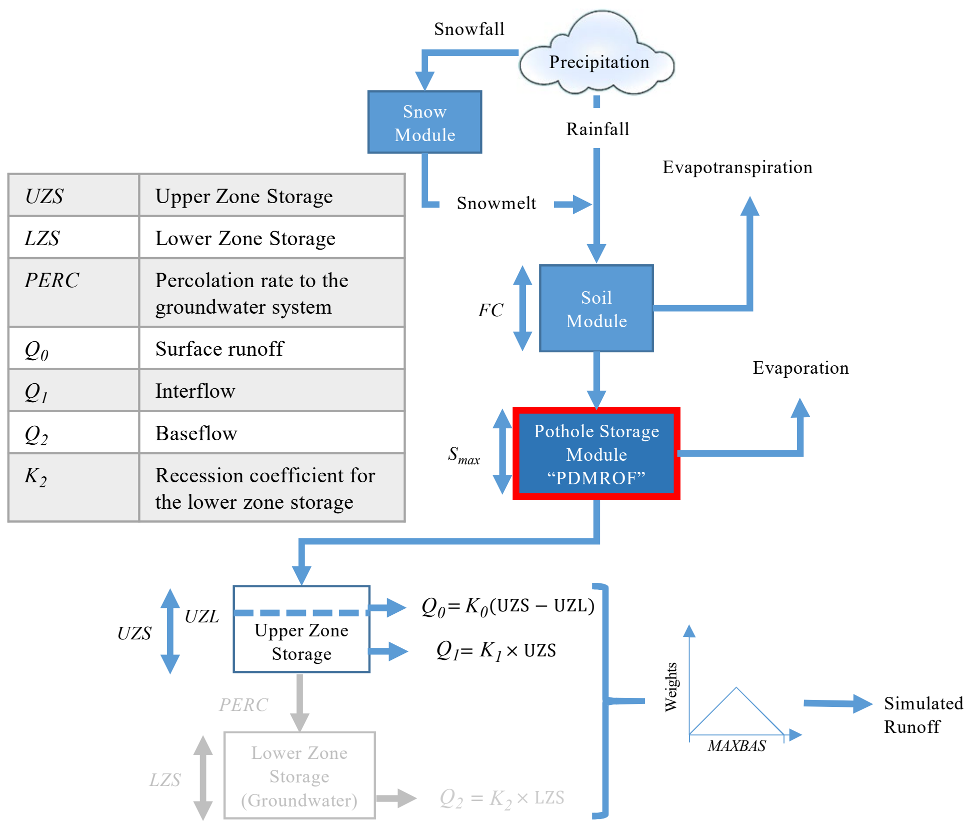

Figure 2.1: Schematic representation of the HYPR model with the incorporation of the PDMROF algorithm (pothole storage module) that is highlighted with a thick red outline. The seepage to the groundwater bucket was fixed at a value close to zero because groundwater has a negligible effect on the prairie streamflow (components highlighted in gray). A full description of the model parameters is presented in Table 2.1.

Table 2.1: Calibration parameters ranges for HYPR.

Model Parameter	Description	Units	Min	Max	Related Module
TT	Air Temperature Threshold for distinguishing rain from snow and for melting/freezing	C°	-3	3	Snow Module
C0	Base melt/degree day factor	mm/C°/day	1	10	
CFR	Refreezing Coefficient	-	0	0.1	
CWH	Water Holding Capacity of snow	-	0	0.2	
SCF	Snowfall Correction Factor to compensate for errors in snowfall measurements and snowpack evaporation.	-	0.4	1	
ETF	Temperature anomaly correction of potential evapotranspiration	1/C°	0	0.3	Soil Module
LP	Limit for potential evapotranspiration	-	0.3	1	
FC	Maximum soil moisture content. Field Capacity of the soil	mm	1	2,000	
BETA	Soil release exponential parameter	-	0	7	
UZL	Near-surface flow threshold	mm	0	100	Storage/ Routing Module
K0	Near-surface flow coefficient	1/day	0.05	2	
K1	Recession coefficient for upper zone storage	1/day	0.01	1	
MAXBAS	Triangular Transfer function parameter	day	1	6	
B	Shape factor for Pareto distribution	-	0.1	30	Pothole Storage Module (PDMROF)
CMAX	Maximum pothole storage depth	mm	500	5,000	
MAXPA	Percent of the watershed area covered by ponded surface water when all potholes are 100% full	-	0.1	0.8	
PWR	Area-depth relationship exponential parameter	-	1	5	

The parameters of the Pothole Storage Module are new and have been added to modify the HBV-light model to work in prairies. The remaining are the HBV-light model parameters.

2.4.2 Study Area and Data

An extensive review of the literature has demonstrated the difficulty in hydrological model applications in the Qu'Appelle River Basin (QRB) in Saskatchewan, Canada (B. Mekonnen *et al.*, 2015, 2016; Hossain, 2018). The QRB, which has an area of almost 50,000 km^2, is one of the best examples of a challenging prairie watershed due to the presence of large non-contributing area (up to 70 % of the watershed area), varying soil type within the basin ranging from gravel-sandy to clay soils, undefined stream network in most of the sub-basins, and the varying-size controlled and uncontrolled lakes/reservoir on the main river (Figure 2.2). Both HBV-light and HYPR models were tested on three pothole-dominated watersheds: Kronau Marsh, Lanigan, and Moose Jaw, within the QRB to show that the modification is needed to arrive at a better streamflow simulation. Then, the HYPR model was validated on the seven remaining watersheds of the .

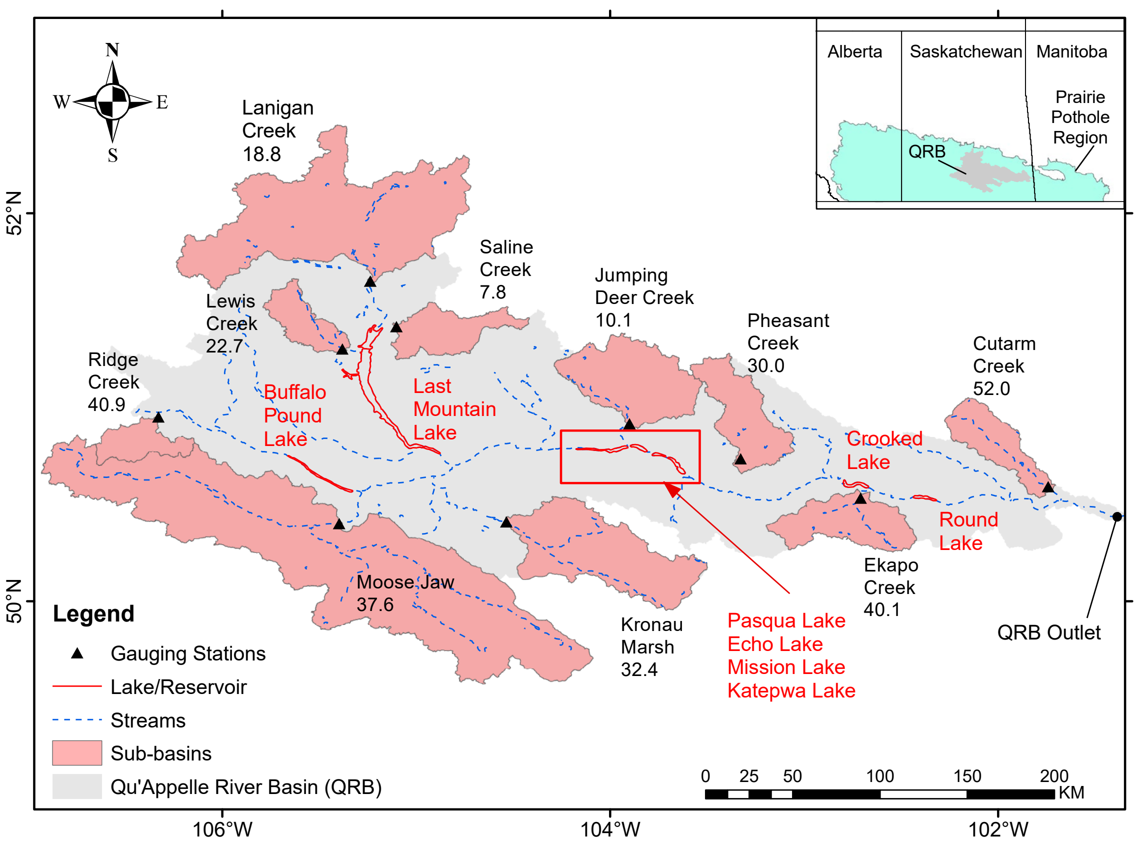

Figure 2.2: The location of the Qu'Appelle River Basin (QRB) and its sub-basins with the managed lake system. Numbers show the percent contributing area for each of the sub-basins.

More than 90 % of the area of the studied watersheds is covered by cropland. The 10 watersheds of the QRB have areas that range from 460 to 9,230 km^2 and percent contributing area for each watershed ranges from 7 % to 52 % of the watershed area (Table 2.2). The contributing area is commonly known as the area that contributes flow to the watershed outlet for events of two years return period or smaller (Godwin and Martin, 1975). The purpose of this study is to test the models' capability in modelling the natural prairie processes, and therefore, the watersheds are selected to be head watersheds with minimum water management impacts on streamflow. Each watershed has a gauging station at its outlet and the observed streamflow data are available through the Water Survey of Canada. The area is characterized by low annual precipitation that ranges from 404 to 474 mm/year (Table 2.2). The average daily streamflow and maximum annual streamflow are less than 1.5 and 15 m^3/sec, respectively, for most of the watersheds. However, these values reach 3.6 and 56.28 m^3/sec, respectively, for the Moose Jaw watershed, which is the largest one in this study area. The low average streamflow is caused by the existence of the potholes that retain a significant amount of rainfall/snowmelt, leaving a minor portion to reach the stream network. Peak flow occurs during spring snowmelt time and during heavy rainfall in summer time with low to no flow during fall, winter, and sometimes summer. The annual runoff ratio does not exceed 0.07 for all watersheds in the basin (Table 2.2).

The model forcing data are precipitation and temperature on a daily time-step. The importance of precipitation forcing, and the difficulty in characterizing the spatial realities of summer-convective type storms in the prairies along with the unavailability of climate ground observation stations led us to adopt the Canadian Precipitation Analysis (CaPA) product (Lespinas *et al.*, 2015) and the Global Environmental Multiscale (GEM) atmospheric model (Mailhot *et al.*, 2006) output as the primary forcing precipitation and temperature fields, respectively. CaPA is a high-resolution precipitation data available by combining precipitation observations with the predicted values from the GEM model using the optimal interpolation technique. The GEM-CaPA gridded data are available at an hourly or sub-hourly temporal scale. Both HBV-light and HYPR models use aggregated total daily values of precipitation from CaPA and average daily temperature from GEM averaged over each of the study watersheds. The GEM-CaPA data are available from 2002 to 2018; however, the simulation period of this study is from 2002 to 2015 because some of the hydrometric station's data are available up to 2015. Each watershed has a separate model setup with a separate parameter set because the parameters in the conceptual model are basin specific and some parameters may represent a combination of watershed properties (Seibert, 1999).

Table 2.2: Study watersheds characteristics for the study period (from 2002 to 2015).

Basin	Gauge Number	Total Drainage Area (km^2)	Effective Drainage Area (km^2)	Mean Streamflow (m^3/sec)	Mean Annual Maximum Streamflow (m^3/sec)	Mean Annual Precipitation (mm) (from CaPA)	Runoff Ratio
Cutarm	05JM015	766	398	0.73	11.66	474.21	0.063
Ekapo	05JM010	1100	441	1.09	16.48	469.98	0.066
Jumping Deer	05JK004	1680	170	0.23	4.14	447.69	0.010
Kronau Marsh	05JF012	2980	966	1.04	18.53	438.11	0.025
Lanigan	05JJ003	2283	429.7	1.62	27.52	421.67	0.053
Lewis	05JH005	572	130	0.20	4.65	428.86	0.026
Moose Jaw	05JE006	9230	3470	3.60	56.28	419.28	0.029
Pheasant	05JL005	1150	345	0.77	14.95	462.83	0.046
Ridge	05JG013	460	188	0.18	8.79	403.97	0.031
Saline	05JJ009	950	74.1	0.23	2.81	432.80	0.018

2.4.3 Model Calibration

The Nash-Sutcliffe Efficiency (NSE; Nash and Sutcliffe, 1970) was used as an objective function for models' calibration. The NSE is traditionally used as a measurement of error in the simulated flows with some emphasis on high flows (Kollat *et al.*, 2012). The model parameters were calibrated, within their respective range in Table 2.1, and validated for each watershed independently using the observed streamflow at the watershed outlet. The only exception being the SCF parameter, which was fixed at a value of 1.0 because we trust the accuracy of the CaPA precipitation product, and hence no correction is needed to compensate for snowfall measurement errors.

The first two years of the simulation period were considered as a spin-up period. The early 2000s were an exceptionally dry period over the Canadian prairies (Bonsal *et al.*, 2013), and thus, the model spin-up was relatively simple and the two years were sufficient to initialize the model. The model results for this period were not used in model calibration or analysis. The calibration period was set from 2004 to 2011, whereas the validation was set from 2012 to 2015 for all the studied watersheds. The calibration period included 2011 to train the model on predicting an actual high flow event, along with the medium and low flows, because the period from 2004 to 2010 did not have a major flood (100-year flood). The selected calibration period contains large hydrologic variability as it contains low, medium, and high flow events. It is known that periods with hydrologic variability are more preferred to be used for model calibration as they contain a lot of information for model parameter identification (Singh and Bárdossy, 2012). The stochastic global optimization Dynamically Dimensioned Search (DDS) algorithm (Tolson and Shoemaker, 2007) was used to calibrate the models by maximizing the NSE to fit the simulated flows to the observed ones with 10 independent optimization trials and 2,000 runs each. The best performing parameter set (out of the 10 sets identified from the 10 trials) with the highest NSE value was used as the calibrated parameter set.

2.4.4 Model Performance Evaluation

The resulting streamflow was evaluated using visual inspection of the hydrograph and the performance measures for the calibration and validation periods, separately. The evaluation criteria were selected based on four performance measures (NSE, NSE_{log}, NSE_{OT}, and PBIAS). The NSE was used to evaluate the model performance in the overall hydrograph, with some emphasis on high flows. NSE_{log} performance criterion is the same as the NSE but gives emphasis to low flows. The NSE_{OT} is the NSE calculated for flows over a pre-set threshold (95th percentile in this study) and was used to assess the goodness of fit for peak flows. The fourth is the percent bias (PBIAS) that was used to assess the model performance in simulating the total runoff volume.

Two more performance metrics were only used in the comparison of the HBV-light and the HYPR models known as Akaike and Bayesian Information Criteria (AIC & BIC). The AIC and BIC measure the goodness of fit between the observed and simulated flow but penalize the model for having more calibration parameters. These two criteria can show if a model, e.g. HYPR, has good performance because of the increased degrees of freedom (calibration parameters), resulting from incorporating the PDMROF algorithm. The AIC and BIC were calculated for the entire study period (2004-2015). The rating criteria, in Table 2.3, were applied to the current study with regard to NSE, NSE_{log} and NSE_{OT}. Further, the model performance can be seen as 'satisfactory' when the PBIAS $\leq \pm 25$ % according to Moriasi *et al.* (2007).

Table 2.3: Rating criteria for the model performance based on the NSE value as proposed by Moriasi *et al.* (2007).

NSE value	**Performance rating**
> 0.75	Very good
> 0.65	Good
> 0.50	Satisfactory
≤ 0.50	Unsatisfactory

2.4.5 A New Approach for Selecting the Proper Calibration Period

A new approach is proposed to help in identifying the proper period for model calibration. This approach can also test the robustness of the HYPR model in simulating the streamflow of Kronau Marsh, Lanigan, and Moose Jaw watersheds, following the calibration steps in *Models Calibration* section, but with different calibration periods. Robustness in hydrological modelling context means that the model should preserve the same good performance when tested in different watersheds (spatially) and time periods (temporally). The performance of a model depends on the information contained in the calibration period (Arsenault *et al.*, 2018). Thus, an approach was proposed in this study to select the proper calibration period based on clustering analysis such that the calibration period has enough information of all flow types and flow triggering mechanisms to better identify the model parameters. Clustering is typically used to identify the similarities of data in a dataset by partitioning/subgrouping them into different groups. The k means method was used for the clustering analysis in this study.

The clustering analysis was conducted such that the watershed has two different clustering groups representing high flows and low to medium flows, and it was conducted on the different hydrological years (October to September) in the study period. The years were clustered based on each year's total snowfall, total antecedent (previous year's) rainfall, which was used as an indicator of the antecedent moisture conditions, and the maximum annual discharge. A temperature threshold of 0 °C was used to distinguish rainfall and snowfall. The edge points in a cluster are the farthest points from the cluster's centroid and they have higher variations/differences in the data than other points inside the cluster. They have unique behavior in terms of watershed response to the meteorological forcing (streamflow triggering mechanism) and sometimes may represent extreme years/events. Thus, the calibration period was selected such that it includes some points from the outermost points of the cluster (unique and/or extreme years) and some other points inside the cluster. In this way, the calibration period contains both extreme and normal events, and, thus, large hydrologic variability, which maximizes the information content of the calibration period, making it useful for parameter identification (Singh and Bárdossy, 2012; Arsenault *et al.*, 2018). The same length of the simulation period (2002 to 2015) was used, with the first two years being considered as a spin-up period. The objective function (NSE) value for model calibration was calculated for the selected years only while considering the remaining years as a validation period.

2.4.6 Sensitivity and Uncertainty Analysis

Sensitivity analysis was conducted to test the sensitivity of the model to different calibration parameters based on the resulting streamflow and to understand how the model works. A Global Sensitivity Analysis (GSA) was performed on the HYPR model for the 10 watersheds of the QRB using NSE and NSE_{log}, separately, as evaluation criteria. The Variogram Analysis of Response Surfaces (VARS; Razavi and Gupta, 2016) was used as a GSA method in this study. The sensitivity analysis was assessed using 20,000 parameter values/sets generated by the VARS star sampling method based on parameters' range (from Table 2.1). The resulting behavioral streamflow simulations, resulting from using the parameter sets from the VARS algorithm, were used to assess the uncertainty in model output. The behavioral streamflow simulations were identified as streamflow simulations that have NSE $\geq$ 0.5. The model output uncertainty is described by 95 % prediction uncertainty bounds, which were calculated at 2.5 % and 97.5 % of the cumulative distribution function of the output streamflow.

2.4.7 Snow Process Simulation

The calibration process can make hydrological models more flexible to the extent that their behavior is less dependent on their structure, which consequently, affects the accuracy of process representation (Kirchner, 2006). Hence, we compared the Snow Water Equivalent (SWE) simulation of HYPR, as an intermediate process, to the measured SWE values to understand how the model works and to test its predictive validity/reliability in process simulation.

The measured SWE data are available through the Saskatchewan Water Security Agency (WSA) for certain watersheds in the QRB at different times. The number of SWE measurements vary from one to ten different locations for each watershed during different dates based on its size. Almost all measurements were recorded over cropland cover, and over a few locations that were close to each other and were poorly scattered over the watersheds. As a result, most of the measured SWE values are not representative enough of the landscape. Since HYPR is a lumped model and its SWE simulation is a watershed average, we compared the simulated SWE to the observations that were recorded over well-distributed locations within the watershed to represent the average basin conditions. For each date, the SWE values were averaged over the locations of measurements per watershed and were used to assess the HYPR SWE simulation. The HYPR model was calibrated for streamflow only and the snow survey data were not used to calibrate the model.

2.5 Results and Analysis

2.5.1 HBV-light vs HYPR streamflow simulation

Figure 2.3 shows the streamflow simulation of both HBV-light and HYPR models in the calibration and validation periods with the observed streamflow for Kronau Marsh, Lanigan, and Moose Jaw watersheds. The HBV-light model, despite using optimal parameters, still had difficulty in simulating flow during the calibration period, except for Lanigan watershed. In the validation period, the performance of the model deteriorated further, and the model showed significant error in estimating the flow magnitude and timing in all watersheds. A good example is the Lanigan flow estimates from HBV-Light in the summer of 2012 (Figure 2.3). In this case, there was a significant rainfall event, but since the potholes were relatively dry, there was ample storage on the landscape to dampen the hydrograph. Also, the model was sensitive to small storms and responded quickly to them (especially in 2014), which is not the case in the prairies due to the storage impact of the potholes in drier years that delays or completely removes the response of the non-contributing parts of the watershed. The HBV-light model considered the watersheds as traditional watersheds with a traditional rainfall/snowmelt runoff response and without the existence of the pothole complexities and the dynamic non-contributing area. The HBV-light model's simulated flows showed unsatisfactory performance scores in all performance measures (Table 2.4). The model was unable to predict the hydrograph, low flows, peak flows, or the variability of the observed flows.

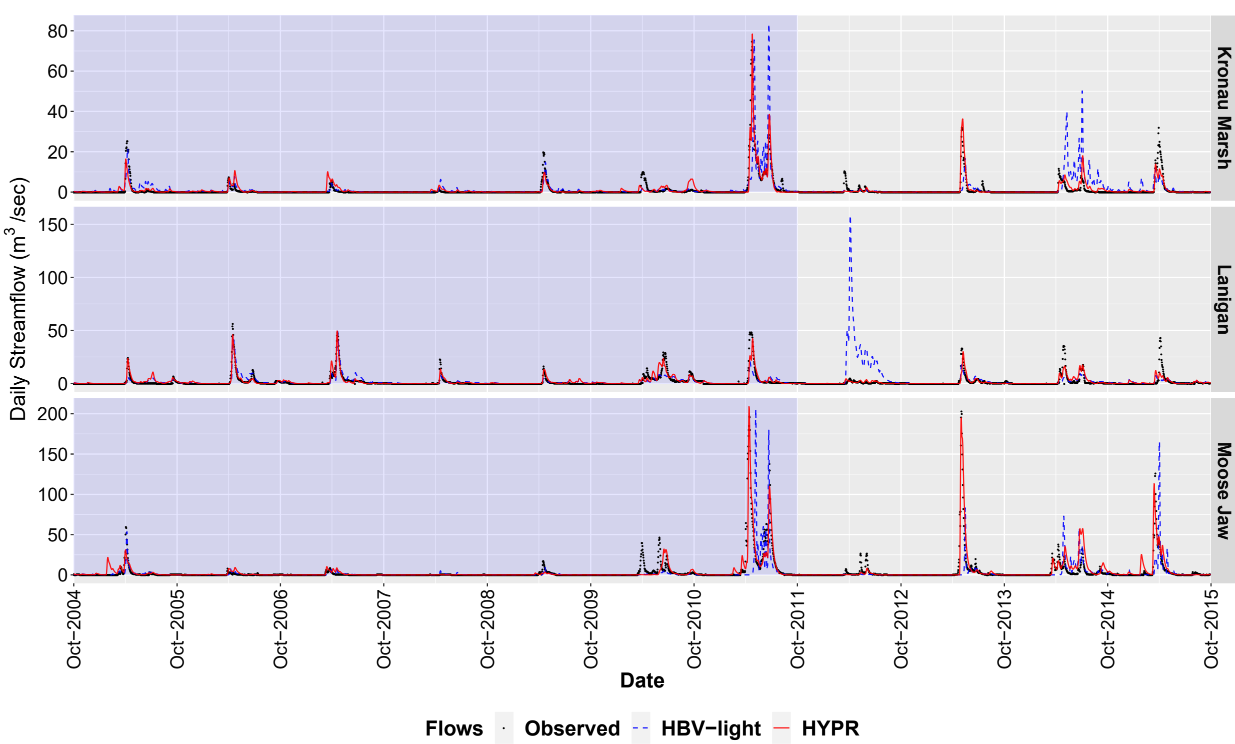

Figure 2.3: Daily streamflow hydrographs of HBV-light and HYPR for Kronau Marsh, Lanigan, and Moose Jaw watersheds. The shaded area represents the calibration period and the remaining period is validation. Each row shows different watershed hydrograph with different y-axis (flow) scale.

For the HYPR model, the modification of the model resulted in an improved streamflow simulation for the three studied watersheds (Figure 2.3). The model was better able to predict the streamflow with respect to the magnitude and timing of peak flows as compared to the HBV-light simulations. HYPR was not sensitive to any rainfall/snowmelt event and responded only to the actual runoff events. In addition, HYPR did not overestimate the low flow period as the case of the HBV-light model. In terms of statistical measures (Table 2.4), HYPR showed good streamflow simulations in both calibration and validation periods with almost NSE of 0.8 and 0.6, respectively, in all watersheds. HYPR also showed very good peak flow prediction, as indicated by NSE_{OT} of almost 0.9 and 0.8 in both the calibration and validation periods, respectively, averaged over all watersheds. The model showed good to satisfactory performance in simulating low flows and in preserving the total runoff volume when looking at the NSE_{log} and PBIAS values (Table 2.4), respectively. The values of AIC and BIC for HYPR were almost one order of magnitude smaller than that of HBV-light (Table 2.4), which concludes that HYPR had good performance because it simulated the conditions of the basin, not because it has more degrees of freedom. Clearly, HYPR was able to simulate the streamflow more effectively, highlighting the essential need for lateral potholes flow controls, such as PDMROF, in this environment.

Table 2.4: Performance measures of daily streamflow for HBV-light and HYPR for the calibration (Cal; 2004 to 2011) and Validation (Val; 2012 to 2015) period.

		NSE		**NSE_{log}**		**NSE_{OT}**		**PBIAS (%)**		**AIC ($x10^4$)**	**BIC ($x10^4$)**	**NSE rating**		**NSE_{OT} rating**	
Watershed	Model	Cal	Val	Cal	Val	Cal	Valid	Cal	Val	Full Period	Full Period	Cal	Val	Cal	Val
Kronau Marsh	HBV-light	0.29	-0.92	0.52	-0.12	0.32	0.07	-18.47	-65.32	1.23	1.24	unsatisfactory	unsatisfactory	unsatisfactory	unsatisfactory
	HYPR	0.84	0.62	0.58	0.66	0.89	0.73	-6.13	-6.22	0.61	0.62	very good	satisfactory	very good	good
Lanigan	HBV-light	0.66	-7.29	0.60	-0.38	0.71	0.41	5.39	-182.83	1.75	1.76	good	unsatisfactory	good	unsatisfactory
	HYPR	0.81	0.54	0.66	0.62	0.89	0.65	-4.73	2.83	0.85	0.86	very good	satisfactory	very good	satisfactory
Moose Jaw	HBV-light	-0.13	-0.11	0.45	0.27	-0.10	-0.01	44.35	36.85	2.26	2.28	unsatisfactory	unsatisfactory	unsatisfactory	unsatisfactory
	HYPR	0.85	0.69	0.59	0.60	0.88	0.82	6.87	-21.15	1.60	1.61	very good	good	very good	very good

2.5.2 HYPR streamflow simulations

In the previous section, HYPR provided improved streamflow simulation as compared to HBV-light in the three tested watersheds. HYPR was validated further on the remaining watersheds of the QRB to test its ability to simulate streamflow of different watersheds of various sizes, conditions, and landscape. The simulated flows agreed with the observed ones in both the calibration and the validation periods for the majority of the watersheds (Figure 2.4). Importantly, the model agreed well with the actual significant peak flood events (e.g., 2011 and 2013) for the majority of the watersheds. In terms of the performance measures (Table 2.5), HYPR showed good hydrograph simulation (NSE) and showed good to very good peak flow simulation (NSE_{OT}). Overall, HYPR showed good to very good performance in the studied watersheds, given the simplicity of this conceptual model. However, the streamflow in Ridge watershed was challenging to simulate and HYPR did not show as good performance in it as the remaining watersheds, especially in the validation period, with an overestimation in the total runoff volume (PBIAS, Table 2.5).

The Ridge watershed-gauging station is located about 0.5 km downstream of a very high embankment (about 8.5 m height) at highway 367. Consequently, this embankment acts as a dam, controlling the outflow of the watershed, and the gauged flow is not the natural response of the watershed (C. Hallborg, WSA, personal communication). This made the simulation to be further challenging and HYPR was unable to simulate the hydrograph, nor the runoff volume as indicated by NSE and PBIAS, respectively. Another possible reason might be issues with precipitation estimates; however, we cannot compare CaPA to ground climate stations, since they are not available within near proximity of the basin.

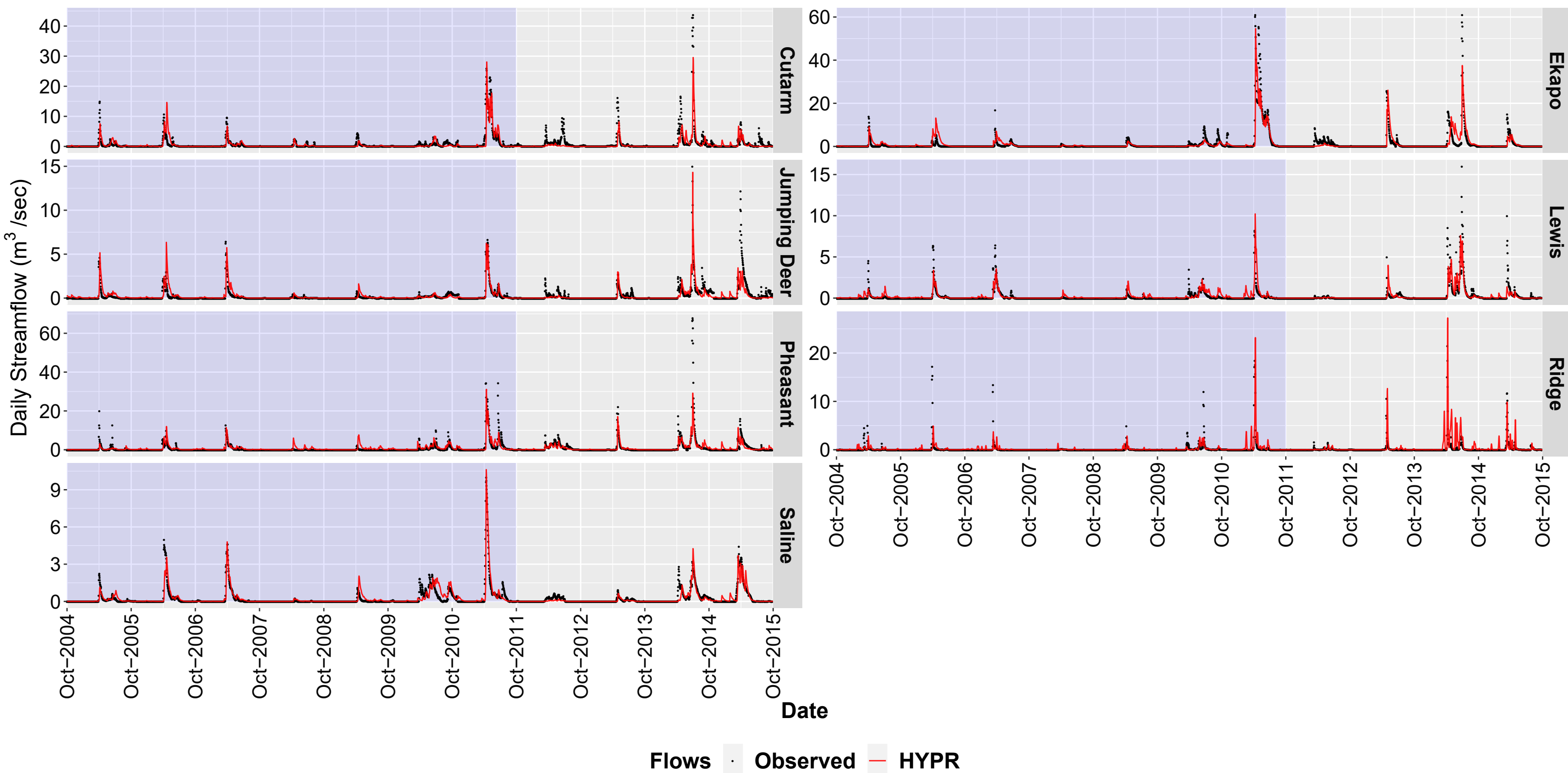

Figure 2.4: Daily streamflow hydrographs of HYPR for the studied watersheds. The shaded area represents the calibration period, and the remaining period is validation. Each subplot shows different watershed hydrograph with different y-axis (flow) scale.

Table 2.5: Performance measures of HYPR daily streamflow for the calibration (Cal; 2004 to 2011) and Validation (Val; 2012 to 2015) period.

	NSE		NSE_{log}		NSE_{OT}		PBIAS (%)		NSE rating		NSEOT rating	
Watershed	Cal	Val	Cal	Val	Cal	Val	Cal	Val	Cal	Val	Cal	Val
Cutarm	0.80	0.65	0.71	0.49	0.86	0.69	6.19	31.54	very good	satisfactory	very good	good
Ekapo	0.82	0.73	0.74	0.70	0.85	0.82	3.37	7.94	very good	good	very good	very good
Jumping Deer	0.75	0.60	0.68	0.62	0.83	0.68	-24.26	34.35	very good	satisfactory	very good	good
Lewis	0.64	0.63	0.54	0.76	0.73	0.68	-32.51	22.26	satisfactory	satisfactory	good	good
Pheasant	0.70	0.59	0.47	0.72	0.79	0.62	-20.06	24.94	good	satisfactory	very good	satisfactory
Ridge	0.56	0.01	0.30	-0.07	0.63	0.41	-10.86	-94.11	satisfactory	unsatisfactory	satisfactory	unsatisfactory
Saline	0.87	0.75	0.80	0.76	0.92	0.81	-4.91	19.03	very good	good	very good	very good

2.5.3 The Proposed Approach for Selecting the Proper Calibration Period

The calibration period was changed to test HYPR's robustness in preserving the same good performance under different calibration scenarios (time periods) and to test the effectiveness of the proposed clustering-based selection criteria of the calibration period. For the first scenario (Figure 2.3), the model was calibrated from 2004 to 2011 and validated from 2012 to 2015. Here, a second calibration scenario was conducted, in which the calibration and validation periods were changed, based on the clustering analysis selection criteria (Figure 2.5), and the resulting streamflow was compared to that of the first scenario for Kronau Marsh, Lanigan, and Moose Jaw watersheds.

Based on the results of the clustering analysis (Figure 2.5), the calibration period was set to 2006 and 2010 to 2014 for Kronau Marsh; whereas it was set to 2006, 2008, and 2010 to 2013 for Lanigan watershed. For Kroanu Marsh watershed, 2006 to 2008 are almost similar (close to each other) in terms of snowfall and antecedent rainfall with low flows, and hence, 2006 was incorporated in the calibration, as it was representative of that period (from 2006 to 2008). The rest of the calibration period are extreme flood (2011) or unique (2010 and 2012 to 2014) years in terms of the three variables used for clustering, as they are on the edge of the cluster (Figure 2.5). For Moose Jaw watershed, the calibration period was set to 2005, 2008, 2010 to 2012, and 2014 (Figure 2.5). We included one year from the high flow cluster group to test the hypothesis that including at least one flooding event in the calibration period, along with the incorporation of years from the other cluster, can have the potential information to properly identify the parameters' values.

For the first scenario, all data points from different clusters were included in the calibration period for the watersheds including the unique/extreme years (Figure 2.5). This gave the model the chance to learn and be trained on different years with different behavior, and thus, the model was successful in simulating the validation period. For the second scenario, although the calibration period length was less than that of the first scenario, the model maintained the same good performance in replicating the overall hydrograph and peak flows when looking at the hydrographs (Figure 2.6) and NSE values (Table 2.6). The selection criteria of the calibration period reached a successful streamflow simulation, proved the robustness of HYPR as it maintained the same good performance as of the first scenario, and sometimes further improved the validation results as in the case of Moose Jaw watershed.

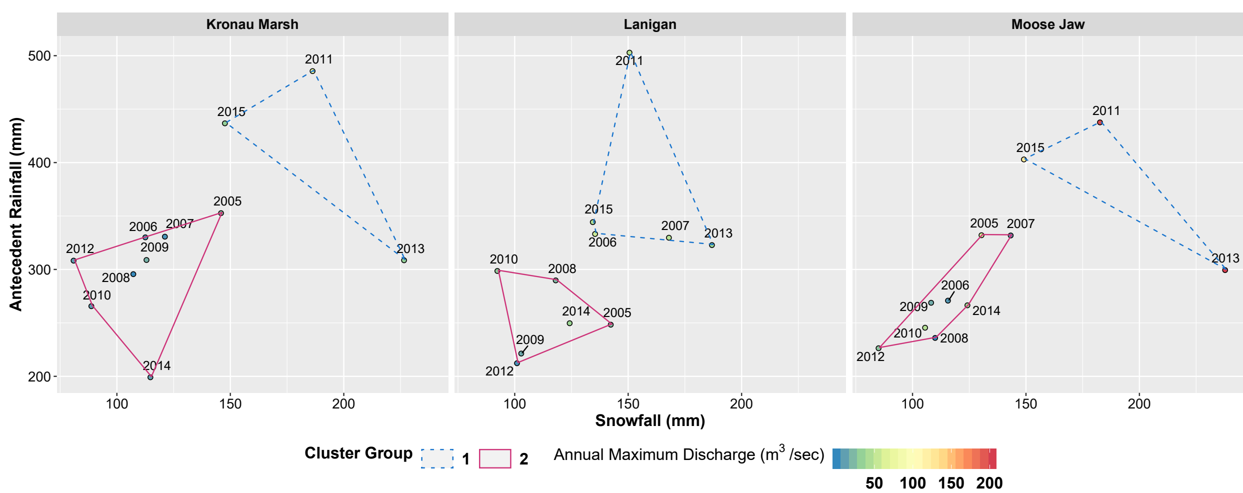

Figure 2.5: Clustering analysis using k means method for the different years in the study period for Kronau Marsh, Lanigan, and Moose Jaw watersheds based on each hydrological year's snowfall, antecedent rainfall, and annual maximum discharge. Cluster group 1 shows high flow years, while the other group shows the low to medium flow years. The cluster analysis was used to help in selecting the proper period for model calibration.

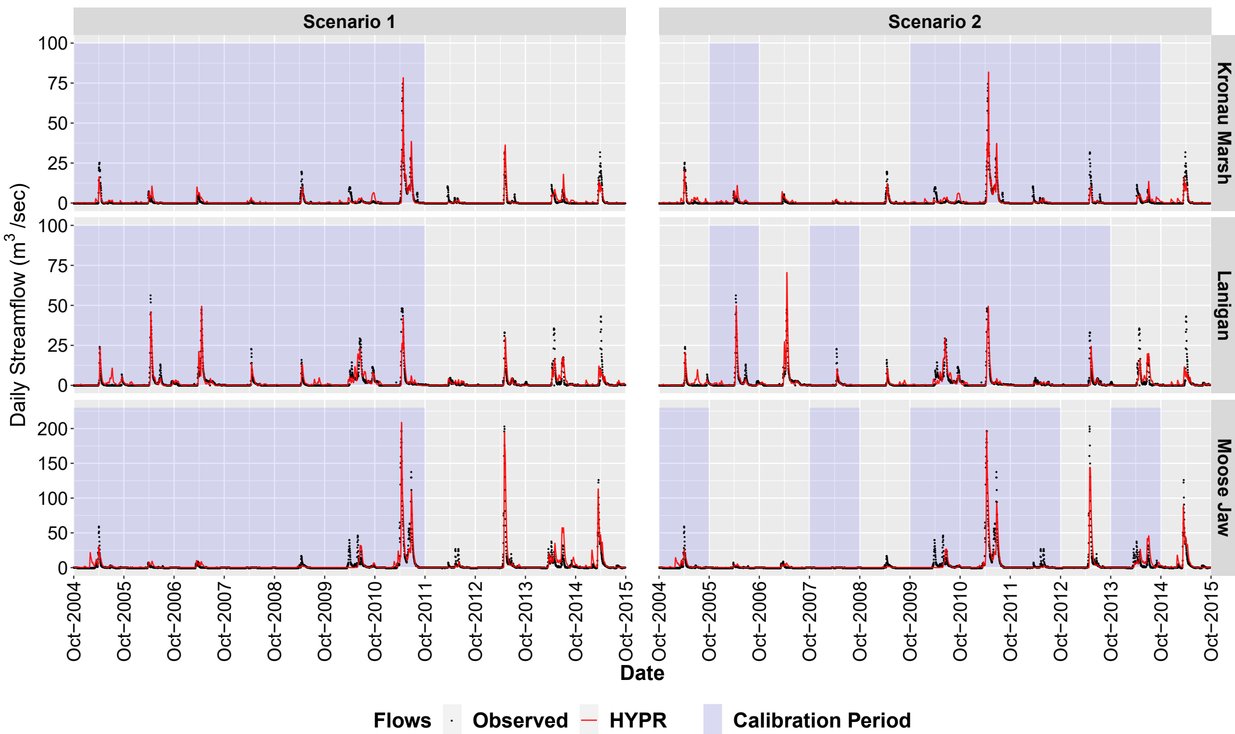

Figure 2.6: HYPR streamflow simulations with the observed ones at the outlet of Kronau Marsh, Lanigan, and Moose Jaw watersheds using different calibration and validation periods. The shaded area represents the calibration period and the remaining period is validation.

Table 2.6: NSE values of the streamflow simulations in Figure 2.6 for the different calibration and validation periods (Scenarios) for the selected watersheds.

Watershed	**Calibration**	**Validation**	**Scenario**
Kronau Marsh	0.84	0.62	Scenario 1
	0.89	0.63	Scenario 2
Lanigan	0.81	0.54	Scenario 1
	0.83	0.53	Scenario 2
Moose Jaw	0.85	0.69	Scenario 1
	0.82	0.85	Scenario 2

2.5.4 Sensitivity and Uncertainty Analysis

When using NSE to evaluate the model parameter sensitivity (Figure 2.7), HYPR showed sensitivity to some of the parameters that control the representation of different hydrological processes, and more importantly to pothole and snow parameters as they are the most important processes controlling the streamflow, especially peak flow, generation in the prairies. When using NSE_{log} to evaluate the parameter sensitivity (Figure 2.7), the model showed sensitivity to the soil, evapotranspiration, and pothole parameters. These parameters are responsible for water storage in soil, potholes, and evapotranspiration, which limit the amount of water reaching the outlet. This is true about the prairies in the low flow period, especially summer time. It also showed some sensitivity to the parameter controlling the interflow (K1). This shows that HYPR simulates the prairies low flow periods (summer time) with high water holding capacity of the soil (BETA), high values of pothole evaporation (MAXPA, PWR) and evapotranspiration (LP), and interflow (K1). Therefore, HYPR is working as expected in generating both peak and low flows.

Figure 2.8 shows the 95 % prediction uncertainty bounds of the HYPR model for the studied watersheds. The Ridge watershed does not have uncertainty bounds because all the resulting streamflow simulations were non-behavioral. The 95 % uncertainty bounds agreed with the observed flows for the remaining watersheds with narrow uncertainty bounds. More than 92 % of the observed flows for the entire study period were within the uncertainty bounds.

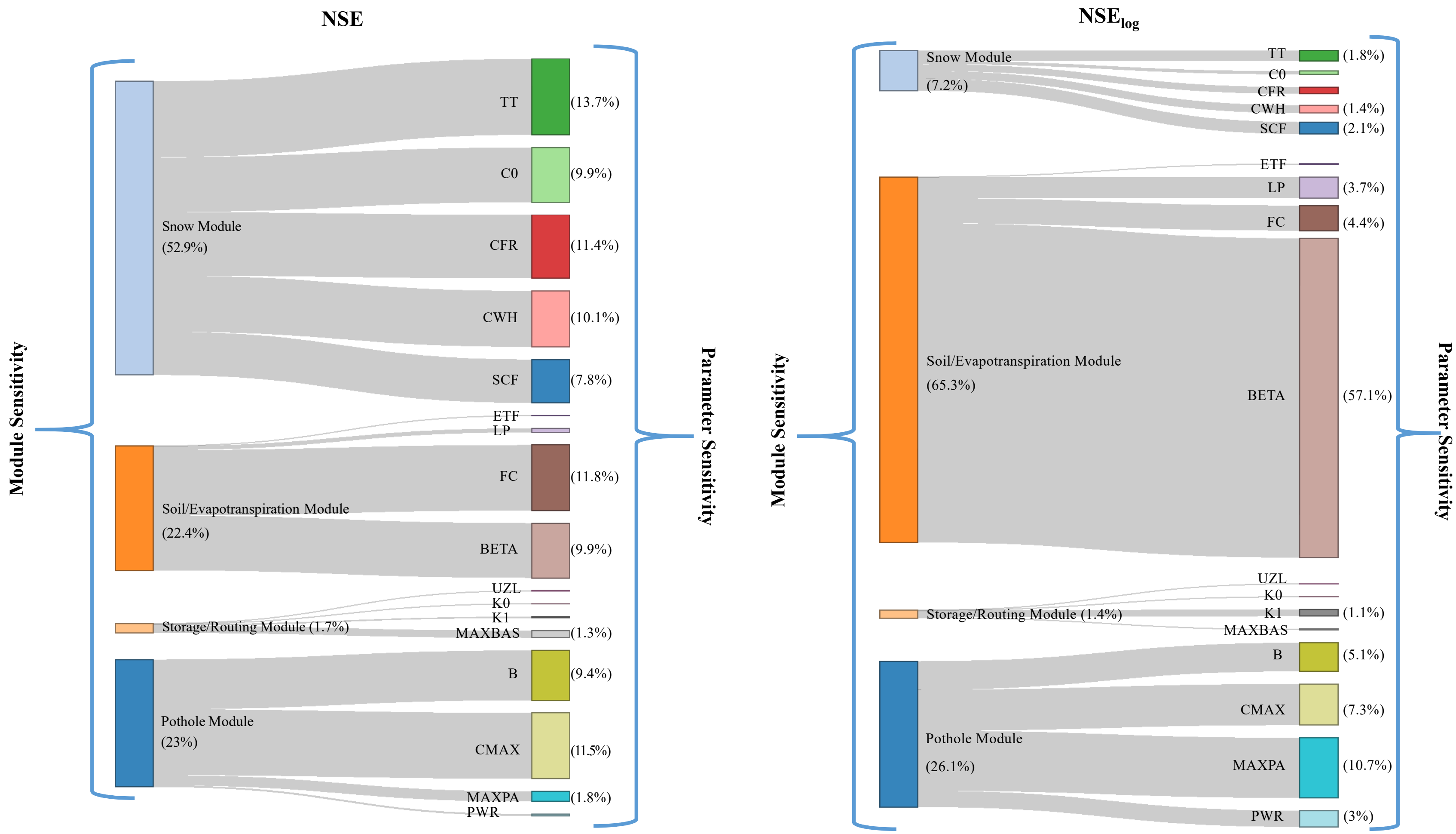

Figure 2.7: Percent of parameter sensitivity for HYPR, averaged over the watersheds of the QRB, using two different evaluation criteria. The parameter sensitivity of individual watersheds is more or less the same as the average values.

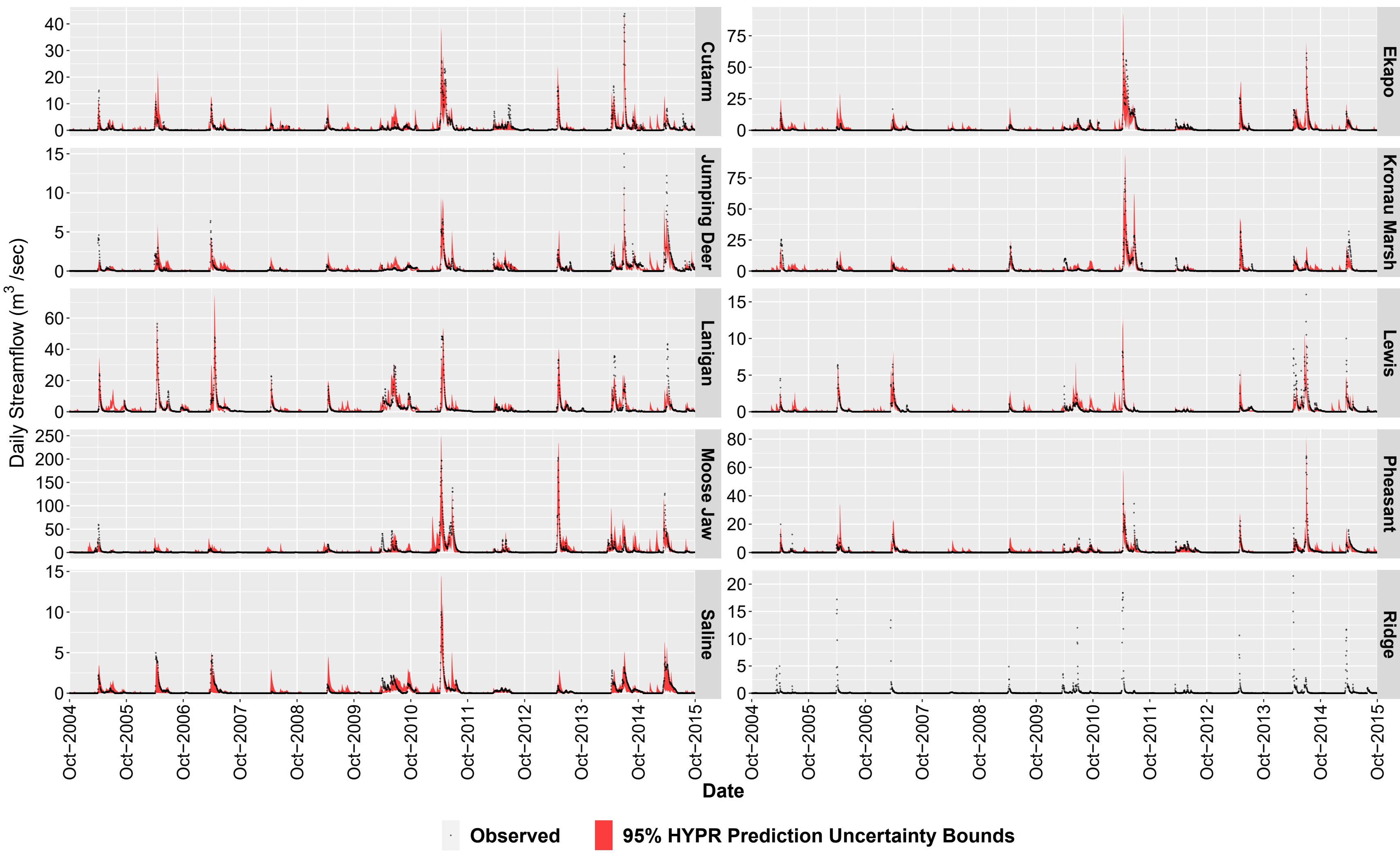

Figure 2.8: 95% prediction uncertainty bounds for HYPR simulations with the observed flows for the studied sub-basins. Prediction uncertainty bounds are unavailable for the Ridge watershed as all simulations were non-behavioral.

2.6 Discussion

The clustering-based selection criteria of the calibration period showed potential for improving the performance of HYPR in streamflow simulation (Figure 2.6 &Table 2.6). Incorporating one flooding event in the calibration period (scenario 1 in all watersheds, Figure 2.4, and scenario 2 in Moose Jaw, Figure 2.6) contributed toward the success of the streamflow simulation, which shows the importance of incorporating at least one peak flow in the calibration as peak flows have a considerable amount of information that is useful for parameter identification. The clustering analysis can also be used as an indication/predictor on when the model may fail in past/future years. If a future/past year is unique in nature, based on the clustering analysis (a data point that lies outside the clusters, or that is not close to any other data point), it is likely that the model may fail in simulating that year. Thus, it is recommended that such a year should be included in the calibration period to reach a successful streamflow simulation.

The use of different objective functions (NSE and NSE_{log}) as evaluation criteria changed the sensitivity of model parameters (Figure 2.7). This was widely validated in the literature for conceptual models (e.g., Lamb, 1999; Gupta *et al.*, 2009; Booij and Krol, 2010; Orth *et al.*, 2015). Consequently, this can affect the parameter identification during the model calibration. In this study, we used the NSE to simulate the hydrograph and peak flows. HYPR showed very good to good streamflow and peak flow simulation, whereas it showed good to satisfactory simulation of the low flows. If the low flows are more important than peak flows (i.e., during droughts), the use of an objective function that focuses on low flows (such as NSE_{log}) will be beneficial in improving the low flow simulation at the cost of affecting the simulation of the peak flows.

Analyzing the snow processes' representation of the HYPR model is beneficial in understanding the accuracy of process simulation and can give an indication on the validity of the model. Processes' representation in conceptual models is simple; however, HYPR showed potential for simulating the SWE with reasonable errors (Table 2.7). Calibrating HYPR for the observed values of the internal variables can further improve the processes representation and model performance. This can be achieved at the cost of affecting the performance of the calibration period as more degrees of freedom are removed due to further constraining the model with an additional calibration target. The reasonable error in the SWE proved that HYPR has a reasonably good representation of internal processes and hence, is dependent on its structure for the streamflow simulation and was not over-parameterized.

Table 2.7: Error in SWE for dates with SWE observations that were well scattered/distributed over the watershed.

Watershed	Date	SWE error (%)	Number of SWE measurements locations in the watershed
Kronau Marsh	2013-03-31	9.67	6
	2014-03-24	-9.84	6
Moose Jaw	2013-03-31	14.22	10

2.7 Conclusions

In this study, the traditional HBV-light model was modified by adding a pothole-modelling component to work in the prairies, resulting in a new conceptual HYdrological model for Prairie Region (HYPR). HYPR provided improved streamflow simulation as compared to HBV-light when tested on different watersheds within the Qu'Appelle River Basin in Saskatchewan, Canada. Some of the main findings of this study are as follows: (1) it is important to incorporate the pothole complexities in hydrological models for successful streamflow simulation in the prairies, (2) the proposed HYPR model is robust and shows potential for simulating the complex prairie streamflow, especially peak flows with narrow uncertainty bounds, (3) HYPR can prove that conceptual models have the potential for working in the complex prairies for streamflow simulation because it simulates the conditions of the basin, not because it has more degrees of freedom resulting from the incorporation of the PDMROF algorithm, (4) HYPR shows potential for simulating the internal processes when comparing the simulated SWE to the observed data, (5) the proposed clustering-based selection criteria show potential for identifying the proper period for model calibration. The outermost points in clusters represent unique/extreme years and at least half of them, along with at least one flooding event, should be included in the calibration period to contribute towards the success of streamflow simulation as they contain considerable information to identify model parameters, and (6) the selection of the objective function for model calibration has a significant effect on changing the sensitivity of the model parameters and outputs. Hence, the selection of the objective function should be based on the application of the model.

The results of this study are promising, and the developed methodologies show potential for solving the streamflow simulation problem in the prairies. However, more investigation is needed to further understand the strengths and limitations of HYPR. Since HYPR is a lumped model, the spatial information of the internal variables are not available. Some of HYPR's parameters represent a group of watershed properties and hence, it might be difficult to map their values to actual measurements. Although a low optimization budget was conducted in this study (with 2,000 evaluations) using the DDS algorithm for model calibration, HYPR performed very well in streamflow simulation over the studied watersheds for both the calibration and validation periods. For future studies and due to HYPR's computational efficiency, a higher optimization budget can be conducted with more evaluations along with the use of other stochastic approaches (e.g., adaptive simulated annealing (ASA), covariance matrix adaptation evolution strategy (CMAES); Arsenault *et al.*, 2014), which can further improve the streamflow simulation of the model.

HYPR can be seen as the engineering solution to the streamflow simulation problem in the prairies and should perform better in forecasting mode. HYPR is a computationally and data inexpensive model as it takes less than 30 minutes to setup and calibrate, and less than one second to simulate the watershed with only two forcing variables and very limited physiographic information. Consequently, HYPR can be used operationally, by water management organizations, for real-time flood forecasting. Further efforts are needed to investigate the transferability of HYPR's parameters (or even specific ones) from one basin to another and compare the performance of the HYPR model with physically based models in the future.

2.8 Data Availability Statement

- The observed snow water equivalent measurements used during the study were provided by a third party (Saskatchewan Water Security Agency). Direct requests for these materials may be made to the provider.
- HYPR's code is available from the corresponding author upon reasonable request.

2.9 Acknowledgment

The financial support of the Natural Sciences and Engineering Research Council of Canada (NSERC) strategic network through the Canadian FloodNet research network is acknowledged

(Grant number: NETGP451456-13). The funding of the Department of Civil, Geological and Environmental Engineering, University of Saskatchewan devolved scholarship is appreciated. The authors acknowledge the Saskatchewan Water Security Agency for providing snow water equivalent measurements.

2.10 References

Akinremi OO, McGinn SM, Cutforth HW. 1999. Precipitation Trends on the Canadian Prairies. Journal of Climate 12 (10): 2996 DOI: 10.1175/1520-0442(1999)012<2996:PTOTCP>2.0.CO;2

Anteau MJ, Wiltermuth MT, van der Burg MP, Pearse AT. 2016. Prerequisites for Understanding Climate-Change Impacts on Northern Prairie Wetlands. Wetlands 36: 299–307 DOI: 10.1007/s13157-016-0811-2

Arsenault R, Brissette F, Martel JL. 2018. The hazards of split-sample validation in hydrological model calibration. Journal of Hydrology 566 (May): 346–362 DOI: 10.1016/j.jhydrol.2018.09.027

Arsenault R, Poulin A, Côté P, Brissette F. 2014. Comparison of Stochastic Optimization Algorithms in Hydrological Model Calibration. Journal of Hydrologic Engineering 19 (7): 1374–1384 DOI: 10.1061/(ASCE)HE.1943-5584.0000938

Beven K. 2001. How far can we go in distributed hydrological modelling? Hydrology and Earth System Sciences 5 (1): 1–12 DOI: 10.5194/hess-5-1-2001

Bonsal BR, Aider R, Gachon P, Lapp S. 2013. An assessment of Canadian prairie drought: past, present, and future. Climate Dynamics 41 (2): 501–516 DOI: 10.1007/s00382-012-1422-0

Booij MJ. 2003. Determination and integration of appropriate spatial scales for river basin modelling. Hydrological Processes 17 (13): 2581–2598 DOI: 10.1002/hyp.1268

Booij MJ, Krol MS. 2010. Balance between calibration objectives in a conceptual hydrological model. Hydrological Sciences Journal 55 (6): 1017–1032 DOI: 10.1080/02626667.2010.505892

Bourdin DR, Fleming SW, Stull RB. 2012. Streamflow modelling: A primer on applications, approaches and challenges. Atmosphere - Ocean 50 (4): 507–536 DOI: 10.1080/07055900.2012.734276

Brimelow J, Stewart R, Hanesiak J, Kochtubajda B, Szeto K, Bonsal B. 2014. Characterization and assessment of the devastating natural hazards across the Canadian Prairie Provinces from 2009 to 2011. Natural Hazards 73 (2): 761–785 DOI: 10.1007/s11069-014-1107-6

Chu X, Yang J, Chi Y, Zhang J. 2013. Dynamic puddle delineation and modeling of puddle-to-puddle filling-spilling-merging-splitting overland flow processes. Water Resources Research 49 (6): 3825–3829 DOI: 10.1002/wrcr.20286

Fang X, Pomeroy JW, Westbrook CJ, Guo X, Minke AG, Brown T. 2010. Prediction of snowmelt derived streamflow in a wetland dominated prairie basin. Hydrology and Earth System Sciences 14 (6): 991–1006 DOI: 10.5194/hess-14-991-2010

Godwin RB, Martin FRJ. 1975. Calculation of gross and effective drainage areas for the Prairie Provinces. In Canadian Hydrology Symposium - 1975 Proceedings, 11-14 August 1975, Winnipeg, Manitoba.Associate Committee on Hydrology, National Research Council of Canada; 219–223.

Gray DM, Landine PG. 1988. An energy-budget snowmelt model for the Canadian Prairies. Canadian Journal of Earth Sciences 25 (8): 1292–1303 DOI: 10.1139/e88-124

Gray DM, Pomeroy JW, Granger RJ. 1989. Modelling Snow Transport, Snowmelt and Meltwater Infiltration in Open, Northern Regions. Northern Lakes and Rivers: 8–22

Gupta H V., Kling H, Yilmaz KK, Martinez GF. 2009. Decomposition of the mean squared error and NSE performance criteria: Implications for improving hydrological modelling. Journal of Hydrology 377 (1–2): 80–91 DOI: 10.1016/j.jhydrol.2009.08.003

Hayashi M, Van Der Kamp G. 2000. Simple equations to represent the volume-area-depth relations of shallow wetlands in small topographic depressions. Journal of Hydrology 237 (1–2): 74–85 DOI: 10.1016/S0022-1694(00)00300-0

Hayashi M, Van Der Kamp G, Rudolph DL. 1998. Water and solute transfer between a prairie wetland and adjacent uplands, 2. Chloride cycle. Journal of Hydrology 207 (1–2): 56–67 DOI: 10.1016/S0022-1694(98)00099-7

Hayashi M, Van Der Kamp G, Schmidt R. 2003. Focused infiltration of snowmelt water in partially frozen soil under small depressions. Journal of Hydrology 270 (3–4): 214–229 DOI: 10.1016/S0022-1694(02)00287-1

Hossain K. 2018. Towards a Systems Modelling Approach for a Large-Scale Canadian Prairie Watershed. Master’s Thesis. Dept. of Civil, Geological and Environmental Engineering, University of Saskatchewan.

Hrachowitz M, Clark M. 2017. HESS Opinions: The complementary merits of top-down and bottom-up modelling philosophies in hydrology. Hydrology and Earth System Sciences Discussions (January): 1–22 DOI: 10.5194/hess-2017-36

Jakeman AJ, Hornberger GM. 1993. How much complexity is warranted in a rainfall-runoff model? Water Resources Research 29 (8): 2637–2649 DOI: 10.1029/93WR00877

van der Kamp G, Hayashi M. 2009. Groundwater-wetland ecosystem interaction in the semiarid glaciated plains of North America. Hydrogeology Journal 17 (1): 203–214 DOI: 10.1007/s10040-008-0367-1

Kirchner JW. 2006. Getting the right answers for the right reasons: Linking measurements, analyses, and models to advance the science of hydrology. Water Resources Research 42 (3): 1–5 DOI: 10.1029/2005WR004362

Kollat JB, Reed PM, Wagener T. 2012. When are multiobjective calibration trade-offs in hydrologic models meaningful? Water Resources Research 48 (3): 1–19 DOI: 10.1029/2011WR011534

Kuczera G, Mroczkowski M. 1998. Assessment of hydrologic parameter uncertainty and the worth of multiresponse data. Water Resources Research 34 (6): 1481–1489 DOI: 10.1029/98WR00496

Lamb R. 1999. Calibration of a conceptual rainfall-runoff model for flood frequency estimation by continuous simulation. Water Resources Research 35 (10): 3103–3114 DOI: 10.1029/1999WR900119

Lespinas F, Fortin V, Roy G, Rasmussen P, Stadnyk T. 2015. Performance Evaluation of the Canadian Precipitation Analysis (CaPA). Journal of Hydrometeorology 16 (5): 2045–2064 DOI: 10.1175/jhm-d-14-0191.1

Te Linde AH, Aerts JCJH, Hurkmans RTWL, Eberle M. 2008. Comparing model performance of two rainfall-runoff models in the Rhine basin using different atmospheric forcing data sets. Hydrology and Earth System Sciences 12 (3): 943–957 DOI: 10.5194/hess-12-943-2008

Lindström G, Johansson B, Persson M, Gardelin M, Bergström S. 1997. Development and test of the distributed HBV-96 hydrological model. Journal of Hydrology 201 (1–4): 272–288 DOI: 10.1016/S0022-1694(97)00041-3

Mailhot J, Bélair S, Lefaivre L, Bilodeau B, Desgagné M, Girard C, Glazer A, Leduc A, Méthot A, Patoine A, et al. 2006. The 15-km version of the Canadian regional forecast system. Atmosphere-Ocean 44 (2): 133–149 DOI: 10.3137/ao.440202

Martin FRJ. 2001. Addendum No. 8 to Hydrology Report #104, Agriculture and Agri-Food Canada PFRA Technical Service: Regina, Saskatchewan, 109 pp. PFRA Hydrology Division, 1983, The Determination of Gross and Effective Drainage areas in the Prairie Provinces, Hydrology Repo.

Mekonnen BA, Mazurek KA, Putz G. 2016. Incorporating landscape depression heterogeneity into the Soil and Water Assessment Tool (SWAT) using a probability distribution. Hydrological Processes 30 (13): 2373–2389 DOI: 10.1002/hyp.10800

Mekonnen BA, Nazemi A, Mazurek KA, Elshorbagy A, Putz G. 2015. Hybrid modelling approach to prairie hydrology: fusing data-driven and process-based hydrological models. Hydrological Sciences Journal 60 (9): 1473–1489 DOI: 10.1080/02626667.2014.935778

Mekonnen MA, Wheater HS, Ireson AM, Spence C, Davison B, Pietroniro A. 2014. Towards an improved land surface scheme for prairie landscapes. Journal of Hydrology 511: 105–116 DOI: 10.1016/j.jhydrol.2014.01.020

Moriasi DN, Arnold JG, Van Liew MW, Bingner RL, Harmel RD, Veith TL, Binger RL, Harmel RD, Veith TL. 2007. Model evaluation guidelines for systematic quantification of accuracy in watershed simulations. Transactions of the ASABE v. 50 (3): 885-0–2007 v.50 no.3 DOI: 10.13031/2013.23153

Muhammad A, Evenson GR, Stadnyk TA, Boluwade A, Jha SK, Coulibaly P. 2019. Impact of model structure on the accuracy of hydrological modeling of a Canadian Prairie watershed. Journal of Hydrology: Regional Studies 21 (December 2018): 40–56 DOI: 10.1016/j.ejrh.2018.11.005

Nash JE, Sutcliffe J V. 1970. River flow forecasting through conceptual models part I - A discussion of principles. Journal of Hydrology 10 (3): 282–290 DOI: 10.1016/0022-1694(70)90255-6

Orth R, Staudinger M, Seneviratne SI, Seibert J, Zappa M. 2015. Does model performance improve with complexity? A case study with three hydrological models. Journal of Hydrology 523: 147–159 DOI: 10.1016/j.jhydrol.2015.01.044

Pokhrel P, Gupta H V. 2011. On the ability to infer spatial catchment variability using streamflow hydrographs. Water Resources Research 47 (8) DOI: 10.1029/2010WR009873

Pomeroy JW, Gray DM, Landine PG. 1993. The Prairie Blowing Snow Model: characteristics, validation, operation. Journal of Hydrology 144 (1–4): 165–192 DOI: 10.1016/0022-1694(93)90171-5

Ponce VM, Hawkins RH. 1996. Runoff Curve Number: Has It Reached Maturity? Journal of Hydrologic Engineering 1 (1): 11–19 DOI: 10.1061/(ASCE)1084-0699(1996)1:1(11)

Razavi S, Gupta H V. 2016. A new framework for comprehensive, robust, and efficient global sensitivity analysis:2. Application. Water Resources Research 52: 440–455 DOI: 10.1002/2015WR017558.A

Reed S, Koren V, Smith M, Zhang Z, Moreda F, Seo D-J, DMIP Participants A. 2004. Overall distributed model intercomparison project results. Journal of Hydrology 298 (1–4): 27–60 DOI: 10.1016/J.JHYDROL.2004.03.031

Refsgaard JC. 1996. Terminology, Modelling Protocol And Classification of Hydrological Model Codes, Chapter 2 in Distributed Hydrological Modelling., Abbott MB, , Refsgaard JC (eds).Springer Netherlands: Dordrecht; 17–39. DOI: 10.1007/978-94-009-0257-2_2

Reggiani P, Schellekens J. 2003. Modelling of hydrological responses: the representative elementary watershed approach as an alternative blueprint for watershed modelling. Hydrological Processes 17 (18): 3785–3789 DOI: 10.1002/hyp.5167

Savenije HHG, Hrachowitz M. 2017. HESS Opinions ‘catchments as meta-organisms - A new blueprint for hydrological modelling’. Hydrology and Earth System Sciences 21 (2): 1107–1116 DOI: 10.5194/hess-21-1107-2017

Seibert J. 1999. Conceptual runoff models -fiction or representation of reality? Acta Univ. Ups., Comprehensive Summaries of Uppsala Dissertations from the Faculty of Science and Technology.

Seibert J. 2005. HBV light version 2, User's manual, Uppsala University, Department of Earth Sciences, Hydrology

Seibert J, Vis MJP. 2012. Teaching hydrological modeling with a user-friendly catchment-runoff-model software package. Hydrology and Earth System Sciences 16 (9): 3315–3325 DOI: 10.5194/hess-16-3315-2012

Shaw DA, Vanderkamp G, Conly FM, Pietroniro A, Martz L. 2012. The Fill-Spill Hydrology of Prairie Wetland Complexes during Drought and Deluge. Hydrological Processes 26 (20): 3147–3156 DOI: 10.1002/hyp.8390

Shook KR, Pomeroy JW. 2011. Memory effects of depressional storage in Northern Prairie hydrology. Hydrological Processes 25 (25): 3890–3898 DOI: 10.1002/hyp.8381

Singh SK, Bárdossy A. 2012. Calibration of hydrological models on hydrologically unusual events. Advances in Water Resources 38: 81–91 DOI: 10.1016/j.advwatres.2011.12.006

Smith MB, Koren V, Zhang Z, Zhang Y, Reed SM, Cui Z, Moreda F, Cosgrove BA, Mizukami N, Anderson EA. 2012. Results of the DMIP 2 Oklahoma experiments. Journal of Hydrology 418–419: 17–48 DOI: 10.1016/j.jhydrol.2011.08.056

Tolson BA, Shoemaker CA. 2007. Dynamically dimensioned search algorithm for computationally efficient watershed model calibration. Water Resources Research 43 (1): 1–16 DOI: 10.1029/2005WR004723

Uhlenbrook S. 2003. An empirical approach for delineating spatial units with the same dominating runoff generation processes. Physics and Chemistry of the Earth, Parts A/B/C 28 (6–7): 297–303 DOI: 10.1016/S1474-7065(03)00041-X

Winter TC. 1989. Hydrologic studies of potholes in the northern prairies. (Ames, ed.). Northern Prairie Wetlands. Iowa: Iowa State University Press.

Zhang B, Schwartz FW, Liu G. 2009. Systematics in the size structure of prairie pothole lakes through drought and deluge. Water Resources Research 45 (4) DOI: 10.1029/2008WR006878

Chapter 3 A Novel Model for Storage Dynamics Simulation and Inundation Mapping in The Prairies

This chapter is a slightly modified version of the published article (Ahmed *et al.*, 2020b), modified to make it consistent with the format and body of the thesis. This chapter is the final accepted draft of the paper prior to copyediting or other production activities by the journal.

Citation: Ahmed MI, Elshorbagy A, Pietroniro A. 2020b. A novel model for storage dynamics simulation and inundation mapping in the prairies. Environmental Modelling & Software 133 (August): 104850 DOI: 10.1016/j.envsoft.2020.104850. The permission of reproduction is presented in Appendix A.2.

Authors Contributions and The Contribution of This Chapter to The Overall Study

The following are the contributions from the different authors of this (chapter) published manuscript. M. I. Ahmed contributed to the conceptualization, methodology, software, validation, formal analysis, investigation, data curation, writing - original draft, and visualization. A. Elshorbagy contributed to the conceptualization, methodology, writing - review & editing, supervision, and funding acquisition. A. Pietroniro contributed to the conceptualization, writing - review & editing, and supervision.

This chapter fills an important gap in flood mapping and storage dynamics simulation of complex prairie landscape by proposing the Prairie Region Inundation MApping (PRIMA) model as a hydraulic routing model. This model can be used to simulate the complexities of the prairie depressions and route the water over prairie watersheds. PRIMA addresses the second objective of this thesis and contributes to solving the problem of inundation mapping over the prairies and it is useful in flood risk assessment and landuse planning.

3.1 Abstract

The Canadian prairies are dominated by numerous depressions, which can modify the lateral transfer of water to prairie streams. Few studies were conducted to simulate the pothole dynamics using their actual spatial distributions. This study proposes a computationally efficient Prairie Region Inundation MApping (PRIMA) model as a hydrologic routing model, for a more accurate and comprehensive storage dynamics simulation and inundation mapping in the prairies. PRIMA shows potential for simulating the potholes' extents when comparing its results with

remote sensing data of pothole areas with an accuracy of 85% averaged over two prairie basins in Saskatchewan, Canada. PRIMA is three ~ eight times as computationally efficient as the recently developed Wetland DEM Ponding Model (WDPM). Due to its computational efficiency and ability to provide a good simulation of inundation extents, PRIMA shows strengths as a possible tool for pothole inundation mapping and storage dynamics simulations.

3.2 Graphical abstract

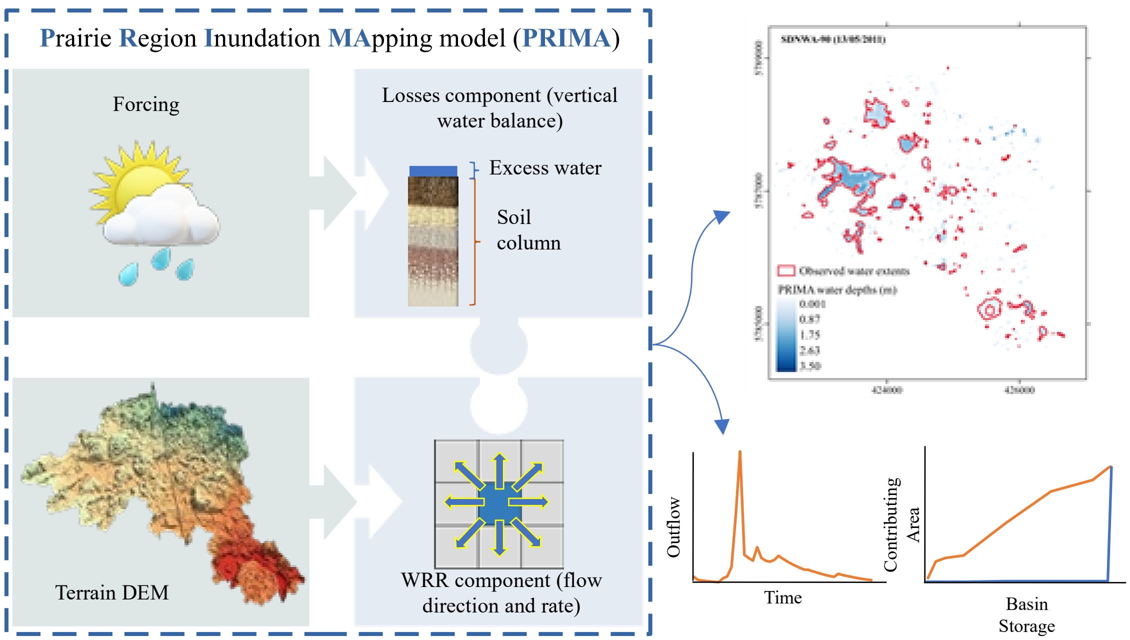

3.3 Introduction

The North American prairies are characterized by numerous depressions (Zhang *et al.*, 2009; Anteau *et al.*, 2016) known as wetlands, sloughs, prairie potholes, puddles, Geographically Isolated Wetlands (GIWs), and dugouts. Due to the existence of these potholes, the runoff production in prairies follows a “fill and spill” mechanism (Shaw *et al.*, 2012), wherein, each pothole contributes flow to downstream potholes after being filled. Therefore, the majority of the prairies are designated as being non-contributing, wherein the surface water runs off into isolated or internally drained basins. The derivation of the non-contributing area map over the prairies was quite subjective and was derived from the visual interpretation of topographic contour maps (Shaw *et al.*, 2013). More details on the non-contributing area map and its derivation are provided in Appendix B, Section B.1.

Potholes can be connected by surface or subsurface flow of water; however, this connection differs dramatically in length and time. The subsurface connection between potholes is slow and can improve the quality of water in the basin, whereas surface connection is fast and limited to significant precipitation events (Ameli and Creed, 2017). Simulating the hydrological behavior of pothole-dominated landscapes is challenging because of the difficulty in characterizing the fill and spill mechanism, which leads to a hysteretic relationship between the basin storage and the contributing area (Shook and Pomeroy, 2011). Thus, the prairies are often referred to as the graveyard of hydrological models.

The prairie potholes complexities can be simulated using conceptual approaches (M. Mekonnen *et al.*, 2014) or satellite (DEM/imageries)-based approaches (Shook and Pomeroy, 2011; Shaw *et al.*, 2012, 2013; Chu *et al.*, 2013; Shook *et al.*, 2013; Muhammad *et al.*, 2019). M. Mekonnen *et al.* (2014) introduced the conceptual PDMROF (Probability Distribution Model based RunOFf generation) approach, which assumes that runoff is a function of the basin storage capacity. In PDMROF, the capacity of different potholes in the basin is assumed to follows a Pareto distribution and the runoff from potholes is calculated by integrating the probability density function. The PDMROF concept showed potential to simulate the prairie streamflow dynamics when implemented into different models such as MESH (M. Mekonnen *et al.*, 2014) and HBV (Ahmed *et al.*, 2020a). However, as a conceptual approximation, the PDMROF cannot represent the spatial extents of pothole water storage, and it might be difficult to map its parameters to field measurements.

Land cover data classified from satellite imageries can be used to identify the potholes (Evenson *et al.*, 2016; Muhammad *et al.*, 2019). Then, each of the identified potholes can be simulated using a separate reservoir that contributes surface flow to the downstream area after exceeding its maximum capacity. This concept of representing potholes as separate reservoirs was used in the conceptual Pothole Cascading Model (PCM; Shook *et al.*, 2013). In PCM, the properties of the potholes are obtained from DEMs and a small number of potholes is used to represent all potholes in the basin. The methodologies that use separate reservoirs to represent the potholes do not represent the fill-merge-split processes of the potholes and some of them may not represent the spatial distribution of water on the landscape.

DEMs can be used to delineate depressions in the basin. For example, the Puddle Delineation (PD) algorithm (Chu *et al.*, 2010) was proposed to delineate the landscape, and it differentiates the landscape into pothole and non-pothole areas. The topographic characteristics of the potholes (cascading order, surface area, and storage) and flow direction for the non-pothole area are obtained from DEMs. The output of the PD algorithm can be used by hydrologic models to route flows and simulate the fill-spill mechanism of the prairies (e.g., Puddle-to-Puddle (P2P) model; Chu *et al*., 2013 and SWAT; Nasab *et al*., 2017).

The Wetland DEM Ponding Model (WDPM) is a DEM-based model that distributes water on the landscape (Shook and Pomeroy, 2011; Shook *et al.*, 2013). WDPM was the first explicit method able to simulate the spatial distribution of water on the prairies and it was used to simulate the contributing area. However, WDPM was found to be computationally expensive, requiring thousands of iterations to reach the steady-state solution (converge), despite not using conventional flow equations to transfer water. DEM-based hydraulic models, such as MIKE SHE (DHI, 1998), and the recently developed HEC-RAS model (Hydrologic Engineering Center, 2016) could be used to simulate the fill and spill phenomena in the prairies. However, these models use the Saint-Venant equation to simulate the movement of water, requiring numerical solutions of the differential equations, which is computationally expensive. There is a need for a computationally efficient model that can simulate the pothole storage dynamics using their actual spatial distributions. This type of model could be easily adapted to simulate the impact of the potholes on the system response in prairie basins, and for inundation mapping and/or flood risk assessments in the prairie pothole region.

The main objective of this study is to develop a novel, computationally efficient Prairie Region Inundation MApping (PRIMA) model, and test its applicability, as a fully distributed simplified hydrological routing model to simulate the spatiotemporal surface water movement and storage dynamics over the landscape. PRIMA is based on the Cellular Automata (CA; Wolfram, 1984) approach as a novel method for simulating filling-spilling and merging-splitting processes of the potholes and calculating the amount and direction of flow over the landscape. PRIMA is based on five necessary modifications of the original CA approach, implemented to improve the computational efficiency and ensure the model is mimicking the behavior of the pothole systems.

3.4 Material and Methods

In this section, the proposed model (PRIMA), the study area, and the validation of the model against remote sensing data of pothole area are fully described. Further, the study consists of models' simulations to compare PRIMA's computational efficiency and performance against WDPM (as a reference) in terms of simulating the complex response of the pothole-dominated watersheds and the spatial extents of water over the landscape. A detailed description of the methodology is given below.

3.4.1 Prairie Region Inundation MApping (PRIMA) model

3.4.1.1 Water Redistribution and Routing (WRR) Component

The novel Water Redistribution and Routing (WRR) component in PRIMA is based on the CA approach, which has been used for simulating the movement of water (Parsons and Fonstad, 2007; Li *et al.*, 2013; Liu *et al.*, 2015; Dimitriadis *et al.*, 2016). CA-based models can replace hydraulics differential equations with a set of rules, which are hydrological simplifications of the Saint-Venant and/or Manning's equations (Bates *et al.*, 2010), to represent the surface water movements (Wolfram, 1984; Di Gregorio and Serra, 1999). The simplicity of the CA models makes them more computationally efficient than other hydraulic models.

The WRR component in PRIMA is based on five modifications, introduced in this study (see Appendix B, Section B.2), to the CA-model (Liu *et al.*, 2015). This component moves water sequentially between DEM cells, following the topography. The WRR component is a combination of the minimization algorithm (Di Gregorio and Serra, 1999) and Manning's equation to determine the amount and timing of flow leaving a central cell to its eight neighboring cells, respectively. The minimization algorithm attempts to minimize the difference in water surface elevation between contiguous cells. A hypothetical example and a flowchart of the WRR component, which is iterative and applied to each cell in the DEM, is presented in Figure 3.1. The following rules apply:

1. Using the water elevation of the current (central) cell (wel_0) and the surrounding cells (wel_i $, i=1:8$), calculate the average water elevation (av) (m) by Eq. (3.1):

$$av = \frac{(wel_0 + \sum_{i=1}^{N} wel_i)}{N+1} \tag{3.1}$$

where N is the number of neighboring cells involved in the calculation of the water redistribution.

2. Eliminate those cells having water elevations greater than the average water elevation (i.e., where $wel_i > av$).
3. Recalculate the average water level for the remaining cells as in step 1 and apply the elimination rule in step 2.
4. Apply step 3 until no more cells can be eliminated from the calculations.
5. Distribute the outflow from the current cell to the remaining neighboring cells such that all of them have the same water elevation (*av*).
6. The travel time is calculated as the quotient of the grid cell size divided by its water velocity from Manning's equation. The velocity (v, m/sec) of water is calculated based on the fraction of water leaving the current cell to its lowest water elevation neighboring cell in the DEM and is assigned to the current cell, assuming a wide cross-section, as:

$$v = \frac{d^{2/3}\sqrt{S}}{n} \tag{3.2}$$

where d is the maximum outflow depth from the current cell to its neighboring cells ($\Delta[3] = 4$ in the given example in Figure 3.1) (m), S is the surface water slope (m/m), and n is Manning's roughness coefficient (unitless).

After applying the WRR component to all cells in the DEM, the following steps are applied: 1) the minimum travel time for all grid cells is assigned as PRIMA's global time step to maintain the simulation stability and to ensure that the water does not cross more than one cell during a single time interval; 2) water reaching the outlet cells is removed from the DEM and stored as outflow volume.

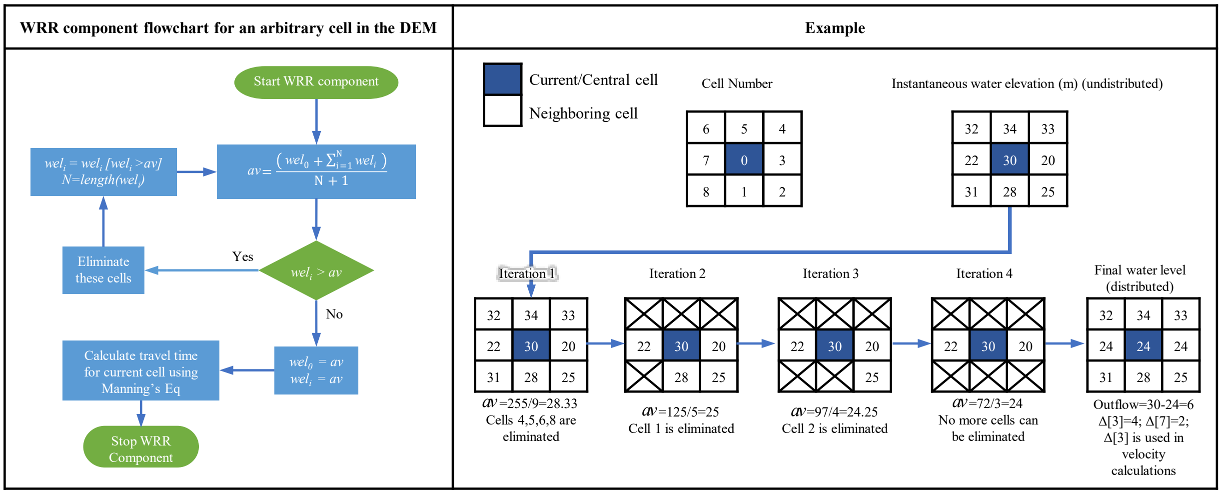

Figure 3.1: A flow chart and a hypothetical example of the Water Redistribution and Routing (WRR) component in PRIMA.

3.4.1.2 Infiltration and Evaporation (losses) Component

Simple vertical water budget calculations were implemented in PRIMA to allow for simulating the spatiotemporal variation of the water extent and the comparison against remote sensing observations. The vertical water budget (infiltration and evaporation processes) were represented in PRIMA using a simple bucket-type approach (Ahmed *et al.*, 2020a). The infiltration to and evapotranspiration from the soil are functions of the soil moisture storage. The evaporation from the potholes is a function of the mean monthly temperature and potential evapotranspiration. A simple degree-day approach was also implemented to allow for distinguishing rainfall and snowfall and calculate the snowmelt rates. The rainfall/snowmelt determined by the degree-day approach was added to the ponded water on each grid cell, then, the amount of infiltration and evaporation were calculated and subtracted from the ponded water. If the grid cell does not have ponded water (i.e., dry cell), the calculated evapotranspiration is subtracted from the soil moisture storage of the cell. After applying the vertical water budget calculations, the remaining ponded water is redistributed over the landscape using the WRR component (Section 3.4.1.1). It is important to note that PRIMA does not allow for horizontal transfer of water in the sub-surface system.

In summary, PRIMA loops through the DEM cells from the highest to the lowest elevation to simulate the water movement from uplands to lowlands, and to reduce the required number of iterations. A flowchart of PRIMA is presented in Figure 3.2. Each run of PRIMA includes the following steps:

1) The DEM cells are sorted by elevation from highest to lowest,
2) Excess water depth (provided as an arbitrary value or calculated by the loss component) is added to or removed from the DEM,
3) The program iterates over each DEM cell in order of elevation: The amount of water exchanged and water velocity are calculated for each grid cell (current cell) and its neighboring cells using the WRR component,
4) The model's global time step is calculated as the minimum travel time among all cells,
5) Water reaching the outlet cell/s is drained/removed from the DEM and stored as outflow volume,
6) The model checks if:
    i. The cumulative global time step is greater than the specific forcing/simulation resolution (e.g., hourly or daily).
    ii. The water depth change is smaller than a user-predefined elevation tolerance. The depth change is the maximum change in water elevation over all cells calculated every *n* iteration (e.g., 1,000).
    iii. The outflow volume change is less than a user-predefined volume tolerance. The volume change is calculated as the change in the cumulative outflow volume every *n* iteration.
7) If any of the conditions above in step (6) is met, the model run terminates. Otherwise, the model re-iterates over the DEM cells (i.e., repeats step 3 to step 7). Step 2 to step 7 are repeated for every addition and/or removal of water.

Depth and volume change are error measurements used to terminate the run because the model may take thousands of iterations to make negligible changes in the water surface elevation. We choose to calculate depth and volume change every *n* iteration interval to ensure that the model was not trapped in a local optima solution (i.e., reached steady-state solution).

PRIMA is a flexible model wherein any component/process can be activated or deactivated (Figure 3.2). As an example, it can allow for the redistribution of water over the landscape without allowing the water to leave through outlet cells. The concept behind the modifications (Appendix B, Section B.2) is to reduce the running time of PRIMA, by draining water from multiple outlet/river cells (Appendix B, Section B.3), and to allow for travel time calculations so that it can be implemented, in the future, into a hydrological land surface model as a runoff generation algorithm. In terms of input and output data, PRIMA requires the topographic data (DEM), outlet cell/s location, elevation and volume tolerance, and the excess water depths (as either uniform or spatially variable), to be distributed over the landscape, as inputs. The excess water depths can be provided as arbitrary depths or calculated by the loss component. If the loss component is used, the model requires precipitation and temperature as input forcings. A preliminary run of PRIMA can help in identifying possible outflow cells and reasonable tolerance values. PRIMA generates water depth raster, value of state variables (soil moisture, snowmelt, snow water equivalent, etc.), outflow volume/rate, and run summary (number of iterations and execution time) as outputs. PRIMA does not do any pre-processing to identify depressions or flat areas in the DEM, the model uses the WRR component to determine if water is trapped in pothole cells or flat area cells.

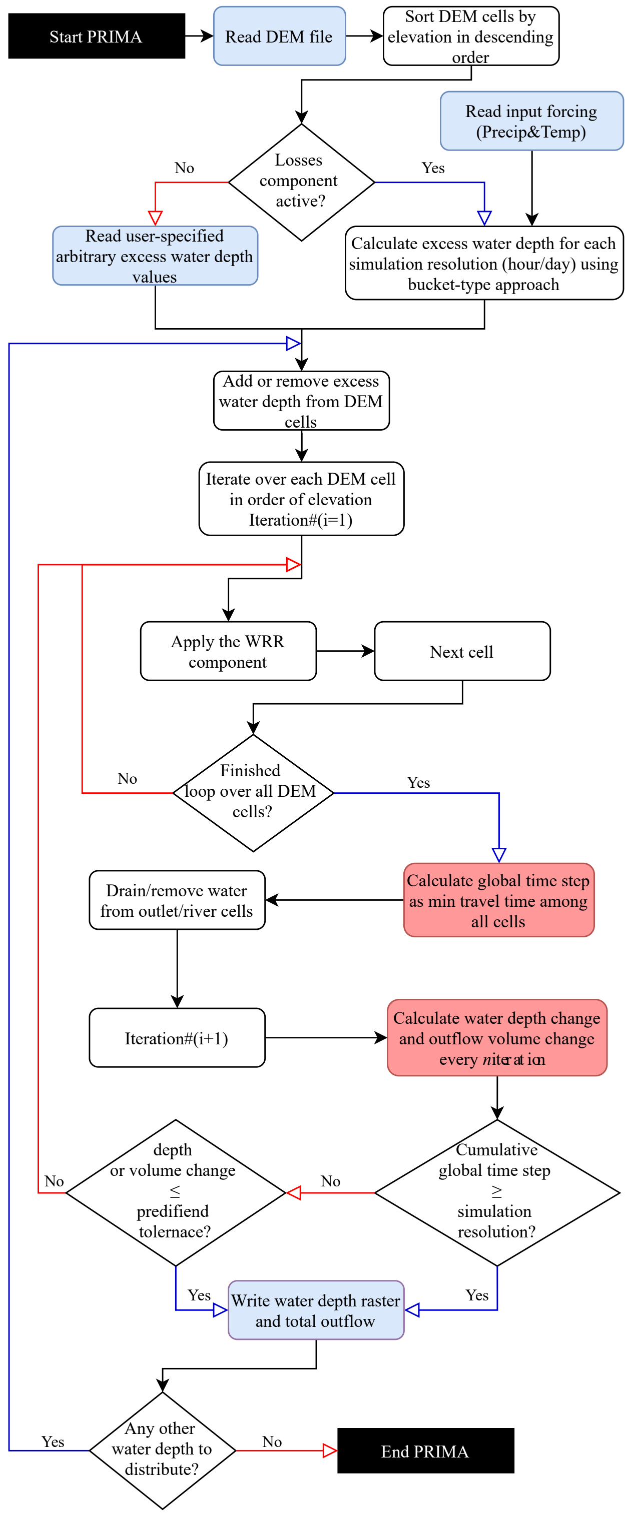

Figure 3.2: A conceptual flowchart of the PRIMA model with its components, inputs, and outputs.

3.4.2 Study area and Data

In order to fully evaluate PRIMA, it was important to test it in areas where DEM at high resolution and remote sensing data of the observed water areas were readily available, and the fill and spill response is well understood and characterized. Thus, Smith Creek Research Basin (subbasin 5, SCRB5) and Saint Denis National Wildlife Area (SDNWA), in Saskatchewan, Canada (Figure 3.3) were selected for this study because of an extensive history of studies in the region (van der Kamp *et al.*, 2003; Fang *et al.*, 2010; Shook and Pomeroy, 2011; Shaw *et al.*, 2012; Mengistu and Spence, 2016). The basins are useful for testing the behavior of the models because they represent two extremes within the variety of topography in the prairie ecozone. SCRB5, with an area of approximately 11 km^2, is relatively flat (slopes of 2-5 %) and has a well-developed stream with a prominent valley. On the other hand, SDNWA is hummocky (slopes of 10 to 15 %), has no defined drainage system, nor an obvious outlet (Figure 3.3), and has an area of approximately 22 km^2. Both basins have more than 1,000 potholes with areas larger than 100 m^2. However, SDNWA is dominated by large potholes/ponds (area > 10,000 m^2) that are scattered over the landscape and occupy almost one-third of the basin area. The dominant land cover on both basins is cropland.

The simulations were performed using available LiDAR-based DEMs for both basins. The SCRB5 LiDAR DEM has a horizontal resolution of 5 m and were collected between the 14th to 16th of October 2008 (Shook and Pomeroy, 2011). The SDNWA LiDAR DEM was collected on the 9th of August 2005 with 5 m horizontal resolutions (Shook *et al.*, 2013). There was some water in the potholes when the LiDAR data were collected at each basin and hence, all modelling and simulations were done relative to the initial conditions of water elevation. The DEMs were not conditioned to account for the existing culverts in the study areas.

The observed water extents/areas were identified from remote sensing data (RapidEye satellite imageries) that are available for SCRB5 and the area above pond 90 within SDNWA (SDNWA-90, Figure 3) for the 2011 spring snowmelt period. The images have a horizontal resolution of 5 m and were captured on May 13, 2011 and May 18, 2011 for SDNWA-90 and SCRB5, respectively (Shook *et al.*, 2013). Water depth observations at different potholes are available at SDNWA-90 (Bam *et al.*, 2018), but they are intermittent and thus, the observation that were available within the 2011 snowmelt period were used. Fourteen different potholes were found to have one recorded water depth during that period; 13 of the measurements were available on May 12, 2011 and the remaining one on May 13, 2011. The locations of the measurements are plotted in Figure 3.3. Both the observed water areas and depths were used to assess PRIMA's performance in simulating the complex potholes' extents, dynamics, and storage.

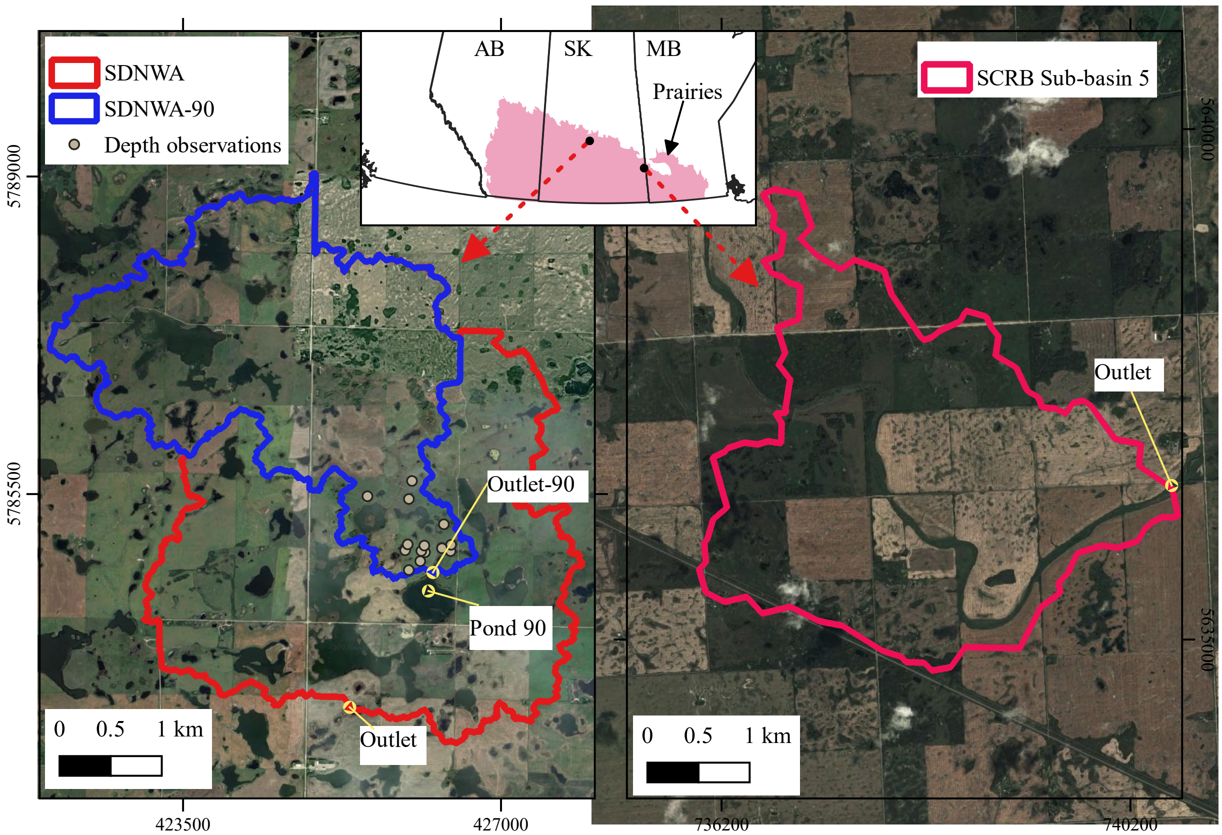

Figure 3.3: A general layout of Smith Creek Research Basin (subbasin 5, SCRB5), Saint Denis National Wildlife Area (SDNWA), and SDNWA above pond 90 (SDNWA-90) with Google satellite imagery in the background and the respective outlet for each area. The points in SDNWA-90 represent depth observation at different potholes during the 2011 snowmelt period. The projection of the figures is UTM-13.

3.4.3 Simulating the extents of surface water areas by PRIMA

The simulation period of PRIMA was set from April 1, 2011 to the date the image was captured for each of the two studied basins (May 13, 2011 and May 18, 2011 for SDNWA-90 and SCRB5, respectively) to simulate the spring snowmelt event. The model used the gridded Canadian Precipitation Analysis (CaPA) product (Lespinas *et al.*, 2015) and the Global Environmental Multiscale (GEM) atmospheric model (Mailhot *et al.*, 2006) output as the respective precipitation and temperature forcing on a daily time scale (Figure 3.4). The forcing was spatially uniform over the basins because each basin was located inside one pixel of the GEM-CaPA data.

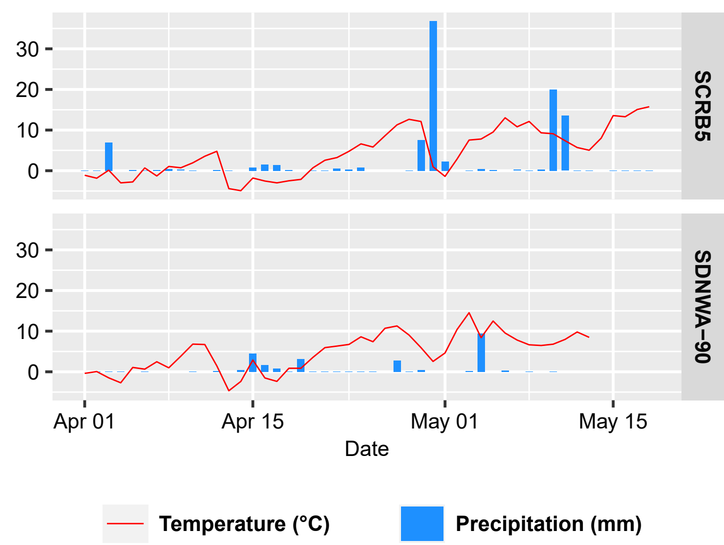

Figure 3.4: GEM-CaPA daily precipitation and temperature for the studied basins for the simulation period of the 2011 spring snowmelt event.

The soil moisture and the potholes almost reached their storage capacity for the studied areas prior to the 2011 flood event (Shook *et al.*, 2013; Mengistu and Spence, 2016). Thus, the initial soil moisture storage was assumed to be close to the water holding capacity. However, we assumed different scenarios for the initial filling conditions of the potholes, assuming that all potholes are 0, 25, 50, 75, and 100 % full to test the effect of the pothole conditions on changing the outflow of the basin and the resulting water extents. The 100 % full condition of the potholes was obtained by adding a significant water depth to the landscape and then redistribute that water using PRIMA's WRR component until all depressions are filled. Then, using QGIS software, the capacity of individual potholes was identified. For each scenario, the depth of stored water in individual potholes was obtained by multiplying its capacity by the fraction of filling (i.e., 0.25 for 25 % full scenario).

In this test, all components of PRIMA were used (i.e., water redistribution and losses). The calculated water depths (from the losses component for each day) were redistributed over the landscape and the excess water was drained from the outlet cells. The accumulated precipitation during fall and winter was used as initial accumulated snow on ground. A summary of PRIMA's parameters and their values are presented in Table 3.1. The parameters were determined from the literature and available landcover data or were set to their default values according to Ahmed *et al.* (2020a). The parameters in Table 3.1 were not calibrated to simulate the observed water areas.

The exceedance probabilities and the spatial distribution of the water areas at the end of the simulation were compared to that of the observed water areas for both basins. The average of absolute deviations was used as a goodness of fit measurement to assess the accuracy of PRIMA's exceedance probabilities of water areas. Two performance metrics were used to further validate PRIMA's spatial water extents against remote sensing data: Sensitivity (S_v) and Specificity (S_c). S_v and S_c quantify the probability of correctly predicting a grid cell within the basin as inundated or non-inundated, respectively (Bharath and Elshorbagy, 2018), and are defined as:

$$S_v = \frac{F_c}{F_c + F_{oc}} \tag{3.3}$$

$$S_C = \frac{NF_c}{NF_c + NF_{oc}} \tag{3.4}$$

where F_c is the total number of observed inundated cells that were correctly predicted as inundated by the model, F_{oc} is the total number of observed inundated cells that were falsely predicted as non-inundated by the model, NF_c is the total number of observed non-inundated cells that were correctly predicted as non-inundated by the model, and NF_{oc} is the total number of observed non-inundated cells that were falsely predicted as inundated by the model. Both Sv and S_c range from 0 to 1 with values closer to 1 demonstrating high probability of accurately predicting inundated and non-inundated areas, respectively. Also, the error in simulating the water depth in the 14 identified potholes over SDNWA-90 was assessed.

Table 3.1: A summary and description of PRIMA's parameters. FC and n values were obtained from the literature/data while the rest of the parameters were assumed to have their default values according to Ahmed *et al.* (2020a).

Parameter	**Value**		**Description [units]**	**PRIMA's component**
	SDNWA	**SCRB5**		
n	0.03		Manning's roughness coefficient based on cropland/grassland cover that is dominant in both areas [-]	Water redistribution and routing component
TT	0		Air temperature for distinguishing rain from snow [ºC]	Infiltration and evaporation (losses) component
C0	5		Melt factor [mm/ ºC/day]	
CFR	0.1		Refreezing factor [-]	
CWH	0.1		Water holding capacity of snow [-]	
SCF	1		Snowfall correction factor [-]	
ETF	0.15		Temperature anomaly correction of potential evapotranspiration [1/Cº]	
LP	0.65		Limit for evapotranspiration [-]	
FC	450	600	Water holding (field) capacity of the soil [mm] (determined from literature, Pomeroy *et al.*, 2010; Mengistu and Spence, 2016)	
BETA	3		Soil release parameter [-]	

3.4.4 Experimental Setup (PRIMA vs WDPM)

It is important to evaluate the computational efficiency and the resulting water extents of PRIMA against another simple hydraulic model (WDPM) that was proven to be successful in redistribution of water over the complex prairie landscape (Shook and Pomeroy, 2011; Shook *et al.*, 2013). WDPM iteratively redistributes excess water over a DEM using the method of Shapiro and Westervelt (1992), in which the water is redistributed from a central cell to its eight-neighboring cells, with each cell taking 1/8 of the water depth difference between itself and the central cell. WDPM does not calculate water velocities or travel time – all water is assumed to flow instantaneously (based on the 1/8 water depth difference rule per iteration). WDPM was used as a reference to further assess the performance and results of the proposed PRIMA model.

For this section and for the sake of comparing the performance of PRIMA to WDPM, the losses component and the travel time calculations were not used, only the WRR component in PRIMA was used, and the water was drained from the outlet cell until both models converged (reached the steady-state solution). The models were tested by applying arbitrary depths of water to the DEM and redistribute them without draining the excess water, which is referred to as "add test". After redistribution of water, the excess water was drained from the basin outlet and this test is referred to as "drain test". This was implemented because WDPM can either add water or drain excess water, unlike PRIMA that can redistribute and drain the water at the same time. There was no attempt to account for groundwater contribution to the outlet. The performance of PRIMA and WDPM were assessed relative to the number of iterations required for convergence because the models' codes are quite different. WDPM was written in C++ for parallel processing, whereas PRIMA was written in Fortran 95 for serial processing. The term "efficiency" in the following discussions refers to the number of iterations required to achieve a model state.

3.4.4.1 Effect of Elevation tolerance on the water distribution of PRIMA and WDPM models

The models' sensitivity to changing the elevation tolerance was tested on SCRB5. SCRB5 was selected to test the effect of changing the models' tolerances on the produced water extents for both the pothole areas and the riverbanks. The models were tested for: (1) the addition and (2) draining of water. The addition tests were carried out at SCRB5 by adding an arbitrary depth of water (100 mm) to the empty DEM and redistributing it until each model converged, for elevation tolerances of 1000, 500, 100, 10, and 1 mm. Because the models' results might be different, we used the final water distribution of PRIMA with 1 mm tolerance as an initial state for the drainage test for both models. This was conducted to test the agreement between both models' results for the same initial condition and water distribution over the landscape. Both models drained the excess water from the landscape, with 1 mm and 1 m^3 as the respective elevation and volume tolerances. The number of iterations and the final spatial distribution of the water over the landscape for the add and drain tests were compared.

3.4.4.2 Simulating the contributing area curves by PRIMA and WDPM

Contributing area fraction curves were generated for both basins using both models. The curves represent the envelope of the relationship between the basin's contributing area fraction and the storage of water. The curves were constructed by repeatedly adding water to an initially empty DEM until all depressions are completely filled for a fine elevation and volume tolerance (1 mm and 1 m^3). Following each addition of water, the basin was drained for both test areas. Then, an incremental water depth of 1 mm was added, and the basin was drained again. The contributing area fraction is calculated as the fraction of the outflow volume corresponding to the added 1 mm.

3.5 Results and Discussion

3.5.1 Suitability of PRIMA for the prairies

The exceedance probability of the observed and the simulated water areas for different pothole initial filling conditions for both basins are shown in Figure 3.5. For SCRB5, the exceedance probability of the near-full scenarios (75 and 100% pothole full) showed good agreement with the exceedance probability of the observed water areas. For SDNWA-90, the exceedance probabilities of the near-full scenarios were almost similar and showed reasonable agreement to that of the observed water areas. In terms of the goodness of fit statistic (Table 3.2), the near-full scenarios showed the smallest error among all scenarios, with the 75% scenario being slightly better than the 100% full scenario.

The near full scenarios showed the best optimal combination of predicting inundated (S_v) and non-inundated areas (S_c) over the two basins (Table 3.2). Although the water extents of the near full scenarios were quite similar in each of the basins, the 100% full scenario tended to slightly overestimate the inundated areas when compared to the 75% full scenario (S_c, Table 3.2). The 75% full scenario showed the best performance in predicting both the inundated (S_v) and non-inundated (S_c) areas in both basins with values of 0.85, and 0.88, respectively (Table 3.2), averaged over the two basins. This agrees with the literature about the conditions of the 2011 flood event, as the potholes were almost full prior to the snowmelt event (Shook *et al.*, 2013; Mengistu and Spence, 2016). The remaining scenarios (0, 25, and 50 %) showed underestimation of the water areas, especially for the larger potholes (Figure 3.5 and S_v Table 3.2).

The actual water extents of the observed water areas and PRIMA's simulated water areas at the end of the simulation period for the 75 % full scenario (best simulation) are shown in Figure 3.6 for both basins. PRIMA showed good agreement with the observed water areas extents, especially for the larger potholes and the upstream portion of the main river at SCRB5. For SDNWA-90, PRIMA's water extents showed good agreement with the observed large potholes; however, there were some over estimation of the ponded area in the central and northeastern parts of the basin (Figure 3.6), with difference between simulated and observed inundated extents in that area of 0.15 km^2. The percent observed and simulated ponded area are 8% and 15%, respectively at SDNWA-90. The model predicted potholes in central and northeastern part of the basin as inundated that were not observed as inundated by the remote sensing data. This overestimation caused some disagreement between the observed and simulated areas exceedance probabilities (Figure 3.5, SDNWA-90). In terms of the simulated water depth in the potholes, the average percent bias for 14 potholes at SDNWA-90 was found to be 2% and the max absolute error was 23% for the 75% full scenario (Figure 3.6, right panel).

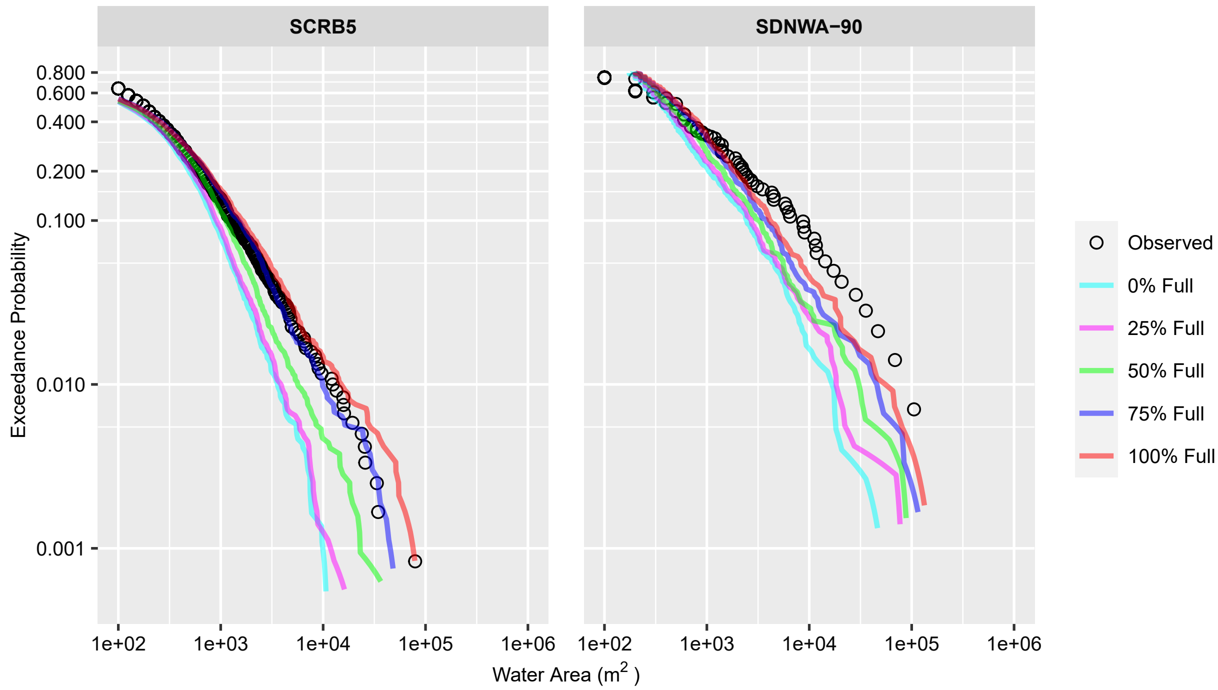

Figure 3.5: The exceedance probability of the observed and PRIMA's water areas at the end of the simulation period for SCRB5 and SDNWA-90 for different pothole filling scenarios on a logarithmic scale.

Table 3.2: The goodness of fit (average of absolute deviations) between the observed and PRIMA's exceedance probabilities and the Sensitivity (S_v) and Specificity (S_c) performance metrics for the different scenarios for both basins.

	SCRB5			SDNWA-90		
Scenario	**average of absolute deviations (x10^{-2})**	S_v	S_c	**average of absolute deviations (x10^{-1})**	S_v	S_c
0%	7.93	0.49	0.92	1.29	0.55	0.94
25%	7.22	0.52	0.91	1.22	0.70	0.94
50%	5.79	0.62	0.89	1.13	0.87	0.92
75%	5.03	0.72	0.86	1.10	0.98	0.89
100%	5.29	0.76	0.82	1.12	0.99	0.86

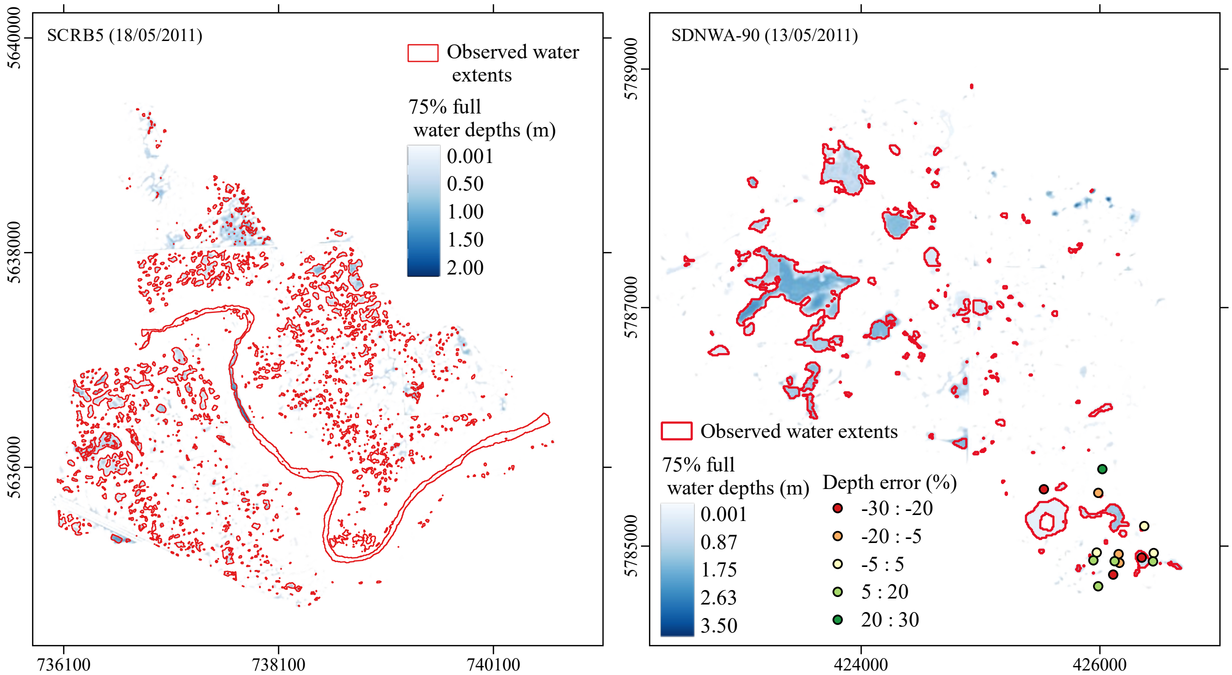

Figure 3.6: The water extents of PRIMA (for the 75% full initial conditions) at the end of the simulation with the observed ones for SCRB5 and SDNWA-90 areas along with the depth error for the selected potholes. The projection is UTM-13.

The average total outflow volume of the below 50% full scenarios (0, 25, and 50 %) was 43,000 m^3 and was smaller than that of the 75 % and 100 % scenarios (almost 56,500 and 191,600 m^3, respectively) for SCRB5. Similarly, for SDNWA-90, the average total outflow volume of the below 50% full scenarios (0, 25, and 50 %) was 350 m^3 and was significantly smaller than that of 75 % and 100 % full scenarios (almost 8,000 and 88,500 m^3, respectively). In the below 50% full scenarios, the potholes did not reach their capacity, especially the larger ones, and hence, most of the water is being stored with little runoff reaching the outlet. However, for the 100 % full scenarios, the majority of the surface runoff can reach the outlet, as all potholes are almost full, and the water might be lost due to infiltration or evaporation.

There is a difference in the outflow volume of the 75 and 100 % full scenarios of SCRB5, while the difference between the same scenarios increased dramatically for SDNWA-90. The biggest pothole has a capacity of almost 1.6×10^5 and 8.8×10^5 m^3 within SCRB5 and SDNWA-90, respectively. In SCRB5, there is a 0.9×10^5 m^3 volume difference between the initial stored water in the largest pothole for the 100 and 75 % full scenario. However, for SDNWA-90, the value reaches 4.8×10^5 m^3 volume difference between the two scenarios, which explains the great difference between the outflow volumes, as there is more available storage within the biggest pothole to reduce the outflow. SDNWA-90 is dominated by large potholes with large storage capacities, when completely filled, caused the outflow volume to change dramatically compared to other scenarios (0 to 75 % full). These results show the great effects of the pothole sizes and initial conditions on changing the outflow dramatically and the corresponding water extents and frequency distribution.

The main idea here was not to model the basins outflow because their outflow observations are not available. However, we used the simple vertical water balance (losses) calculations, without calibrating some of its parameters, because outflows were not of interest and our main interest was to assess PRIMA's novel WRR component in reproducing reasonable water extents. We did this to run the model with reasonable fluxes rather than assuming different arbitrary depths to fit the observations. Although a simple processes representation, without calibration, was incorporated to represent the fluxes, the model showed reasonable to good agreement with the observed water areas exceedance probability (Figure 3.5 and Table 3.2) and extents and depths (Figure 3.6) for the 75 % full scenario. If the basin response is of interest, the model should be calibrated to accurately simulate the outflows, and this should further improve the water extent simulation.

There were differences between the best simulated scenario (75% full) and observed water extents and exceedance probabilities for both test basins. These differences may stem from different simplifications, assumptions, and/or used data. For instance, the initial conditions (snow on ground, soil moisture, % filling of potholes) were assumed to be uniform over the basins. It is known that these values are spatially variable, and this assumption might have affected the results. For example, wind can redistribute snow on ground and results in a heterogeneous snow cover. Further, sublimation and mid-winter melt events can reduce the accumulated snow on ground during winter (Shook *et al.*, 2015). These processes affect the amount of snow available for melt on each basin area/grid-cell and consequently affect the amount of flow to certain potholes. However, the calculations of these processes or the spatially variable initial conditions required either detailed observations, which are not available or a detailed physically based model implementation over the basins, which is beyond the scope of this work. Further, the DEMs were collected 3 and 6 years prior to the date the remote sensing data were acquired for SCRB5 and SDNWA-90, respectively. During that period, the artificial drainage might have affected the potholes' extents, capacity, and/or connectivity. Also, there was some water when the DEMs were collected and this might have affected the actual capacity of the depressions. Despite of the afro-mentioned assumptions/limitations, the reasonable to good agreement between PRIMA's results and the observations suggests that PRIMA's novel WRR is working reasonably well. Integrating PRIMA with a land surface model should help in better identification of initial conditions and in forcing the model with more accurate fluxes, which should result in improved results and more realistic use of PRIMA.

3.5.2 PRIMA vs WDPM

3.5.2.1 Effect of elevation tolerance

PRIMA and WDPM required the same number of iterations (2,000) to distribute the added water when using a coarse elevation tolerance (more than 100 mm), as shown in Figure 3.7-a, and consequently, the water extents of the coarse elevation tolerances were similar for both models. However, PRIMA was three times as efficient for the very fine tolerance (1 mm) for both the adding and draining tests. WDPM was twice as efficient when adding water for the 10 mm tolerance. Figure 3.7-b demonstrates that the maximum water depth, which occurs at the basin outlet, increased for both WDPM and PRIMA as increasingly fine tolerances are used. The use of fine tolerances increased the number of iterations required in each run, allowing water to be distributed more effectively over the DEM. The PRIMA runs demonstrated that the maximum water depths increased compared to WDPM, indicating that PRIMA was more efficient at redistributing water toward the outlet (Figure 3.7-b). When the water was drained, both WDPM and PRIMA had very similar values for the maximum depth of water on their DEMs. Despite the use of very different algorithms, the quantity of water retained by the drained DEM is essentially the same.

Similar results are shown in Figure 3.7-c, which plots the fractional water-covered area. The fractional water areas were reduced as increasingly fine tolerances were used, which was also expected as the use of more iterations would be expected to further concentrate the water in smaller areas. In all cases, PRIMA produced smaller water areas than did the WDPM, which when combined with the greater maximum depths for the PRIMA runs (seen in Figure 3.7-b) implies that PRIMA concentrates the water more rapidly than does WDPM. There was a negligible change in PRIMA's fractional water-covered area with tolerances of 10 mm compared to tolerance of 1 mm (Figure 3.7-c). This shows the efficiency of the PRIMA model in concentrating more water in smaller areas and moving more water downstream the river (near the outlet) with less number of iterations (10 mm iterations compared to 1 mm iterations; Figure 3.7-a). As with the maximum water depths, the drained water areas produced by PRIMA and WDPM are essentially the same for tolerances of 1 mm. Further discussion and analysis on the effect of elevation tolerance are provided in Appendix B, Section B.4.

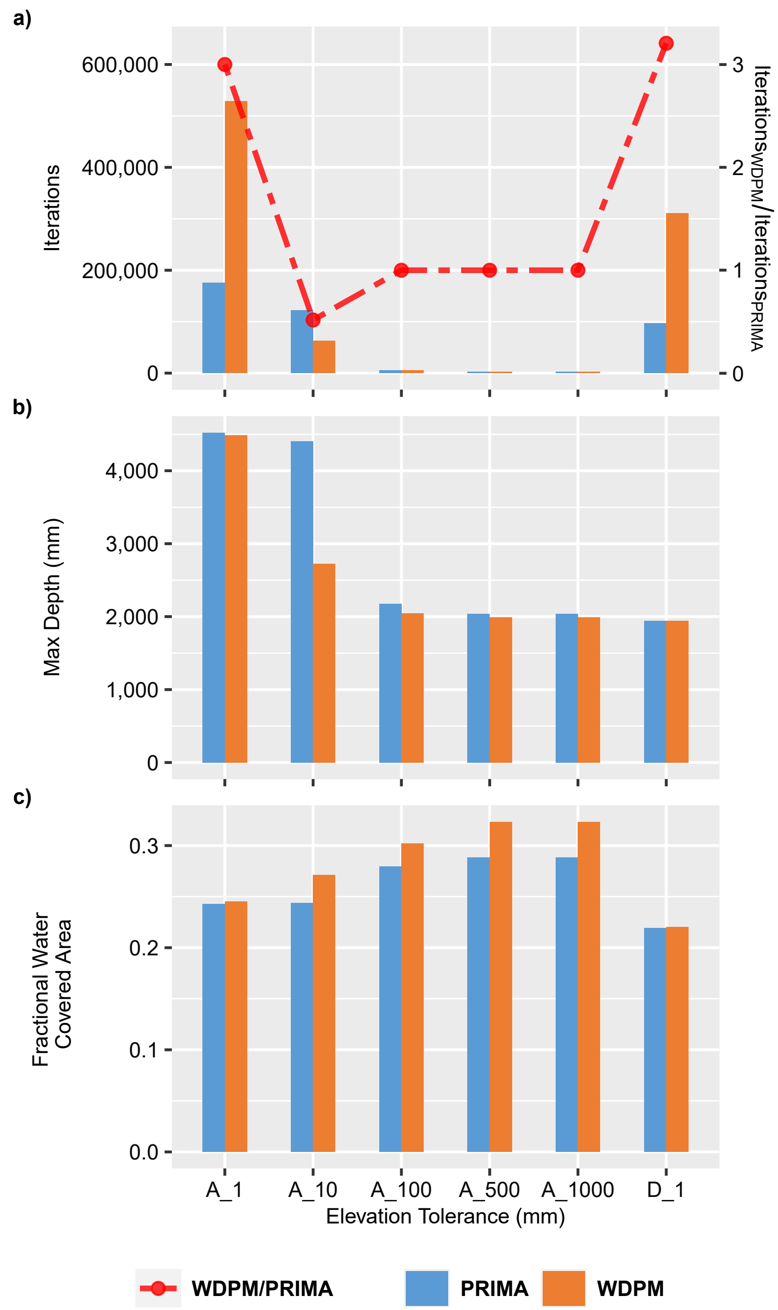

Figure 3.7: Summary statistics of water distribution of both models for SCRB5 for both add and drain test using different elevation tolerance. The x-axis refers to Add (A) or Drain (D) test used followed by the used elevation tolerance in mm for the case of adding 100 mm to the empty DEM.

3.5.2.2 Contributing area curves

Figure 3.8 shows the contributing area fraction of the basin vs. the volumetric fraction of storage for SCRB5 and SDNWA, as computed by both WDPM and PRIMA. The SCRB5 curves required the addition of up to 400 mm of water. The plots of both models are very similar – the greatest difference being that the draining of the final addition of water required more than 4 times as many iterations (1.58 million) by WDPM as by PRIMA (0.36 million).

The SDNWA curves required the addition of up to 500 mm of water, the contributing area fraction for both models being essentially identical. PRIMA was again more efficient than WDPM, requiring ~1.6 million iterations, as opposed to ~6.5 million iterations, to drain the final addition of water. The shape of the SDNWA curves is very different from the SCRB5 curves (Figure 3.8), explaining the greater depth of water required to fill the basin and the very large number of iterations required to drain it. As described above, SDNWA has no permanent drainage system and does not have an obvious outlet. The basin outlet, shown in Figure 3.3, is the lowest point on the divide and lies above much of the basin. The large pond near the outlet (also visible in Figure 3.3) acted as a gatekeeper (Phillips *et al.*, 2011), preventing any outflow until it was filled. It has been demonstrated that PRIMA gives similar results to WDPM but with a reduced computational cost. A detailed comparison of both models' performance and a discussion on why PRIMA is more computationally efficient than WDPM is presented in Appendix B, Section B.4.

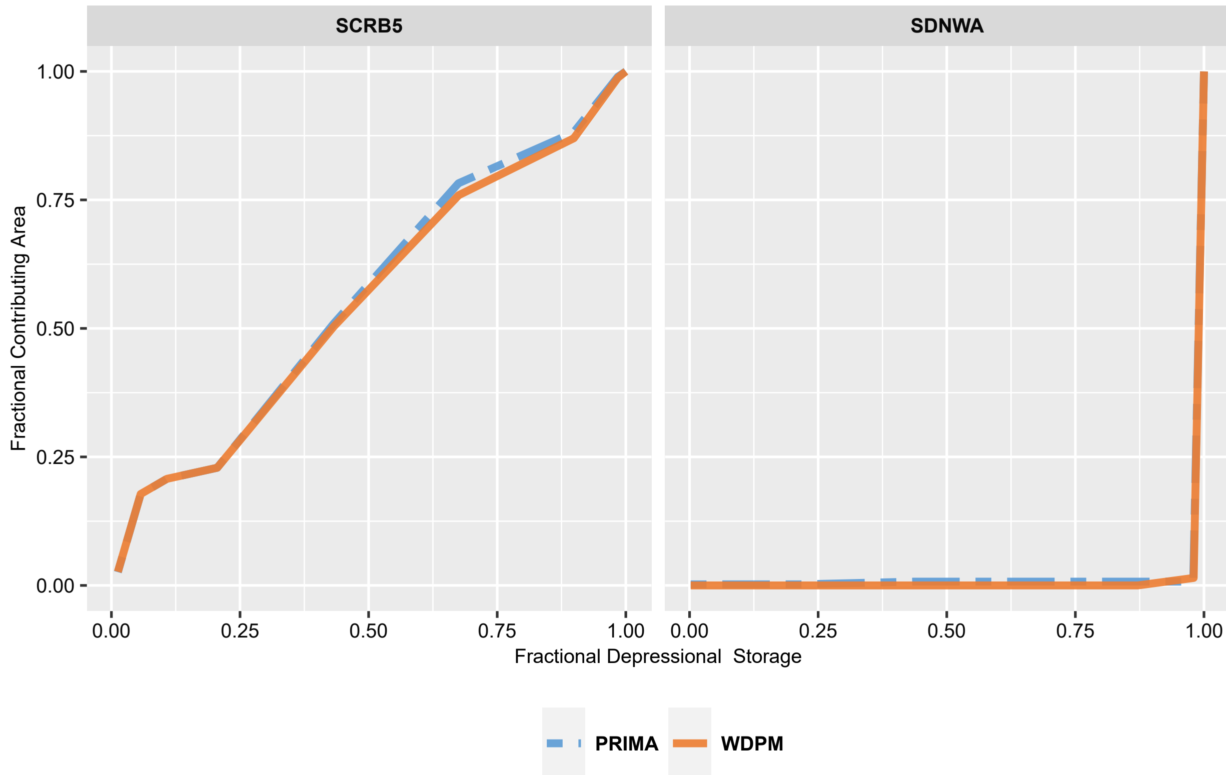

Figure 3.8: Fractional contributing area vs fractional depressional storage for SCRB5 and SDNWA for both PRIMA and WDPM.

3.6 Conclusions

The Prairie Region Inundation MApping model (PRIMA) is proposed as a simplified and comprehensive fully distributed hydrological routing model to allow for a more accurate simulation of the complex pothole systems in the prairies. PRIMA can simulate the infiltration and evaporation losses, movement of surface runoff with travel time calculations, pothole storage dynamics, the fill and spill mechanism, and the spatial extent of the water over the prairie landscape. A number of modifications are implemented to develop PRIMA as an improved and computationally efficient CA-based surface runoff generation algorithm in the prairies.

PRIMA showed reasonable to good simulation of the pothole water extents when compared against remote sensing data of water areas with an accuracy of 85% averaged over the two basins. The percent bias in simulating the water depth in the potholes was 2% averaged over all available pothole depth records at SDNWA-90. The model showed some overestimation in the inundated areas because of some assumption that were made during the simulation (e.g., uniform initial conditions, snow on ground). The initial conditions of the potholes have significant effects on changing the outflow volume and the resulting water extents of the potholes. When the new river cell approach, developed in this study, was used for draining water, the number of iterations required by PRIMA was reduced by almost 48 times compared to the traditional outlet cell approach (Appendix B, Section B.3). Overall, PRIMA was three to eight times as computationally efficient as WDPM in terms of the number of iterations used to arrive at the final water distribution.

Both WDPM and PRIMA took many hours to run. The number of iterations required by the model and their execution time are functions of the applied depth, the complexity (i.e., the number, size, and connectivity of the potholes) and the area of the basin, the grid resolution of the DEM, and the specified tolerance(s). PRIMA runs were performed in a serial mode whereas WDPM runs were performed in a parallel mode. As a test of their relative computational costs, WDPM was also run in a serial mode on the same machine (using a 3.4 GHz Intel Core i7 processor and 16 GB of RAM) as was PRIMA, for the case of draining 100 mm of added water. In this test, PRIMA executed 97,000 iterations in 10,247 sec (0.105 sec/iteration) whereas WDPM executed 311,000 iterations in 15,337 sec (0.049 sec/iteration). PRIMA is more efficient in that it moves more water per iteration, but WDPM had approximately half of the computational cost of PRIMA per iteration. PRIMA filters out the neighboring cells with water elevation higher than the average of the water elevation of the central cell and the neighboring cells, which requires more calculations per iteration compared to WDPM. Although each PRIMA iteration required more CPU time, the total CPU time was reduced by about one third compared to WDPM.

PRIMA showed potential for simulating the pothole flooding extents using a very small number of iterations (2,000), for a basin with a well-developed drainage system and a prominent stream valley. Due to its efficiency, PRIMA can be used for inundation mapping purposes, like WDPM, but with a reduced computational cost, to identify the pothole flooding and associated flood risk, which is useful in urban planning and decision-making. More importantly, PRIMA has the potential to be implemented into hydrologic models, as a prairie runoff generation algorithm, for accurate simulation of the prairie spatiotemporal dynamics and connectivity, which can help in better simulation of the prairie hydrology. Further efforts are needed to parallelize PRIMA code, test the effect of DEM resolutions on the simulation of the storage dynamics and flooding extents, and to test the applicability of integrating PRIMA into a land surface model.

3.7 Acknowledgment

The authors would like to thank Kevin Shook for providing the LiDAR DEM, remote sensing data, and WDPM results for the two study basins and for providing insights and technical support. The financial support of the Natural Sciences and Engineering Research Council of Canada (NSERC) strategic network through the Canadian FloodNet research network is acknowledged (Grant number: NETGP451456-13). The funding of the Department of Civil, Geological and Environmental Engineering, University of Saskatchewan devolved scholarship is greatly appreciated. Compute Canada is also acknowledged for providing the computing facilities to run PRIMA. WDPM was downloaded from https://www.usask.ca/hydrology/WDPM.php.

3.8 References

Ahmed MI, Elshorbagy A, Pietroniro A. 2020a. Toward Simple Modeling Practices in the Complex Canadian Prairie Watersheds. Journal of Hydrologic Engineering 25 (6): 04020024 DOI: 10.1061/(ASCE)HE.1943-5584.0001922

Ameli AA, Creed IF. 2017. Quantifying hydrologic connectivity of wetlands to surface water systems. Hydrology and Earth System Sciences 21 (3): 1791–1808 DOI: 10.5194/hess-21-1791-2017

Anteau MJ, Wiltermuth MT, van der Burg MP, Pearse AT. 2016. Prerequisites for Understanding Climate-Change Impacts on Northern Prairie Wetlands. Wetlands 36: 299–307 DOI: 10.1007/s13157-016-0811-2

Bam E, Brannen R, Budhathoki S, Ireson A, Spence C, Van der Kamp G. 2018. Atmospheric, soil, surface and groundwater data from the St Denis National Wildlife Area, Saskatchewan, Canada DOI: 10.20383/101.0115

Bates PD, Horritt MS, Fewtrell TJ. 2010. A simple inertial formulation of the shallow water equations for efficient two-dimensional flood inundation modelling. Journal of Hydrology 387 (1–2): 33–45 DOI: 10.1016/j.jhydrol.2010.03.027

Bharath R, Elshorbagy A. 2018. Flood mapping under uncertainty: a case study in the Canadian prairies. Natural Hazards 94 (2): 537–560 DOI: 10.1007/s11069-018-3401-1

Chu X, Yang J, Chi Y, Zhang J. 2013. Dynamic puddle delineation and modeling of puddle-to-puddle filling-spilling-merging-splitting overland flow processes. Water Resources Research 49 (6): 3825–3829 DOI: 10.1002/wrcr.20286

Chu X, Zhang J, Chi Y, Yang J. 2010. An Improved Method for Watershed Delineation and Computation of Surface Depression Storage. Watershed Management 2010: 333–342 DOI: doi:10.1061/41143(394)100

DHI. 1998. MIKE SHE Water Movement – User Guide and Technical Reference Manual, Edition 1.1.

Dimitriadis P, Tegos A, Oikonomou A, Pagana V, Koukouvinos A, Mamassis N, Koutsoyiannis D, Efstratiadis A. 2016. Comparative evaluation of 1D and quasi-2D hydraulic models based on benchmark and real-world applications for uncertainty assessment in flood mapping. Journal of Hydrology 534: 478–492 DOI: 10.1016/j.jhydrol.2016.01.020

Evenson GR, Golden HE, Lane CR, D'Amico E. 2016. An improved representation of geographically isolated wetlands in a watershed-scale hydrologic model. Hydrological Processes 30 (22): 4168–4184 DOI: 10.1002/hyp.10930

Fang X, Pomeroy JW, Westbrook CJ, Guo X, Minke AG, Brown T. 2010. Prediction of snowmelt derived streamflow in a wetland dominated prairie basin. Hydrology and Earth System Sciences 14 (6): 991–1006 DOI: 10.5194/hess-14-991-2010

Di Gregorio S, Serra R. 1999. An empirical method for modelling and simulating some complex macroscopic phenomena by cellular automata. Future Generation Computer Systems 16 (2–3): 259–271 DOI: 10.1016/S0167-739X(99)00051-5

Hydrologic Engineering Center. 2016. HEC-RAS, River Analysis System, Hydraulic Reference Manual. Version 5.0. Davis, California. Available at: http://www.hec.usace.army.mil/software/hec-ras/documentation/HEC-RAS 5.0 2D Modeling Users Manual.pdf van der Kamp G, Hayashi M, Gallén D. 2003. Comparing the hydrology of grassed and cultivated catchments in the semi-arid Canadian prairies. Hydrological Processes 17 (3): 559–575 DOI: 10.1002/hyp.1157

Lespinas F, Fortin V, Roy G, Rasmussen P, Stadnyk T. 2015. Performance Evaluation of the Canadian Precipitation Analysis (CaPA). Journal of Hydrometeorology 16 (5): 2045–2064 DOI: 10.1175/jhm-d-14-0191.1

Li Y, Gong J, Zhu J, Song Y, Hu Y, Ye L. 2013. Spatiotemporal simulation and risk analysis of dam-break flooding based on cellular automata. International Journal of Geographical Information Science 27 (10): 2043–2059 DOI: 10.1080/13658816.2013.786081

Liu L, Liu Y, Wang X, Yu D, Liu K, Huang H, Hu G. 2015. Developing an effective 2-D urban flood inundation model for city emergency management based on cellular automata. Natural Hazards and Earth System Sciences 15 (3): 381–391 DOI: 10.5194/nhess-15-381-2015

Mailhot J, Bélair S, Lefaivre L, Bilodeau B, Desgagné M, Girard C, Glazer A, Leduc A, Méthot A, Patoine A, et al. 2006. The 15-km version of the Canadian regional forecast system. Atmosphere-Ocean 44 (2): 133–149 DOI: 10.3137/ao.440202

Mekonnen MA, Wheater HS, Ireson AM, Spence C, Davison B, Pietroniro A. 2014. Towards an improved land surface scheme for prairie landscapes. Journal of Hydrology 511: 105–116 DOI: 10.1016/j.jhydrol.2014.01.020

Mengistu SG, Spence C. 2016. Testing the ability of a semidistributed hydrological model to simulate contributing area. Water Resources Research 52 (6): 4399–4415 DOI: 10.1002/2016WR018760

Muhammad A, Evenson GR, Stadnyk TA, Boluwade A, Jha SK, Coulibaly P. 2019. Impact of model structure on the accuracy of hydrological modeling of a Canadian Prairie watershed. Journal of Hydrology: Regional Studies 21 (December 2018): 40–56 DOI: 10.1016/j.ejrh.2018.11.005

Nasab MT, Singh V, Chu X. 2017. SWAT modeling for depression-dominated areas: How do depressions manipulate hydrologic modeling? Water (Switzerland) 9 (1) DOI: 10.3390/w9010058

Parsons JA, Fonstad MA. 2007. A cellular automata model of surface water flow. Hydrological Processes 21 (16): 2189–2195 DOI: 10.1002/hyp.6587

Phillips RW, Spence C, Pomeroy JW. 2011. Connectivity and runoff dynamics in heterogeneous basins. Hydrological Processes 25 (19): 3061–3075 DOI: 10.1002/hyp.8123

Pomeroy J, Fang X, Westbrook C, Minke A, Guo X, Brown T. 2010. Prairie Hydrological Model Study Final Report

Shapiro M, Westervelt J. 1992. An Algebra for GIS and Image Processing. Champaign, Illinois.

Shaw DA, Pietroniro A, Martz LW. 2013. Topographic analysis for the prairie pothole region of Western Canada. Hydrological Processes 27 (22): 3105–3114 DOI: 10.1002/hyp.9409

Shaw DA, Vanderkamp G, Conly FM, Pietroniro A, Martz L. 2012. The Fill-Spill Hydrology of Prairie Wetland Complexes during Drought and Deluge. Hydrological Processes 26 (20): 3147–3156 DOI: 10.1002/hyp.8390

Shook K, Pomeroy J, van der Kamp G. 2015. The transformation of frequency distributions of winter precipitation to spring streamflow probabilities in cold regions; case studies from the Canadian Prairies. Journal of Hydrology 521: 394–409 DOI: 10.1016/j.jhydrol.2014.12.014

Shook K, Pomeroy JW, Spence C, Boychuk L. 2013. Storage dynamics simulations in prairie wetland hydrology models: Evaluation and parameterization. Hydrological Processes 27 (13): 1875–1889 DOI: 10.1002/hyp.9867

Shook KR, Pomeroy JW. 2011. Memory effects of depressional storage in Northern Prairie hydrology. Hydrological Processes 25 (25): 3890–3898 DOI: 10.1002/hyp.8381

Wolfram S. 1984. Cellular automata as models of complexity. Nature 311 (5985): 419–424 DOI: 10.1038/311419a0

Zhang B, Schwartz FW, Liu G. 2009. Systematics in the size structure of prairie pothole lakes through drought and deluge. Water Resources Research 45 (4) DOI: 10.1029/2008WR006878

Chapter 4 Dynamic Representation of Non-Contributing Area in Land Surface Models for Better Simulation of Prairie Hydrology

This chapter was submitted to the journal of hydrology. This chapter is a slightly modified version of the submitted article, modified to make it consistent with the format and body of the thesis.

Citation: Ahmed, M. I., Elshorbagy, A., Pietroniro, A., & Princz, D. (2020). Dynamic Representation of Non-Contributing Area in Land Surface Models for Better Simulation of Prairie Hydrology. Journal of Hydrology (submitted on December 3rd, 2020).

Authors Contributions and The Contribution of This Chapter to The Overall Study

The following are the contributions from the different authors of this (chapter) submitted manuscript. M. I. Ahmed contributed to the conceptualization, methodology, software, validation, formal analysis, investigation, data curation, writing - original draft, and visualization. A. Elshorbagy contributed to the conceptualization, writing - review & editing, supervision, and funding acquisition. A. Pietroniro contributed to the conceptualization, writing - review & editing, supervision, and project administration. D. Princz contributed to the software, data curation, and writing - review & editing.

This chapter fills an important gap in the physically based simulation of floods and the spatiotemporal changes in the flooding extents and the non-contributing area in the prairies by coupling PRIMA (proposed in chapter 3) with the MESH land surface model. MESH-PRIMA can be used to simulate the hydrograph and peak flows and for mapping flood extents and spatial non-contributing areas, while keeping the integrity of capturing the overall hydrological cycle in the prairies. MESH-PRIMA addresses the third objective of this thesis and contributes to solving the problem of flood prediction as well as assessment of the impacts of climate and landuse change on the hydrology of the prairies. This is the first attempt to add an explicit and dynamic prairie pothole solution to an earth system model.

4.1 Abstract

The hydrology of the Canadian prairie region is complicated by the existence of numerous land depressions that change the contributing area dynamically and result in a non-linear and hysteretic basin response. Depressions are represented conceptually in most hydrologic models using lumped or a series of reservoirs approaches. These conceptual approaches are simplified, and do not adequately represent the dynamics of the depressions and the changing non-contributing area either temporally or spatially, and therefore, the simulation of streamflow remains challenging. This study advances towards a more physically based simulation of the hydrology, streamflow, and spatiotemporal pluvial/nival flooding extents and the associated non-contributing area in the prairies. This is achieved by coupling the MESH hydrology-land surface model with a newly developed surface routing component designed to explicitly deal with the prairie-pothole issue (PRIMA) and is referred to as MESH-PRIMA. In this model, MESH handles the classical vertical water and energy balance calculations while PRIMA routes the water over the landscape and quantifies the depressional storage and runoff. The streamflow simulation of MESH-PRIMA is compared against that of MESH with its current conceptual prairie algorithm (MESH-PDMROF) on the Smith Creek Research Basin in Saskatchewan, Canada. MESH-PRIMA shows an improved streamflow and flood simulation compared to MESH-PDMROF and is able to replicate the non-linear and hysteretic relationship of the basin response. MESH-PRIMA allows for mapping the spatial distribution of water (pluvial/nival flooding) and the non-contributing area over landscape for different events. The results of MESH-PRIMA can help in updating the non-contributing area map and in identifying pluvial/nival flooding hazard, which is useful in flooding contexts.

4.2 Introduction

The prairies are characterized by sequences of flat and undulating terrain with numerous land depressions of glacial origin, referred to as prairie potholes (Anteau *et al.*, 2016). These potholes can retain considerable amounts of runoff (van der Kamp and Hayashi, 2009; Shook and Pomeroy, 2011) and consequently change the basin response to be complex, non-linear, and hysteretic (Shook *et al.*, 2013). The amount of retained runoff depends on the available storage in the land depressions that vary in area and volume (Ahmed *et al.*, 2020b). These potholes are usually disconnected from the stream network and thus, they do not contribute to streamflow under dry conditions (Martin, 2001; Hayashi *et al.*, 2003). Therefore, most of the praries are designated as non-contributing area wherein these areas do not contribute flow to the basin outlet for events with return periods of 2 years or smaller (Godwin and Martin, 1975). Prairie potholes can contribute flow to the stream network under wet conditions. In this situation, the surface area of potholes is expanded and many of them may connect/merge to form larger potholes (Shook and

Pomeroy, 2011). The potholes are connected by surface or subsurface flow through a fill and spill mechansim (Shaw *et al.*, 2012), wherein a depression spills/contributes flow to downstream areas after being filled. Such a mechanism results in a dynamic non-contributing area that increases the hydrological complexities of the prairies and makes traditional hydrological models inapplicable (M. Mekonnen *et al.*, 2014; B. Mekonnen *et al.*, 2016; Ahmed *et al.*, 2020a). Further, cold region processes, such as blowing snow (Fang et al., 2007), snowmelt, and frozen soil infiltration (Gray and Landine, 1988; Pomeroy *et al.*, 2007) pose a challenge for streamflow simulation in the Canadian prairies and it becomes more challenging with the existence of the land depressions.

Efforts have been made to handle the pothole complexities in hydrological models using satellite-based (Chu *et al.*, 2013; Shook *et al.*, 2013; Evenson *et al.*, 2016; Nasab *et al.*, 2017) or conceptual approaches and algorithms (M. Mekonnen *et al.*, 2014). Evenson *et al.* (2016) introduced an approach to obtain pothole properties from land cover data, which are classified from satellite imagery. Digital Elevation Models (DEMs) can also be used to obtain the properties (area, depth, and cascading order) of different potholes in the basin (Chu *et al.*, 2010; Shook *et al.*, 2013). In most of these approaches, flow is routed between individual potholes that are represented using simple buckets, and a pothole contributes flow to downstream areas after being filled. Such approaches do not represent the spatial connection and/or extents of the water between potholes in a fully dynamic and distributed manner (Ahmed *et al.*, 2020b). Other attempts were made to understand the effect of the prairie potholes on changing the system response using DEMs by implementing simple hydraulic models to move water over prairie landscapes (Shook and Pomeroy, 2011; Shook *et al.*, 2013; Ahmed *et al.*, 2020b). However, these models do not have full hydrologic process representation and thus, they are not useful in conducting full hydrologic simulations.

The conceptual Probability Distribution Model based RunOFf generation (PDMROF) algorithm was introduced by M. Mekonnen *et al.* (2014) to handle pothole complexities in hydrologic models. In the PDMROF algorithm, the capacity of different potholes can be drawn from a Pareto distribution, and runoff is calculated as a function of the storage in potholes. The PDMROF algorithm was shown to improve the streamflow simulation in prairie basins when implemented in different models (B. Mekonnen *et al.*, 2016; Ahmed *et al.*, 2020a). However, this algorithm does not represent the spatial distribution of water in potholes across the land surface.

Despite the attempts that have been made to handle the pothole complexities in hydrological models, the streamflow simulation remains challenging due to the poor/simplified representation of potholes, as most of these approaches use a lumped or a series of reservoirs to represent the potholes in which a reservoir contributes flow after exceeding its capacity, and it becomes even more challenging when peak flow prediction is emphasized (Ahmed *et al.*, 2020a). The HYdrological model for Prairie Region (HYPR, Ahmed *et al.*, 2020a) was proposed as an engineering solution to this problem. HYPR was based on the conceptual HBV model for process representation and the PDMROF algorithm for pothole representation. Although HYPR showed potential to simulate both the overall hydrograph and peak flows in multiple prairie watersheds, it simply cannot represent the spatial water extents because it is based on PDMROF (Ahmed *et al.*, 2020a).

In the past decade, the prairie region has been impacted by many flooding events that resulted in severe damages. For example, the 2013 flood that caused widespread damage in excess of CAD $1 billion over the prairie region (Brimelow *et al.*, 2014). In the prairies, flood damages are not associated with fluvial flooding only; pluvial/nival flooding can also cause major issues to agricultural and urban areas that reside near potholes. Pluvial/nival flooding is typical in the prairies under wet conditions as potholes can be filled and their surface area expanded, causing the surrounding areas to be flooded (Shook *et al.*, 2015). However, assessing flooding impacts has been typically limited to fluvial flooding (e.g., Elshorbagy *et al.*, 2017; Bharath and Elshorbagy, 2018) with less attention to landscape pluvial/nival flooding. Thus, it is important to accurately estimate the magnitude of floods and the corresponding areal extents of water over the landscape to contribute to the proper assessment of combined flood risks in the prairies. There is a need for a land surface model that has sound physical representation of the complex prairie hydrological processes and can predict the spatial water distribution over prairie landscape and the progression of pluvial/nival flood water, in addition to the prediction of the hydrograph, including peak flows. Such a model can be used to further understand the prairie complexities and the mechanisms of generating different runoff and flood regimes in both fluvial and pluvial/nival dominated events.

This study is an attempt towards improving the understanding of non-contributing area dynamics and pothole representation in land surface models with emphasis on peak flow simulation and pluvial/nival flood hazard mapping in pothole-dominated areas. We argue that adding a prairie-customized routing component to handle pothole complexities in a land surface model can yield (i) an improved overall streamflow and peak flow simulations, and (ii) an improved understanding and simulation of the progression of pluvial/nival flooding, while keeping the integrity of capturing the overall hydrological cycle in the prairies. These are key factors for understanding floods and their various generation mechanisms, and for assessing their impacts in prairie landscapes. In this paper, the physically based "Modélisation Environnementale communautaire" - Surface Hydrology model (MESH; Pietroniro *et al.*, 2007) was modified by adding a physically based Prairie Region Inundation MApping model (PRIMA; Ahmed *et al.*, 2020b) to simulate streamflow, peak flow, spatial water and flooding extents, and spatial dynamic non-contributing areas. This model is referred to as MESH-PRIMA and is considered a hydrologic-hydraulic model.

4.3 Methodology

The MESH model was coupled with PRIMA to improve the streamflow simulation and allow for local scale flood and non-contributing area mapping in the prairie region. MESH-PRIMA and MESH-PDMROF were calibrated and validated against streamflow observations and the uncertainty in the output streamflow was assessed. The non-contributing area map, generated by MESH-PRIMA, was compared against the existing static non-contributing area map, which is currently being used to evaluate prairie basins and their contributing area by both researchers and practitioners. The resulting flooding extents over the basin obtained from MESH-PRIMA was used to understand the spatial connection between potholes and to assess the pluvial/nival flooding hazard over the basin. A detailed methodology is provided below.

4.3.1 The MESH-PRIMA Model

4.3.1.1 The MESH Model

The "Modelisation Environmentale Communautaire" (Communal Environment Model – MEC) was an initiative developed by Environment and Climate Change Canada (ECCC) to simulate different components of an Earth Systems Model (ESM). It was configured to form a new modelling platform called MESH (MEC – Surface Hydrology) to couple land-surface and hydrological models (Pietroniro *et al.*, 2007). The MESH model was proposed to provide a framework for coupling the robust physically based land surface schemes of regional and global climate models with hydrological processes to better represent the land surface, which can further be coupled with distributed routing models for streamflow simulation. The components in the MESH model solve both the energy and water balances of the land surface provided meteorological driving data, and the water balance of a stream network provided runoff fields. In most cases, these components are run in a coupled mode, where the hydrologic land surface scheme provides the runoff field to route flow through the stream network. MESH has shown potential for simulating streamflow and other hydrological processes in Canada (MacLean, 2009; M. Mekonnen *et al.*, 2014; Haghnegahdar *et al.*, 2015; Davison *et al.*, 2016; Mengistu and Spence, 2016; Yassin *et al.*, 2017; Budhathoki *et al.*, 2020).

MESH consists of three main components: (1) a prognostic land surface component that calculates the vertical water and energy budget and the exchange of vertical fluxes between land surface (soil column, snow, surface ponded water, and vegetation canopy) and the atmosphere; (2) a runoff generation component that calculates the lateral fluxes and generates surface and subsurface runoff; and (3) a river routing component that routes the lateral fluxes through the channel/stream network to the watershed outlet.

MESH commonly uses the Canadian Land Surface Scheme (CLASS; Verseghy, 1991; Verseghy *et al.*, 1993) to calculate the vertical water and energy budget for soil, snow, ponded water, and vegetation. Other vertical water budgets components such as the Soil-Vegetation-Snow (SVS) system, which is currently being implemented in the Canadian numerical weather prediction model (Alavi *et al.*, 2016) are also available in MESH. CLASS uses Richard's equation to calculate the soil moisture for different layers (typically three layers) in the soil column. There are three alternative runoff generation components/algorithms in MESH. The first is the traditional CLASS runoff algorithm that calculates the total runoff as excess surface runoff and baseflow runoff. Surface runoff occurs when water, which cannot infiltrate into the soil, exceeds a specific minimum ponding depth, whereas baseflow runoff occurs when there is drainage from the bottom of the soil column and this drainage depth is used in Darcy's equation to calculate the baseflow. The second runoff generation algorithm is WATROF (Soulis *et al.*, 2000), which is based on the concept of sloped soil layers with a horizontal hydraulic conductivity that decreases as the soil depth increases. WATROF calculates surface runoff using Manning's equation and interflow (from saturated and unsaturated zones) using Richard's equation. Baseflow is generated in the same way as by the traditional CLASS runoff algorithm. The third runoff generation algorithm is the PDMROF (M. Mekonnen *et al.*, 2014), which incorporates land depressions by integrating the probability density function of the Pareto distribution to generate surface runoff. PDMROF does not generate interflow. Baseflow is generated in the same way as by the traditional CLASS runoff algorithm. As for the routing component, MESH uses the "WATROUTE" algorithm from the WATFLOOD model (Kouwen *et al.*, 1993) to route the flows through the stream network using the continuity and Manning's equations.

The spatial heterogeneity of the basin properties is handled in MESH using the Grouped Response Unit approach (GRU; Kouwen *et al.*, 1993), in which areas with the same properties are combined together in one GRU. This makes the MESH model computationally efficient and reduces the required number of model parameters. The stream network and drainage properties for MESH are typically discretized into regular grid cells. The hydrologic information of each cell (e.g. elevation, slope, hydrologic connectivity to other grid cells) is derived by processing a hydrologically conditioned DEM. Both hydrologic land surface schemes currently coded in MESH require seven meteorological driving variables (incoming shortwave and longwave radiation, total precipitation rate, air temperature, wind speed, barometric surface pressure, and specific humidity) as input at a sub-daily temporal scale.

4.3.1.2 PRIMA Model

The Prairie Region Inundation MApping model (PRIMA; Ahmed *et al.*, 2020b) is a distributed hydraulic model that simulates the movement of water over prairie landscapes. PRIMA consists of two main components: A Water Redistribution and Routing (WRR) component and a losses component. The WRR component in PRIMA uses a set of rules along with Manning's equation (in an iterative way) to quantify the magnitude and direction of flow, travel time, and flow rate from cell to cell over the DEM that represents the landscape. The losses component was proposed in PRIMA based on the HBV model approach (Ahmed *et al.*, 2020a) to simulate a simple vertical water budget (infiltration and evaporation) to allow for comparison against remote sensing data. PRIMA, when used in conjunction with a conceptual hydrological system like HBV, was shown to be successful in simulating the movement of water over the complex prairie landscape when compared against remote sensing data (Ahmed *et al.*, 2020b).

In this study, PRIMA was coupled with MESH to improve the non-contributing area and pothole representation and streamflow simulation in the prairies. PRIMA's losses component was not used; only the WRR component was used, as excess (net) water depths are obtained from MESH based on its detailed physically based methods. PRIMA was implemented to replace the PDMROF algorithm in MESH and to increase the information that MESH can produce by allowing for a more explicit formulation to characterize the pothole problem. It is well understood that prairie depressions are connected through overland and interflow runoff from the shallow soil layers (Hayashi *et al.*, 1998, 2016; van der Kamp and Hayashi, 2009). Therefore, PRIMA receives input water as the surface runoff depth (ROFO) and the interflow depths from the first two soil layers ($ROFS_{1,2}$), both calculated by the WATROF algorithm (Figure 4.1). Losses (infiltration and evaporation) from ponded water in PRIMA were calculated by MESH. Then, the net water input to PRIMA (the difference between input water and losses) was added to the DEM (Figure 4.1) and PRIMA redistributes that water iteratively, quantifies the storage in the depressions, and calculates the net outflow reaching the stream network. The net outflow from PRIMA (i.e., from depressions) and the remaining runoff depths (interflow runoff from the third soil layer ($ROFS_3$) and baseflow from the bottom of the soil column (ROFB), Figure 4.1) go directly to the routing component of MESH to quantify the streamflow. More details on the technical implementation of PRIMA inside MESH are provided in the Appendix C, Section C.1.

In the MESH-PRIMA setup, MESH calculates the vertical fluxes at a coarse meso grid-scale (subbasin scale, which is typically $\geq$ 10 km) and PRIMA redistributes excess water laterally on a very fine micro grid-scale for the specific subbasin (DEM scale, which is $\leq$ 30m). In other words, MESH-PRIMA has two different layers for each MESH coarse grid/subbasin; one (hydrologic) layer for the land surface model to handle the vertical water balance and hydrological processes representation ($\geq$ 10 km) and a fine resolution (hydraulic) layer ($\leq$ 30 m DEM resolution) for PRIMA to redistribute water over the landscape, identify spatial water distribution, and quantify the storage and outflow (Figure 4.1).

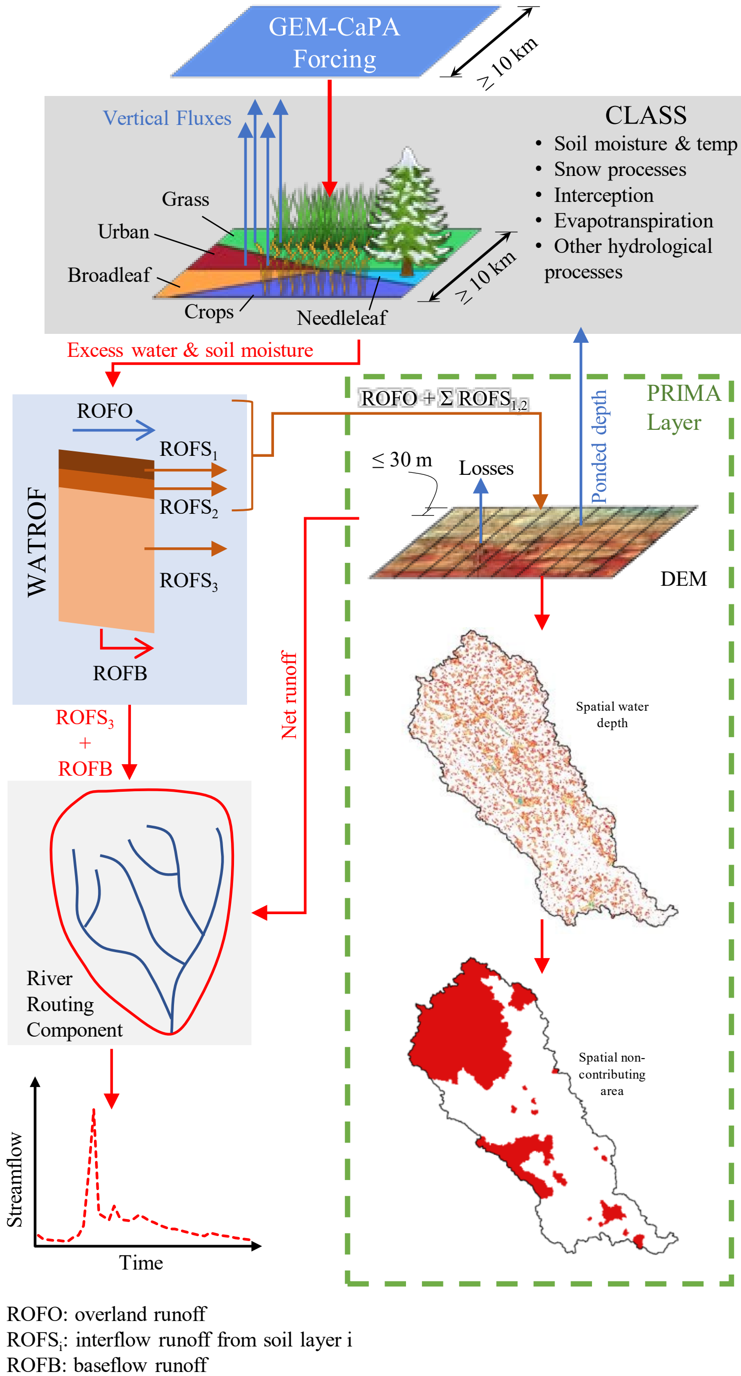

Figure 4.1: A schematic representation of the MESH modelling framework with the incorporation of PRIMA component (highlighted in a dashed green box).

4.3.2 Study Area and Data

It is important to test the proposed model (MESH-PRIMA) and the MESH model with its current accepted conceptual approach, namely MESH-PDMROF on a prairie watershed with sufficient streamflow records, minimum level of flow regulation, and a good understanding of the complexities of the prairie pothole (Fang *et al.*, 2010; Shook and Pomeroy, 2011; Shook *et al.*, 2013; Dumanski *et al.*, 2015; Ahmed *et al.*, 2020b). Therefore, Smith Creek Research Basin (SCRB, Figure 4.2) was chosen as a study area to test the performance of MESH-PRIMA. SCRB has a total area of 435 km^2 and an effective area of 57.8 km^2 according to the existing, static non-contributing area map that shows the non-contributing area of events with a 2-year return period or smaller (Figure 4.2). The landscape of SCRB is relatively flat (almost 3% average slope) with cropland and pasture as the dominant landcover.

SCRB was represented in MESH using one grid cell (~ 30 km resolution) and one GRU with five different landcover types. The landscape was represented in PRIMA using the Canadian Digital Surface Model (CDSM) with a resolution of ~ 20 m as input DEM, which was downloaded from https://open.canada.ca/data/en/dataset/768570f8-5761-498a-bd6a-315eb6cc023d. We used the CDSM instead of the Canadian DEM because the latter is void filled and contains no depressions with which to represent potholes. The SCRB was delineated using the CDSM and the resulting streams that match the rivers observed on available satellite imageries were selected as the SCRB main rivers (Figure 4.2). All cells that lie on the centerline of the main rivers were considered as outlet cells in PRIMA. Any water reaching these outlet cells, while PRIMA iterates for the specific time step to distribute water over landscape, was removed from the landscape and was passed to the routing component of MESH to route the water to the outlet.

Landcover types were identified from the Canadian Land Cover data (Circa 2000, https://open.canada.ca/data/en/dataset/97126362-5a85-4fe0-9dc2-915464cfdbb7). The vegetation parameters in the model were set to their recommended values from literature (Verseghy, 2011) and the soil texture information was acquired from the Canadian Soil Information System (CanSIS, http://sis.agr.gc.ca/cansis). The rest of the model parameters were calibrated within their range (Table 4.1) to best fit the observed flow for MESH-PRIMA and MESH-PDMROF.

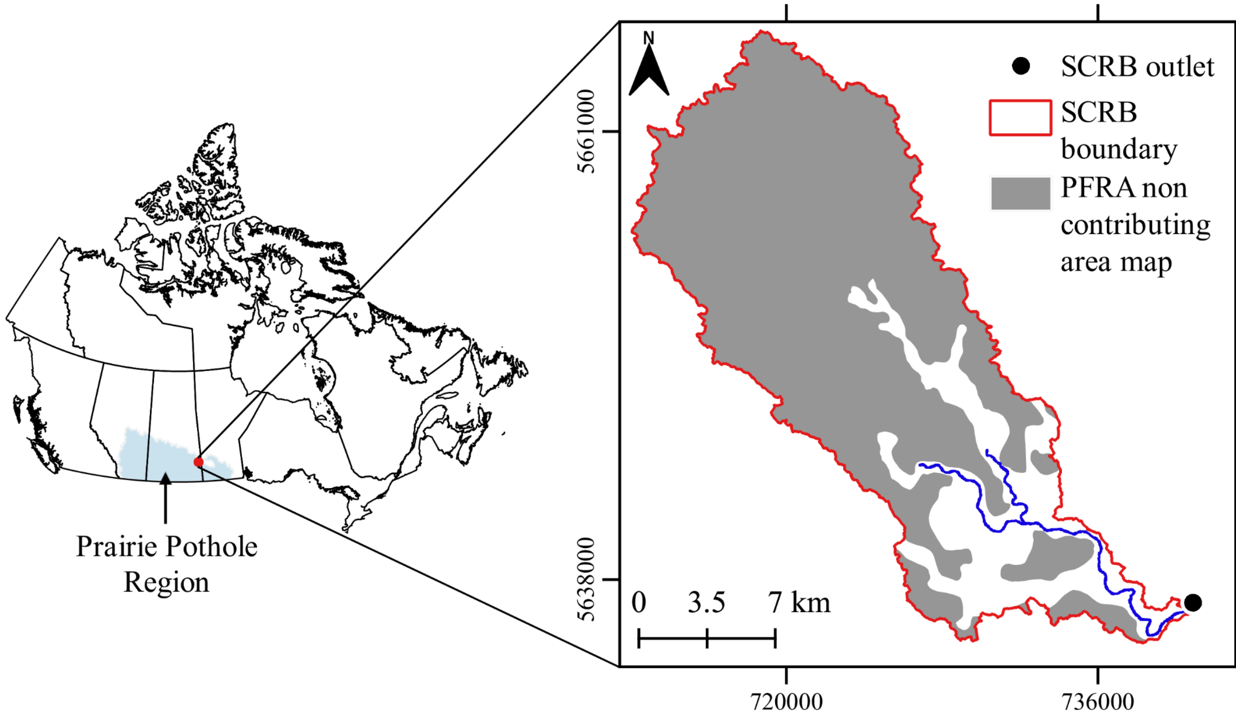

Figure 4.2: A general layout of the Smith Creek Research Basin (SCRB) and the Prairie Farm Rehabilitation Administration (PFRA) static non-contributing area map. The projection of the figure is UTM-13.

The precipitation input for the models was obtained from the Canadian Precipitation Analysis (CaPA; Lespinas *et al.*, 2015) whereas the rest of the meteorological inputs were obtained from the Global Environmental Multiscale atmospheric model (GEM; Mailhot *et al.*, 2006). Data were acquired for the period from 2005 to 2020. Streamflow records were obtained from the Water Survey of Canada (WSA) from 1975 to 2017 (Gauge DID: 05ME007). The simulation period was chosen based on the availability of both meteorological and streamflow data (2005 to 2017; hydrologic year, October to September).

4.3.3 Model Calibration and Output Uncertainty

The Nash-Sutcliffe Efficiency (NSE) was used as an objective function for model calibration to compare simulated to observed flows at the watershed outlet. Each of the two models (MESH-PDMROF and MESH-PRIMA) was calibrated independently to best fit the calibrated parameters to the strengths of each model. The first three years of the simulation were considered as a spin-up period. The results of the models during these years are excluded from the calculation of the objective function and any analysis. The period from 2008 to 2011 was considered as a calibration period and the period from 2012 to 2017 was considered as a validation period. The calibration period includes the 2011 flood event, which is useful for model parameter identification (Ahmed *et al.*, 2020a). The Dynamically Dimensioned Search (DDS) algorithm (Tolson and Shoemaker, 2007) within the OSTRICH optimization toolkit (Shawn Matott, 2017) was used for model calibration by maximizing the NSE value using 1,000 runs. The parameters in Table 4.1 were calibrated within their respective range with the objective to have the simulated flows best fit observed ones. The simulations with a relatively good fit, which were identified during the model calibration process as simulations with NSE ≥ 0.5 for the entire simulation period, were used to assess the uncertainty in the flow simulation. These are identified as "behavioral" runs.

Table 4.1: Calibration parameters and their ranges for PRIMA and PDMROF.

Name	Description [units]	Parameter range		Model configuration
		min	max	
R2N	Manning's roughness coefficient for channel routing [-]	0.01	0.2	PRIMA & PDMROF
R1N	Manning's roughness coefficient for floodplain and between potholes routing [-]	0.01	0.2	PRIMA & PDMROF
ZSNL	Snow depth above which the area is considered 100% snow covered [m]	0.05	0.3	PRIMA & PDMROF
DRN	Drainage index, which is a fraction to control the seepage from the bottom of the soil column [-]	0	1	PRIMA & PDMROF
SDEP	Permeable depth of soil column [m]	0.01	4.1	PRIMA & PDMROF
ZPLS*	Maximum ponding water depth allowed to be stored on the ground for snow covered area [m]	0.05	0.3	PRIMA
ZPLG*	Maximum ponding water depth allowed to be stored on the ground for snow-free area [m]	0.05	0.3	PRIMA
KSAT*	Saturated hydraulic conductivity of the soil [m/s]	0.0001	0.01	PRIMA
DD*	Drainage density [km/km^2]	1	120	PRIMA
B	Shape factor for Pareto distribution to control the connectivity of potholes [-]	0	10	PDMROF
CMAX	Maximum pothole storage [m]	0	5.0	PDMROF
* the parameters that are associated with PRIMA only are WATROF parameters that are used to calculate the interflow and overland runoff depths, which are passed to PRIMA. The only parameter inside PRIMA itself is Manning's roughness, which was assumed to equal the R1N parameter of the MESH routing algorithm. **No new calibration parameters were added to the MESH system as a result of introducing PRIMA**.				

4.3.4 Streamflow Performance Evaluation

The resulting streamflow from each model (MESH-PRIMA and MESH-PDMROF) was compared separately against observed flows using visual inspection of the hydrograph and four quantitative performance measures (NSE, NSE_{OT}, NSE_{log}, PBIAS). NSE was used to assess the model performance for the overall hydrograph with some focus on peak flow. NSE_{OT} was calculated using the NSE formula but for flows over a defined threshold (95th percentile) and was used to assess the goodness of fit in peak flow simulation. NSE_{log} uses the logarithmic transformation of flows within the NSE formula to assess the simulation of low flows. PBIAS was used to assess the performance in preserving the overall runoff volume. The Akaike and Bayesian information criterion (AIC and BIC) were used to assess the goodness of fit between observed and simulated hydrograph (for the entire simulation period) with penalizing the models for having more calibration parameters (more degrees of freedom). AIC and BIC can show if a model outperforms others because it possesses higher degrees of freedom (calibration parameters).

4.3.5 Dynamic Non-Contributing Area Delineation

The spatial distribution of water over the landscape, resulting from MESH-PRIMA, was also used to assess the changing (dynamic) non-contributing area for different events over the course of the simulation. Multiple functions/algorithms from the Whitebox tools (WBT, Lindsay, 2016), which is a free open source GIS toolbox, were used to delineate the landscape to quantify the contributing and non-contributing areas of the basin. The following are the main steps in non-contributing area delineation. The depressions and their capacity were identified from the DEM using the "depth in sink" function from WBT. Then, the filling state (current storage) of each depression (identified from the resulting water depth raster, from MESH-PRIMA, for a specific event/time step) was compared to the capacity of the respective depression. The non-filled depressions (for the specific event/time step) were identified as depressions with storage smaller than their capacity. A raster containing the locations of the non-filled depressions and the main rivers is generated for each event. This raster and the flow direction raster (corresponding to a filled DEM) were used in the "watershed" function. The resulting raster, from the "watershed" function, contains the contributing areas that contributes flow (connected) to the rivers, and the non-contributing areas that are dominated by the non-filled depressions.

4.3.6 Non-Contributing Area Evaluation Metrics

The currently available PFRA non-contributing area map (Figure 4.2) is static and was delineated based on visual interpretation of available topographic maps for events with a magnitude of a 2-year return period or smaller (Shaw *et al.*, 2013; Ahmed *et al.*, 2020b). Thus, that map was used as a reference to further validate the non-contributing area map generated by MESH-PRIMA for an event that has a magnitude of 2 years return period. It is important to note that MESH-PRIMA was calibrated to fit the streamflow observations only and no calibration was conducted to fit the non-contributing area of MESH-PRIMA to the PFRA map. The non-contributing area map of MESH-PRIMA is dynamic, and changes based on the magnitude of the event. The dynamic non-contributing area maps can be seen as an update of the currently used non-contributing area map over the studied basin and the entire prairie region in future.

Two performance metrics were used to assess the ability of MESH-PRIMA to replicate the spatial non-contributing area of the PFRA (as an observed data) for the 2008 spring snowmelt peak that is equivalent to a 2 years return period event, namely: the Hit Rate (HR) and the False Alarm Ratio (FAR) (Sampson *et al.*, 2015). These metrics are typically used to assess the spatial agreement between observations and predictions of flooded areas. However, they are used in this study to assess the spatial agreement between observed and simulated non-contributing area. The Hit Rate (HR) or the probability of detection is used to measure agreement between the simulated and observed non-contributing area without penalizing the model for overprediction the non-contributing areas. HR is expressed as follows:

$$HR = \frac{A_{sim} \cap A_{obs}}{A_{obs}} \tag{4.1}$$

where A_{sim} and A_{obs} are the simulated (MESH-PRIMA) and observed (PFRA) non-contributing areas. HR values range from 0 to 1 with a value of 1 indicating an exact match (spatially) between observed and simulated non-contributing areas. The False Alarm Ratio (FAR) was used to indicate overprediction of the non-contributing area (i.e., areas that were falsely predicted as non-contributing by MESH-PRIMA but were observed as contributing by the PFRA map) and is expressed as follows:

$$FAR = \frac{A_{sim} \setminus A_{obs}}{(A_{sim} \cap A_{obs} + A_{sim} \setminus A_{obs})} \tag{4.2}$$

FAR ranges from 0 to 1 with a value of 0 indicating exact match between observations and simulations with no false alarms (overprediction).

4.3.7 Flood Extents/Hazard Maps

The average inundation depth and the percentage of inundation (percentage of time a DEM cell was inundated) for each DEM cell in the study area, resulting from the water depth raster that MESH-PRIMA generated over the simulation period, were used to understand and quantify the spatial connectivity between land depressions and their ephemerality. The percentage of inundation (POI_i), for any DEM cell *i*, is expressed as:

$$POI_i = \frac{N_i}{N_t} \tag{4.3}$$

where N_i is the number of times a DEM cell i was inundated over the course of the simulation period and N_t is total number of time steps in MESH-PRIMA simulations. The percentage of inundation raster was used as an indication of the areas that are highly likely to be flooded either permanently or during flooding events. The average inundation depth over the simulation period (calculated for each DEM cell) and percentage of inundation combined were used as an indicator of pluvial/nival flood hazard over the basin.

4.4 Results and Analysis

4.4.1 Streamflow Performance (MESH-PDMROF vs MESH-PRIMA)

The streamflow simulation of MESH-PDMROF and MESH-PRIMA for SCRB are shown in Figure 4.3. The MESH-PDMROF model showed a good streamflow simulation during the calibration period as indicated by the NSE value (Table 4.2). However, during the validation period, the performance of MESH-PDMROF deteriorated and the model missed many events and had errors in estimating the magnitude of the remaining events. It had an unsatisfactory performance in replicating the overall hydrograph (NSE), peak flows (NSE_{OT}), low flows (NSE_{log}), and the runoff volume (PBIAS) in the validation period (Table 4.2).

The MESH-PRIMA model showed satisfactory streamflow simulation in the calibration period based on the performance metrics (Table 4.2) and was better able to capture small peaks (e.g., 2010) and overestimated the 2011 flooding event (Figure 4.3). Even though the calibration period length was smaller than that of the validation period, the performance of MESH-PRIMA improved further in the validation period and the model was able to capture peak flow events, especially the 2014 spring snowmelt and summer events (Figure 4.3). MESH-PRIMA shows satisfactory performance in replicating the overall hydrograph, and low flows in the calibration and validation periods (NSE, and NSE_{log}, respectively, Table 4.2). It also shows satisfactory and good simulation of the peak flows as indicated by NSE_{OT} (Table 4.2) for the calibration and validation periods, respectively, and a satisfactory performance in preserving the total runoff volume during the calibration period. However, the performance was affected during the validation period (PBIAS, Table 4.2). MESH-PRIMA underestimated the runoff volume in the validation period because it missed some peaks (e.g., summer 2012 and 2016) and underestimated the magnitude of the 2015 and 2017 peak flows (Figure 4.3). None of the two models (Figure 4.3) nor the behavioral runs of MESH-PRIMA (Figure 4.4) were able to capture the correct magnitude of the events. This was caused by some underestimation in the CaPA precipitation compared to available observations (Figure C.2) for those specific events. It was also shown that CaPA underestimates summer rainfall when compared against observations in another prairie basin (Budhathoki *et al.*, 2020). When CaPA was used to drive the MESH model, the simulations completely miss or underestimate summer and sometimes winter events in multiple prairie and non-prairie basins (M. Mekonnen *et al.*, 2014; Davison *et al.*, 2016; Budhathoki *et al.*, 2020). Overall, MESH-PRIMA showed an improved streamflow and peak flow simulation compared to MESH-PDMROF. Although the performance of the latter was better in the calibration period, MESH-PRIMA outperformed MESH-PDMROF in the overall simulation period, especially in the validation period when looking at the hydrograph (Figure 4.3) and the performance metrics (Table 4.2).

The streamflow of the SCRB is complex and the results are satisfactory by MESH-PRIMA model, given that a low optimization budget was used to calibrate the model and the underestimation in CaPA precipitation. It can be clearly seen that the incorporation of PRIMA within MESH improved the streamflow simulation of the MESH model compared to MESH-PDMROF. Both AIC and BIC for MESH-PRIMA were smaller than that of MESH-PDMROF (Table 4.2), which indicates that the higher degrees of freedom is not the reason why MESH-PRIMA had good performance, rather it is because MESH-PRIMA simulated the actual characteristics of the basin. Since PDMROF is a conceptual algorithm, it did well when it was forced to replicate the observation (i.e., during the calibration period). However, it was unable to preserve the same good performance in the validation period. MESH-PRIMA showed narrow uncertainty bounds and it had an acceptable agreement with the observed flows. The uncertainty bounds include 73 % of the observed flows within the entire study period. 275 model simulation out of the 1,000 runs of model calibration were identified as behavioral runs. The remaining of the simulated flows were not captured within the uncertainty bounds of the model, which might be caused by the inaccurate forcing fields as mentioned above (Figure 4.4). The mean simulated flows, averaged from the behavioral streamflow simulations, showed satisfactory performance to replicate the observed flows as assessed by the performance measures (Figure 4.4). An uncertainty plot for MESH-PDMROF is not presented as the model failed to show behavioral flow simulations for the entire period. More details on the comparison of MESH-PDMROF and MESH-PRIMA is provided in the discussion section.

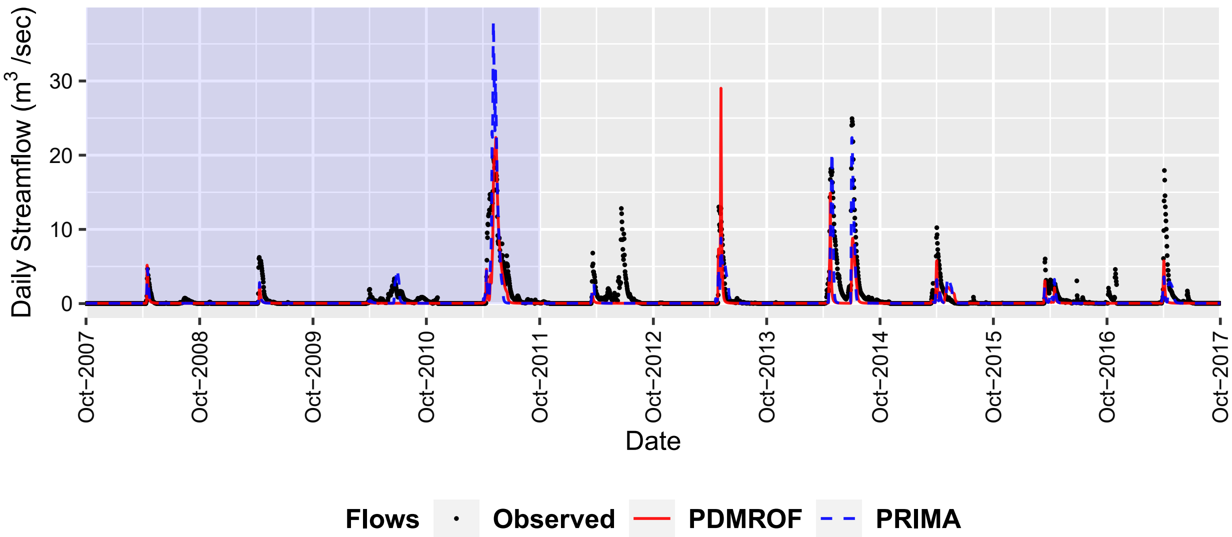

Figure 4.3: Daily simulated streamflow hydrographs of MESH-PDMROF and MESH-PRIMA for SCRB. The blue shaded area represents the calibration period, and the remaining is the validation period.

Table 4.2: Performance measures of daily streamflow for MESH-PDMROF and MESH-PRIMA. AIC and BIC were calculated for the full study period.

	MESH-PDMROF		MESH-PRIMA	
	Calibration	**Validation**	**Calibration**	**Validation**
NSE	0.67	0.34	0.51	0.58
NSE_{OT}	0.71	0.40	0.55	0.65
NSE_{log}	0.54	0.31	0.54	0.40
PBIAS (%)	49.37	72.21	27.06	57.00
AIC ($x10^3$)	4.57		3.95	
BIC ($x10^3$)	4.61		4.00	

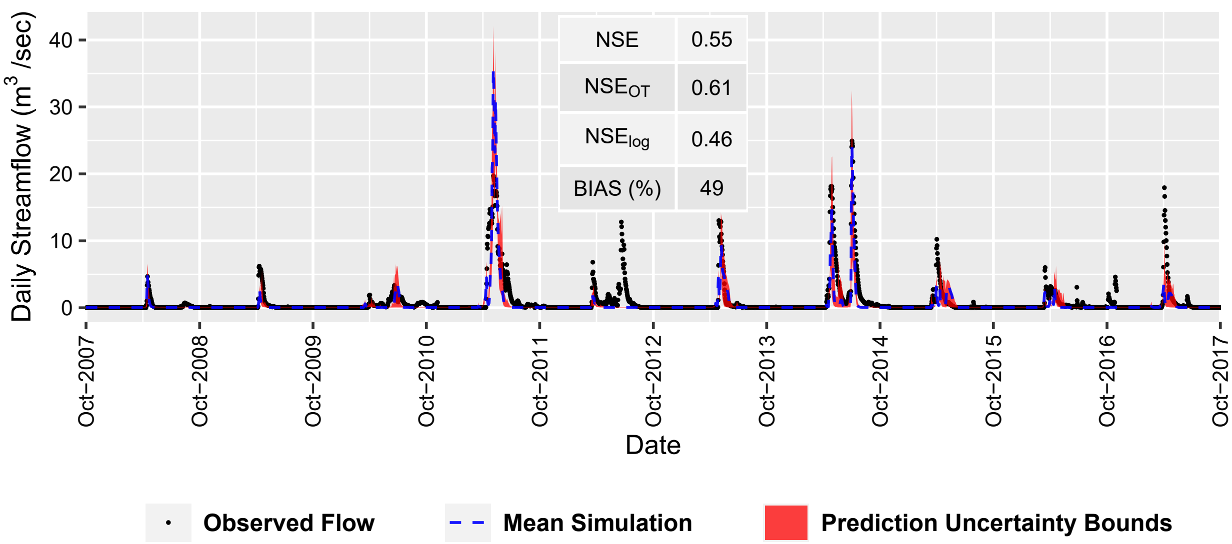

Figure 4.4: The prediction uncertainty bounds with the mean simulated flows of MESH-PRIMA models against observed flows for SCRB. Numbers show the performance metrics for the mean simulated flows for the entire simulation.

4.4.2 Dynamic Non-Contributing Area Map Generated by MESH-PRIMA

The spatial extent of the non-contributing area of the basin can be obtained from MESH-PRIMA only since MESH-PDMROF does not explicitly solve for the non-contributing area over the basin. Overall, the simulated non-contributing area for 2008 showed a good agreement with the observed PFRA map, especially for the northern and north-western parts of the basin (Figure 4.5). The simulated non-contributing area of 2008 replicated the PFRA map with a HR value of 0.90. MESH-PRIMA slightly overestimated the non-contributing area when compared to the PFRA map, especially the area south of the two streams confluence with a FAR of 0.10 (Figure 4.5). These areas have many depressions that are clearly visible on available satellite images and the used DEM, with no prominent streams that can connect them to the main river. Thus, it can be assumed that this area is unlikely to contribute flow to the river network for events with such a low magnitude. Due to MESH-PRIMA's ability to fit the PFRA map well, the prediction of non-contributing area of MESH-PRIMA is accurate and sound. Consequently, MESH-PRIMA was used to investigate the non-contributing areas for different events during the simulation period.

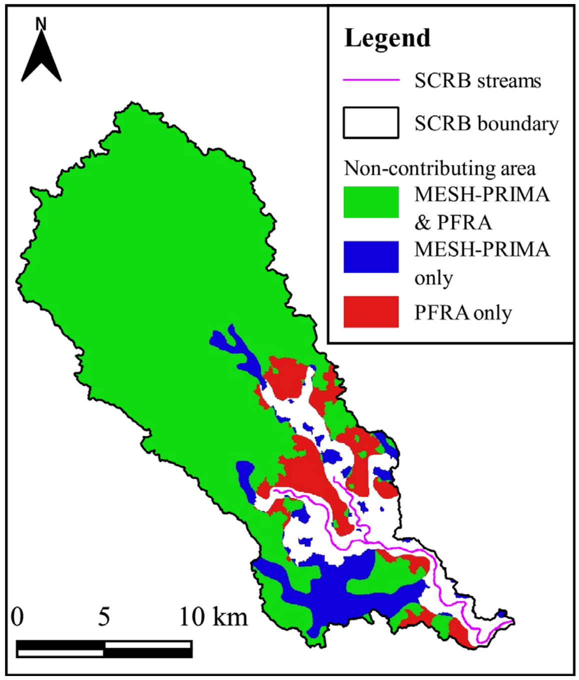

Figure 4.5: A map showing the agreement between the non-contributing area resulting from MESH-PRIMA for spring snowmelt period of 2008 and the static non-contributing area map of PFRA as a benchmark data. Green areas represent matching of the non-contributing area between observed and simulated, blue areas represent non-contributing area predicted by MESH-PRIMA only, red areas represent non-contributing area identified from the observations only.

The non-contributing area maps generated by MESH-PRIMA that correspond to peak spring snowmelt events for different years in the simulation period are shown in Figure 4.6. The spatial extent of the non-contributing area changes from year to year based on the storage in the depressions. Flood years (e.g., 2011, 2013, and 2014) have small non-contributing area with 2014 being the smallest. Low flow years (e.g., 2008 to 2010 and 2016) have greater non-contributing area extents compared to flood years (Figure 4.6). The river-bank area always contributes flow to the river network during both low flow and flood years as it has direct connection to the streams/outlet and no depressions can retain water.

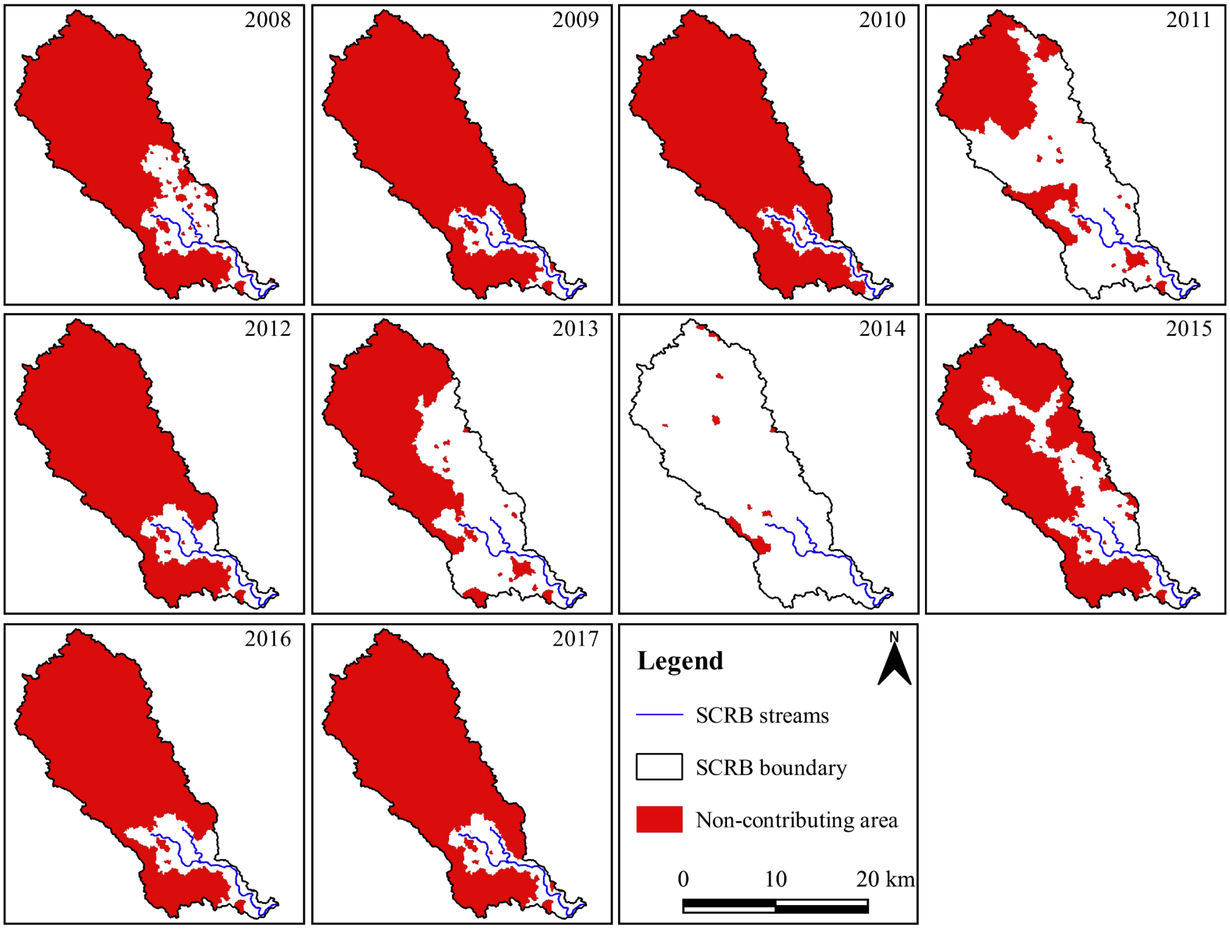

Figure 4.6: The spatial non-contributing area predicted by MESH-PRIMA that corresponds to the spring snowmelt peak time for different years in the simulation period.

4.4.3 Contributing Area, Storage, and Streamflow Curves

The relationship between the average ponded depth (storage) and the fractional contributing area of the SCRB for the different hydrologic years based on MESH-PDMROF and MESH-PRIMA is shown in Figure 4.7. MESH-PDMROF did not show hysteresis nor nonlinearity in the relationship between the contributing area and the average ponded depth over the basin. MESH-PDMROF almost followed the same linear curve during filling and emptying the potholes as indicated by increasing or decreasing the storage (Figure 4.7). On the other hand, MESH-PRIMA showed a clear non-linear and hysteretic clockwise loop for different years. The shape of the relationship is very different from year to year in MESH-PRIMA as it is a function of the storage. The contributing area increase with the increase in storage (wetting phase of potholes) in a clockwise direction, especially for high flow years such as 2011 and 2014. In flood years, the contributing area increase until the total basin contributes flow to the outlet (e.g., 2014). The removal of water from the potholes due to infiltration and/or evaporation (drying of potholes) can cause sudden reduction in the contributing area in a clockwise direction in almost all years (Figure 4.7). Nested hysteretic loops are found when there were multiple consecutive wetting and drying cycles due to significant snowmelt or rainfall events of the years (e.g., 2011, 2014, and 2015, Figure 4.7).

MESH-PDMROF assumes that the basin has no contributing area and the entire basin does not contribute flow if the depressions are near empty (small ponded depths, Figure 4.7). On the other hand, MESH-PRIMA assumes that there is a minimum contributing area (riverbank area) that always contributes flow to the outlet, even when the depressions are near empty (small ponded depth). MESH-PDMROF ignores the fact that defined streams/rivers and their banks always contribute flow to the outlet, and this has to be considered in SCRB that has a well-developed river. It is known that the relationship between contributing area and ponded depth is non-linear and hysteretic (Shook and Pomeroy, 2011). Since MESH-PRIMA shows the non-linear hysteretic relationship between contributing area and ponded depth (Figure 4.7), it is simulating the actual signature of the prairie landscape characteristics.

Both MESH-PDMROF and MESH-PRIMA show non-linear and clockwise hysteretic relationship between contributing area and streamflow in different years (Figure 4.8) and this is very different from the ones in Figure 4.7. There are some instances where a high streamflow is associated with low or medium contributing area (e.g., 2011 and 2014 for both models). This shows the contribution from interflow (from the third soil layer) and baseflow (from the bottom of the soil column) to the stream network directly. The non-contributing area was defined based on the connection between potholes that occur mostly due to surface water (for MESH-PDMROF) and surface and interflow from the first two soil layer (MESH-PRIMA) and it does not account for the contribution from third soil layers or from the bottom of the soil column. The high streamflow that was associated with almost 0.97 contributing area fraction for 2014 in MESH-PRIMA (Figure 4.8) is associated with the spring snowmelt peak flow of that year in which, the flood was generated by surface runoff between depression. On the other hand, the high streamflow associated with small contributing area of almost 0.25 for 2014 is associated with the summer event of 2014, which was driven mainly by contribution from the third soil layer ($ROFS_3$) and the baseflow from the bottom of the soil column (ROFB) that contribute directly to the river (Figure 4.8). This is very important as it shows the usefulness of land surface models, which can help in tracing and investigating different flood triggering mechanisms in the prairies.

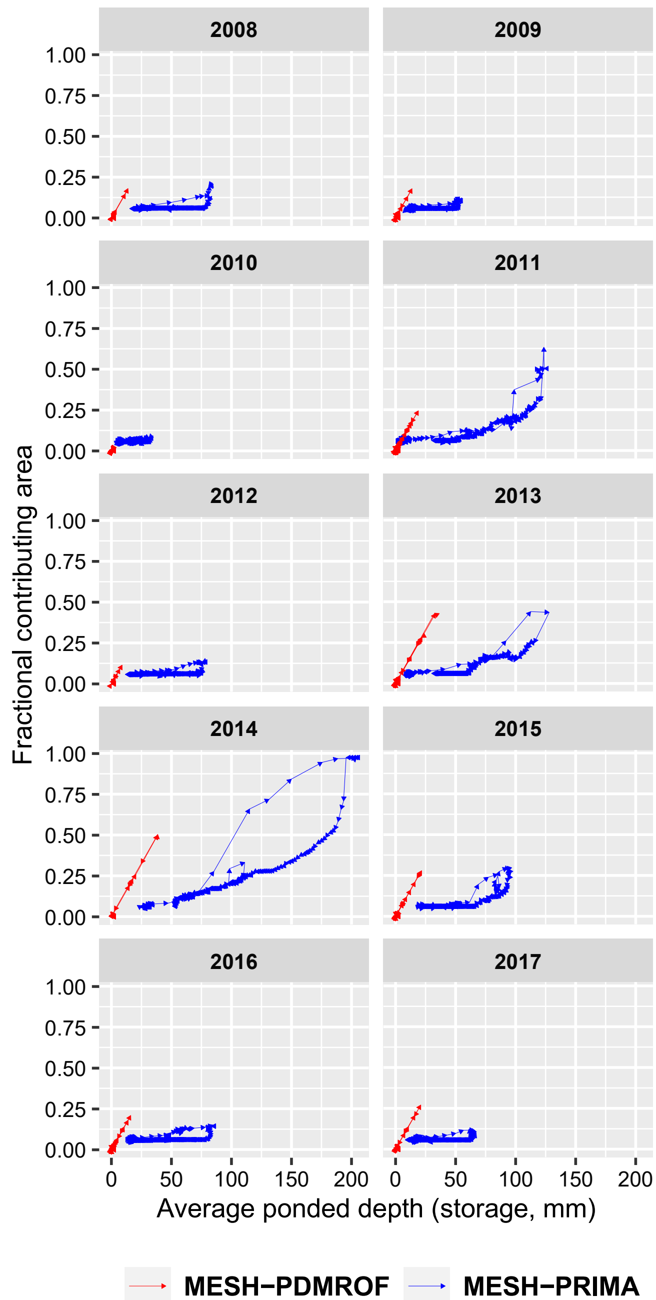

Figure 4.7: The fractional contributing area and average ponded depth (storage) over the basin for the different years in SCRB based on MESH-PDMROF and MESH-PRIMA. Each plot refers to a specific hydrologic year with arrows showing the direction of the loop.

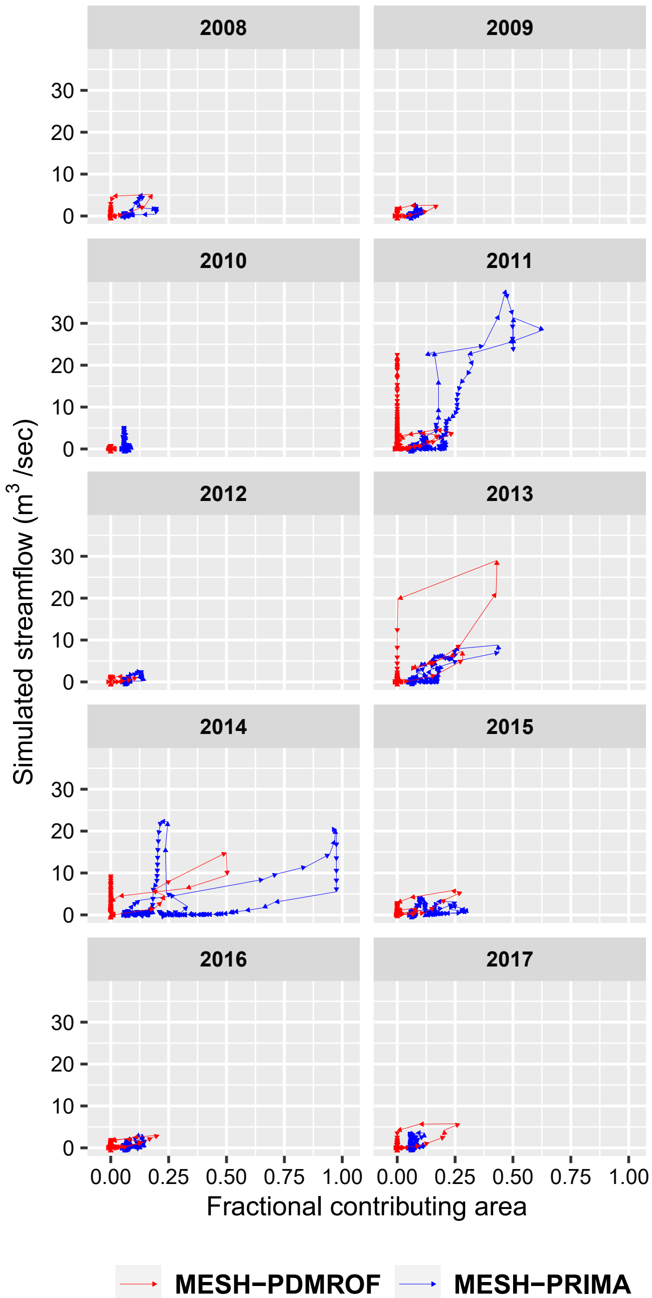

Figure 4.8: The fractional contributing area and simulated streamflow for the different years in SCRB for MESH-PDMROF and MESH-PRIMA. Each plot shows refers to a specific hydrologic year with arrows showing the direction of the loop.

4.5 Discussion

4.5.1 On the Relationship Between Streamflow Performance, Storage, and Contributing Area (PRIMA vs PDMROF)

MESH-PRIMA showed an improved and successful simulation of the streamflow compared to MESH-PDMROF (Figure 4.3 and Table 4.2) and also was able to identify the spatial distribution of water (Appendix C, Section C.3) and the spatial non-contributing area over the landscape (Figure 4.6). MESH-PRIMA also showed improved flood simulation (flood magnitude, timing, and pluvial/nival flooding extents), which is needed to assess non-fluvial flooding impacts. Such information, especially the pluvial/nival flooding extents, cannot be obtained using MESH-PDMROF. MESH-PRIMA is more computationally demanding compared to MESH-PDMROF as it needs to redistribute the water over very fine grid cells and due to the amount of information that it produces. Although a low computational budget was used to calibrate the models (e.g., 1,000 model trial), MESH-PRIMA showed potential to simulate the complex prairie hydrology-hydraulics. This also shows the robustness of MESH-PRIMA as it was able to show satisfactory to good simulation of streamflow and peak flow using a small number of trials for model calibration. Increasing the computational budget should further improve the streamflow simulation results.

PDMROF is a conceptual component and it is based on certain simplifying assumptions that make it partially valid for the prairie region. The most important and critical assumption that affects the simulation of PDMROF is that it assumes that the depressions are sorted in an ascending order with the smallest depression being close to outlet. This is partially true but in many cases in the prairies and in SCRB, the distribution of the depressions varies over the basin and it might be difficult to link the size of the depression to the proximity to the outlet. Further, the parameters of PDMROF are conceptual parameters, which means that it is difficult to relate these parameters to field observations. This also affects the simulation of PDMROF as it might need more model calibration trials to improve the streamflow simulation. More importantly, PDMROF is unable to simulate the hysteretic relationship between contributing area and ponded depth, which further affects its theoretical credibility as well as its ability to capture the complexities of the potholes and consequently, the streamflow.

On the other hand, PRIMA can be considered as a physically based algorithm that simulates the complexities of the prairie potholes. It simulates the fill-spill and merge-split mechanisms between depressions in a fully distributed and dynamic manner. Further, it shows potential to simulate the hysteretic relationship between contributing area and storage. The only parameter inside PRIMA itself is manning's roughness coefficient, which can be related to field observations when they are available. Even if roughness value is not known, a low computational budget for model calibration can be sufficient to arrive at a good simulation of flow and the corresponding inundation extents.

Figure 4.7 suggests that the relationship between contributing area and storage (average ponded water depth) is non-linear and the shape of the curve changes based on the storage of the potholes. The relationship has a different non-linear behavior for different years, and it might be difficult to come up with a single equation that can describe this relationship during different hydrologic years/events of varying magnitude. This shows why conceptual algorithms (i.e., PDMROF) have difficulties in producing acceptable flow simulation since they use a fixed equation to describe the relation between contributing area and storage. Further, It is important to differentiate between the hysteresis in the contributing area and storage curves (Figure 4.7) and the contributing area and streamflow curves (Figure 4.8). A model that can predict the first is simulating the actual physics and connections among depressions (e.g., MESH-PRIMA). However, the latter hysteretic relationship is unlikely related to the ability to simulate the dynamics or actual conditions of the depressions correctly. MESH-PDMROF failed to show hysteretic relationship in Figure 4.7, and consequently, did not show satisfactory streamflow simulation. However, it showed hysteresis in the contributing area and streamflow relationship (Figure 4.8). The hysteretic relation in Figure 4.8 is caused by the effect of flow routing in the channel. It is known that the relationship between active contributing area and the streamflow is hysteretic even for non-prairie watersheds (Nippgen *et al.*, 2015) and this is caused by the effect of the routing that changes the contributing area, for the same flow, on the rising and falling limb of the hydrograph. Another possible reason for the hysteresis in that curve is the contribution from baseflow to the streamflow, which may associate low contributing area to high streamflow caused by that contribution (Figure 4.8).

4.5.2 Progression of Flooding and Pluvial/Nival Flooding Hazard in The Prairies

Observations related to the spatial distribution of water over SCRB are not publicly available to be used to further validate/assess the simulation of water distribution over the basin by MESH-PRIMA. However, it was assumed that MESH-PRIMA simulated the flooding extents in potholes reasonably well since it successfully simulated both the streamflow and the non-contributing area compared to observations. Therefore, the results of the model were used to investigate the spatial extents of pluvial/nival flooding over the basin. It was shown that a flood can be triggered by different responses from surface and/or subsurface flow. The 2011 spring flood event was generated by a combined contribution from surface (flow between depressions) and subsurface flow. The 2014 spring flood event was mainly driven by contribution from surface flow. The magnitude of different components controlling the generation of flow (e.g., snowpack depth, antecedent moisture conditions of the pothole and soil, available energy to melt the snowpack) can be manipulated to investigate which combination generates high or low flow. Such information would help in further understanding of the complex prairie hydrology and flood/flow generation in the prairies using the proposed physically based model (MESH-PRIMA) in future studies.

Average inundation depth map (Figure 4.9) can be generated and used to explore the possible connections between potholes. It can be noticed also that most of the potholes in the basin are ephemeral (having very shallow to shallow depth with very low to low percentage of inundation time, Figure 4.9) while the deep potholes are constantly wet as indicated from the same figure. The depressions are connected through very shallow flow paths/areas that are ephemeral/intermittent (as indicated by the percentage of inundation plot, Figure 4.9). Once these connections are established, many potholes can merge to form larger depressions and increase the contributing area significantly (e.g., central and northern parts of the basin; Figure C.3 for 2014, and average inundation depth in Figure 4.9).

Maps similar to the average inundation depth or the percentage of inundation time generated by MESH-PRIMA can be generated under storms (conditions) of known probabilities to produce hazard maps such as the one shown in Figure C.3 for 2014 flood. Such information, in pothole dominated areas, has not been studied extensively and are needed to help practitioners, decision makers, and the public in assessing the situation of the agricultural, residential, and commercial properties that reside near potholes. The hazard maps are important in assessing the urban expansion and investigating future development locations. Such maps are also valuable in assessing the vulnerability of different areas in the basin to floods, which can contribute to the reduction of the associated flooding risks in the prairie environment.

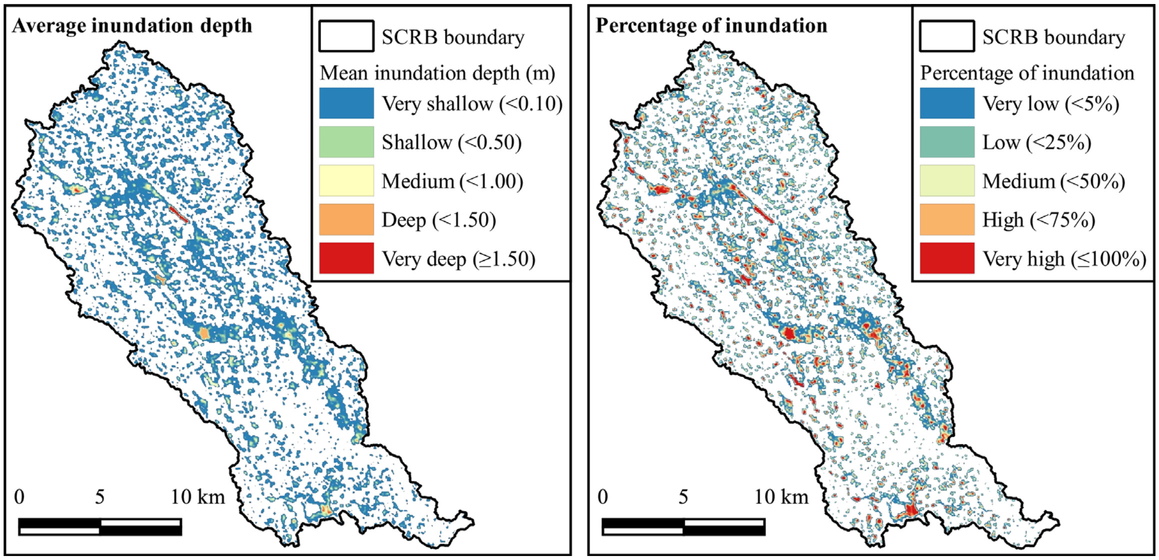

Figure 4.9: Maps showing the average inundation depth and the percentage of inundation for each DEM grid cells in SCRB over the course of the simulation.

4.6 Conclusions

The MESH model was modified by adding a physically based algorithm (PRIMA) to improve the representation of prairie potholes and the non-contributing area dynamics in land surface models. The performance of MESH-PRIMA and the MESH model with its current prairie algorithm (MESH-PDMROF) was tested on the Smith Creek Research Basin (SCRB) in Saskatchewan, Canada. MESH-PRIMA showed improved streamflow and peak flow simulation in the SCRB compared to MESH-PDMROF. More importantly, MESH-PRIMA simulated the potholes in a fully dynamic and distributed manner and was able to identify the spatial distribution of water and the spatial extents of the non-contributing area over the basin. MESH-PRIMA showed non-linear and hysteretic relationship between the contributing area and the ponded water depth, unlike MESH-PDMROF that failed to show the same behavior. The non-contributing area map generated by MESH-PRIMA for an event with a magnitude of a 2-year return period showed a good agreement with the commonly used PFRA static non-contributing area map. MESH-PRIMA generated dynamic non-contributing area maps that change based on the magnitude of the event. The flooding extents over the basin generated by MESH-PRIMA can be used to assess pluvial/nival flood hazard over the basin.

The use of PFRA map in assessing the non-contributing area of different basins in the prairies is valuable but it is limited to low flow events and it cannot be used during floods. The dynamic non-contributing area maps, which can be generated by MESH-PRIMA, would be useful in assessing/predicting the outflow/contributing area from the basins for different events. Such maps would be valuable in re-evaluating the different basins in the prairie region. This can help both researchers and practitioners in a quick estimation of the contributing area when full hydrologic modelling of the basin is not readily available.

The developed MESH-PRIMA model can be seen as a coupled hydrologic-hydraulic modelling platform. The incorporation of PRIMA within MESH improves its capabilities as a research tool (for example, to investigate different flood triggering mechanisms), and as a prediction tool. The new MESH-PRIMA model can be used to understand the actual spatiotemporal dynamics of the hydrologic connectivity in the prairies, which can lead to understanding of the prairie flood triggering mechanisms under different conditions and should be useful in assessing the impacts of climate change on the prairie hydrology. It can also help in updating the static non-contributing area map of the prairie in the future.

4.7 Acknowledgment

The financial support of the Natural Sciences and Engineering Research Council of Canada (NSERC) strategic network through the Canadian FloodNet research network is acknowledged (Grant number: NETGP451456-13). The funding of the Department of Civil, Geological and Environmental Engineering, University of Saskatchewan devolved scholarship is greatly appreciated. Compute Canada is acknowledged for providing the computing facilities to run the MESH model. The MESH code is available on the MESH wiki knowledge page (https://wiki.usask.ca/display/MESH/Releases). The OSTRICH toolkit was downloaded from http://www.civil.uwaterloo.ca/envmodelling/Ostrich.html. Whitebox tools was downloaded from https://jblindsay.github.io/ghrg/WhiteboxTools/download.html, and there is also a frontend package available in R and Python to run it.

4.8 References

Ahmed MI, Elshorbagy A, Pietroniro A. 2020a. Toward Simple Modeling Practices in the Complex Canadian Prairie Watersheds. Journal of Hydrologic Engineering 25 (6): 04020024 DOI: 10.1061/(ASCE)HE.1943-5584.0001922

Ahmed MI, Elshorbagy A, Pietroniro A. 2020b. A novel model for storage dynamics simulation and inundation mapping in the prairies. Environmental Modelling & Software 133 (August): 104850 DOI: 10.1016/j.envsoft.2020.104850

Alavi N, Bélair S, Fortin V, Zhang S, Husain SZ, Carrera ML, Abrahamowicz M. 2016. Warm Season Evaluation of Soil Moisture Prediction in the Soil, Vegetation, and Snow (SVS) Scheme. Journal of Hydrometeorology 17 (8): 2315–2332 DOI: 10.1175/JHM-D-15-0189.1

Anteau MJ, Wiltermuth MT, van der Burg MP, Pearse AT. 2016. Prerequisites for Understanding Climate-Change Impacts on Northern Prairie Wetlands. Wetlands 36: 299–307 DOI: 10.1007/s13157-016-0811-2

Bharath R, Elshorbagy A. 2018. Flood mapping under uncertainty: a case study in the Canadian prairies. Natural Hazards 94 (2): 537–560 DOI: 10.1007/s11069-018-3401-1

Brimelow J, Stewart R, Hanesiak J, Kochtubajda B, Szeto K, Bonsal B. 2014. Characterization and assessment of the devastating natural hazards across the Canadian Prairie Provinces from 2009 to 2011. Natural Hazards 73 (2): 761–785 DOI: 10.1007/s11069-014-1107-6

Budhathoki S, Rokaya P, Lindenschmidt K-E, Davison B. 2020. A multi-objective calibration approach using in-situ soil moisture data for improved hydrological simulation of the Prairies. Hydrological Sciences Journal 65 (4): 638–649 DOI: 10.1080/02626667.2020.1715982

Chu X, Yang J, Chi Y, Zhang J. 2013. Dynamic puddle delineation and modeling of puddle-to-puddle filling-spilling-merging-splitting overland flow processes. Water Resources Research 49 (6): 3825–3829 DOI: 10.1002/wrcr.20286

Chu X, Zhang J, Chi Y, Yang J. 2010. An Improved Method for Watershed Delineation and Computation of Surface Depression Storage. Watershed Management 2010: 333–342 DOI: doi:10.1061/41143(394)100

Davison B, Pietroniro A, Fortin V, Leconte R, Mamo M, Yau M. 2016. What is Missing from the Prescription of Hydrology for Land Surface Schemes? Journal of Hydrometeorology: 2013–2039 DOI: 10.1175/JHM-D-13-055.1

Dumanski S, Pomeroy JW, Westbrook CJ. 2015. Hydrological regime changes in a Canadian Prairie basin. Hydrological Processes 29 (18): 3893–3904 DOI: 10.1002/hyp.10567

Elshorbagy A, Bharath R, Lakhanpal A, Ceola S, Montanari A, Lindenschmidt KE. 2017. Topography-and nightlight-based national flood risk assessment in Canada. Hydrology and Earth System Sciences 21 (4): 2219–2232 DOI: 10.5194/hess-21-2219-2017

Evenson GR, Golden HE, Lane CR, D'Amico E. 2016. An improved representation of geographically isolated wetlands in a watershed-scale hydrologic model. Hydrological Processes 30 (22): 4168–4184 DOI: 10.1002/hyp.10930

Fang X, Minke A, Pomeroy J, Brown T, Westbrook C, Guo X. 2007. A Review of Canadian Prairie Hydrology : Principles , Modelling and Response to Land Use and Drainage Change A Review of Canadian Prairie Hydrology : Principles , Modelling and Response to Land Use and Drainage Change. Review Literature And Arts Of The Americas (July)

Fang X, Pomeroy JW, Westbrook CJ, Guo X, Minke AG, Brown T. 2010. Prediction of snowmelt derived streamflow in a wetland dominated prairie basin. Hydrology and Earth System Sciences 14 (6): 991–1006 DOI: 10.5194/hess-14-991-2010

Godwin RB, Martin FRJ. 1975. Calculation of gross and effective drainage areas for the Prairie Provinces. In Canadian Hydrology Symposium - 1975 Proceedings, 11-14 August 1975, Winnipeg, Manitoba.Associate Committee on Hydrology, National Research Council of Canada; 219–223.

Gray DM, Landine PG. 1988. An energy-budget snowmelt model for the Canadian Prairies. Canadian Journal of Earth Sciences 25 (8): 1292–1303 DOI: 10.1139/e88-124

Haghnegahdar A, Tolson BA, Craig JR, Paya KT. 2015. Assessing the performance of a semi-distributed hydrological model under various watershed discretization schemes. Hydrological Processes 29 (18): 4018–4031 DOI: 10.1002/hyp.10550

Hayashi M, van der Kamp G, Rosenberry DO. 2016. Hydrology of Prairie Wetlands: Understanding the Integrated Surface-Water and Groundwater Processes. Wetlands 36: 237–254 DOI: 10.1007/s13157-016-0797-9

Hayashi M, Van Der Kamp G, Rudolph DL. 1998. Water and solute transfer between a prairie wetland and adjacent uplands, 2. Chloride cycle. Journal of Hydrology 207 (1–2): 56–67 DOI: 10.1016/S0022-1694(98)00099-7

Hayashi M, Van Der Kamp G, Schmidt R. 2003. Focused infiltration of snowmelt water in partially frozen soil under small depressions. Journal of Hydrology 270 (3–4): 214–229 DOI: 10.1016/S0022-1694(02)00287-1

van der Kamp G, Hayashi M. 2009. Groundwater-wetland ecosystem interaction in the semiarid glaciated plains of North America. Hydrogeology Journal 17 (1): 203–214 DOI: 10.1007/s10040-008-0367-1

Kouwen N, Soulis ED, Pietroniro A, Donald J, Harrington RA. 1993. Grouped response units for distributed hydrologic modelling By N . Kouwen , l Member , ASCE , E . D . Soulis , 2 A . Pietronirofl J . Donald , 4 captured using small subbasin elements often called hydrologic response units (HRUs) (Leavesley and Stannar. Journal of Water Resources Planning and Management 119 (3): 289–305

Lespinas F, Fortin V, Roy G, Rasmussen P, Stadnyk T. 2015. Performance Evaluation of the Canadian Precipitation Analysis (CaPA). Journal of Hydrometeorology 16 (5): 2045–2064 DOI: 10.1175/jhm-d-14-0191.1

Lindsay JB. 2016. Whitebox GAT: A case study in geomorphometric analysis. Computers and Geosciences 95: 75–84 DOI: 10.1016/j.cageo.2016.07.003

MacLean A. 2009. Calibration and analysis of the MESH hydrological model applied to cold regions.University of Waterloo.

Mailhot J, Bélair S, Lefaivre L, Bilodeau B, Desgagné M, Girard C, Glazer A, Leduc A, Méthot A, Patoine A, et al. 2006. The 15-km version of the Canadian regional forecast system. Atmosphere-Ocean 44 (2): 133–149 DOI: 10.3137/ao.440202

Martin FRJ. 2001. Addendum No. 8 to Hydrology Report #104, Agriculture and Agri-Food Canada PFRA Technical Service: Regina, Saskatchewan, 109 pp. PFRA Hydrology Division, 1983, The Determination of Gross and Effective Drainage areas in the Prairie Provinces, Hydrology Repo.

Mekonnen BA, Mazurek KA, Putz G. 2016. Incorporating landscape depression heterogeneity into the Soil and Water Assessment Tool (SWAT) using a probability distribution. Hydrological Processes 30 (13): 2373–2389 DOI: 10.1002/hyp.10800

Mekonnen MA, Wheater HS, Ireson AM, Spence C, Davison B, Pietroniro A. 2014. Towards an improved land surface scheme for prairie landscapes. Journal of Hydrology 511: 105–116 DOI: 10.1016/j.jhydrol.2014.01.020

Mengistu SG, Spence C. 2016. Testing the ability of a semidistributed hydrological model to simulate contributing area. Water Resources Research 52 (6): 4399–4415 DOI: 10.1002/2016WR018760

Nasab MT, Singh V, Chu X. 2017. SWAT modeling for depression-dominated areas: How do depressions manipulate hydrologic modeling? Water (Switzerland) 9 (1) DOI: 10.3390/w9010058

Nippgen F, McGlynn BL, Emanuel RE. 2015. The spatial and temporal evolution of contributing areas. Water Resources Research 51 (6): 4550–4573 DOI: 10.1002/2014WR016719

Pietroniro A, Fortin V, Kouwen N, Neal C, Turcotte R, Davison B, Verseghy DL, Soulis ED, Caldwell R, Evora N, et al. 2007. Using the MESH modelling system for hydrological ensemble forecasting of the Laurentian Great Lakes at the regional scale. Hydrology and Earth System Sciences 3 (4): 1279–1294 DOI: 10.5194/hess-11-1279-2007

Pomeroy JW, Gray DM, Brown T, Hedstrom NR, Quinton WL, Granger RJ, Carey SK. 2007. The cold regions hydrological model: A platform for basing process representation and model structure on physical evidence. Hydrological Processes 21 (19): 2650–2667 DOI: 10.1002/hyp.6787

Sampson CC, Smith AM, Bates PD, Neal JC, Alfieri L, Freer JE. 2015. A high-resolution global flood hazard model. Water Resources Research 51 (9): 7358–7381 DOI: 10.1002/2015WR016954

Shaw DA, Pietroniro A, Martz LW. 2013. Topographic analysis for the prairie pothole region of Western Canada. Hydrological Processes 27 (22): 3105–3114 DOI: 10.1002/hyp.9409

Shaw DA, Vanderkamp G, Conly FM, Pietroniro A, Martz L. 2012. The Fill-Spill Hydrology of Prairie Wetland Complexes during Drought and Deluge. Hydrological Processes 26 (20): 3147–3156 DOI: 10.1002/hyp.8390

Shawn Matott L-. 2017. OSTRICH – An Optimization Software Toolkit for Research Involving Computational Heuristics Documentation and User ' s Guide by L . Shawn Matott , Ph . D . State University of New York at Buffalo Center for Computational Research: 79 Available at: www.eng.buffalo.edu/~lsmatott/Ostrich/OstrichMain.html.

Shook K, Pomeroy J, van der Kamp G. 2015. The transformation of frequency distributions of winter precipitation to spring streamflow probabilities in cold regions; case studies from the Canadian Prairies. Journal of Hydrology 521: 394–409 DOI: 10.1016/j.jhydrol.2014.12.014

Shook K, Pomeroy JW, Spence C, Boychuk L. 2013. Storage dynamics simulations in prairie wetland hydrology models: Evaluation and parameterization. Hydrological Processes 27 (13): 1875–1889 DOI: 10.1002/hyp.9867

Shook KR, Pomeroy JW. 2011. Memory effects of depressional storage in Northern Prairie hydrology. Hydrological Processes 25 (25): 3890–3898 DOI: 10.1002/hyp.8381

Soulis EDD, Snelgrove KRR, Kouwen N, Seglenieks F, Verseghy DLL. 2000. Towards closing the vertical water balance in Canadian atmospheric models: Coupling of the land surface scheme class with the distributed hydrological model watflood. Atmosphere-Ocean 38 (1): 251–269 DOI: 10.1080/07055900.2000.9649648

Tolson BA, Shoemaker CA. 2007. Dynamically dimensioned search algorithm for computationally efficient watershed model calibration. Water Resources Research 43 (1): 1–16 DOI: 10.1029/2005WR004723

Verseghy D. 2011. Class – the canadian land surface scheme (version 3.6)

Verseghy DL. 1991. Canadian Land Surface Scheme for GCMS I. Soil model. International Journal of Climatology 11: 111–133 DOI: 10.1002/joc.3370110202

Verseghy DL, McFarlane NA, Lazare M. 1993. Class—A Canadian land surface scheme for GCMS, II. Vegetation model and coupled runs. International Journal of Climatology 13 (4): 347–370 DOI: 10.1002/joc.3370130402

Yassin F, Razavi S, Wheater H, Sapriza-Azuri G, Davison B, Pietroniro A. 2017. Enhanced identification of a hydrologic model using streamflow and satellite water storage data: A multicriteria sensitivity analysis and optimization approach. Hydrological Processes 31 (19): 3320–3333 DOI: 10.1002/hyp.11267

Chapter 5 Summary and Conclusions

5.1 Summary and Conclusions

In this thesis a set of models to improve streamflow, especially peak flow, prediction in the complex environment of the prairie pothole region was modified and/or developed. The first model is the new conceptual HYdrological model for Prairie Region (HYPR), which was proven to improve the streamflow and flood simulation in multiple prairie watersheds using limited input variables in a computationally efficient manner. The second model is the novel Prairie Region Inundation MApping model (PRIMA), which was shown to improve the simulation of the pothole complexities, while being computationally efficient compared to other available hydraulic models (e.g., WDPM). The third model is the modified land surface model (MESH-PRIMA), which showed an improved hydrograph and flood simulation compared to the existing MESH-PDMROF and was able to identify the spatiotemporal changes of the non-contributing area and water extents over the landscape.

HYPR was proposed based on the HBV model for hydrological processes representation and PDMROF for potholes representation. The HYPR model that can predict floods with good accuracy, within a timely manner and without the need for expensive computational resources, was presented in ***Chapter 2***. HYPR showed potential to predict peak flows and the overall hydrograph with narrow uncertainty bounds in the 10 watersheds of the Qu'Appelle River Basin in Saskatchewan, Canada. Sensitivity analysis showed that HYPR is working in a way that agrees with our conceptual understanding of prairie hydrology, with snow processes and pothole storage controlling the runoff, which eventually contributes to the streamflow. The selection of the objective function for model calibration had a significant effect on changing the sensitivity of HYPR model parameters. Therefore, the selection of the objective function can affect the model outputs. Although HYRP is a conceptual model, it showed potential to simulate some internal hydrological processes (e.g. snow on ground). The results of HYPR (***Chapter 2***) showed that conceptual models can work in the prairie environment when they account for pothole complexities.

PRIMA was developed as a simple hydraulic routing model in the prairies. PRIMA uses a set of rules and Manning's equation to route the flow over prairie landscape and quantify flow direction and magnitude. PRIMA can simulate the spatiotemporal changes in the inundation extents because it calculates travel time and losses (infiltration and evaporation) from ponded water. PRIMA showed potential to simulate the pothole complexities and identify the actual spatial distribution and connections among potholes when compared against remote sensing data over two prairie watersheds namely, St. Denis National Wildlife Area and Smith Creek Research Basin, in Saskatchewan, Canada. The results of PRIMA (***Chapter 3***) showed that antecedent moisture conditions of potholes can change both the outflow of the watershed and the associated flooding extents significantly. Further, PRIMA provided almost the same results as the existing WDPM, but with a significant reduction in the computational cost. The computational efficiency of PRIMA, along with its ability to calculate travel times, gives it the potential to be used for better understanding of the effects of potholes on the system response in various prairie watersheds of different size, location, and complexities.

The MESH land surface model was modified in ***Chapter 4*** by coupling it with PRIMA (MESH-PRIMA) to improve the streamflow and flood simulation within more complex land surface models. In MESH-PRIMA model, MESH handles the vertical energy and water budget calculations while PRIMA routes the water over the depressions and quantify the storage and net outflow reaching the stream network. MESH-PRIMA provided improved simulations of both the overall hydrograph and peak flows when compared with MESH-PDMROF over Smith Creek Research Basin in Saskatchewan, Canada. MESH-PRIMA allows for identifying the spatial non-contributing areas and the pluvial-nival flooding extents. More importantly, MESH-PRIMA showed a non-linear and hysteretic relationship between contributing area and watershed storage, unlike PDMROF that failed to show the same behavior. This property of MESH-PRIMA provides additional assurance that the model improves the simulation accuracy based on capturing the physics and subtle dynamics of prairie hydrology.

5.2 Research Significance and Contributions

HYPR fills in an important gap in operational hydrology in the prairie region (***Chapter 2***); it is the first lumped-conceptual model that can be used to predict prairie flows while accounting for the potholes' complexities. This model can help practitioners in predicting prairie flows and floods with limited input data and computational cost, which might be useful for real-time flood forecast. It has been argued for many decades that only complex physically based models have the potential to work in the prairies. However, with its ability to produce good streamflow simulations and acceptable internal hydrologic processes representation, HYPR can prove that conceptual lumped hydrologic models have the potential to work in the prairie environment for practical and engineering purposes. Due its many advantageous, HYPR is currently being used by the Saskatchewan water security agency for flow forecasting. HYPR is also available freely within the Raven hydrologic modelling framework (http://raven.uwaterloo.ca/).

PRIMA fills an important gap in the simulation of pothole storage dynamics and the pluvial-nival flood mapping in the prairie region (***Chapter 3***). It is the first distributed hydraulic routing model in the prairie region that can route the water over prairie landscapes (using their actual spatial distribution) and calculate the travel time of water in a computationally efficient manner. PRIMA is useful in urban planning and decision-making process in the prairies. This model can contribute to the management of flood risk in the prairie environment by predicting the pluvial-nival flood hazard over the landscape. The outputs of PRIMA can help public, practitioners, and decision makers in assessing the situation of the agricultural, residential, and commercial properties at stake and investigating possible areas of future development.

MESH-PRIMA is a leap forward towards proper simulation of earth system dynamics by implementing a hydraulic routing component to handle the pothole complexities (PRIMA) within the MESH modelling framework (***Chapter 4***). MESH-PRIMA is the first coupled hydrologic-hydraulic model to be used and applied to the Canadian prairie region and it is the first model that simulates the potholes using their actual spatial distribution in a fully dynamic and distributed manner. MESH-PRIMA can be used to provide both hydrologic and hydraulic outputs. It produces good streamflow and flood simulation based on sound physical representation of the complex prairie processes and generates flood inundation/hazard and non-contributing area maps, which have not been investigated extensively before. The dynamic non-contributing area maps, which can be generated by MESH-PRIMA, are useful in assessing and predicting the outflow and the contributing area from watersheds for different hydrologic events. The incorporation of PRIMA within MESH can transform MESH into a hydrologic exploratory and modeling-to-understand platform rather than only a prediction tool. The new MESH-PRIMA model can be used to understand the actual spatiotemporal dynamics of the hydrologic connectivity in the prairies, which leads to understanding the prairie flood triggering mechanisms under different conditions and should be useful in assessing the impacts of climate change on the prairie hydrology. MESH-PRIMA can be integrated with Regional Climate Models (RCMs), General Circulation Model (GCMs), or Numerical Weather Prediction models (NWP) to provide in more reliable simulation of climate projections and better assessment of the impact of climate change on the hydrology of the prairies. MESH-PRIMA is freely available on the MESH wiki knowledge page (https://wiki.usask.ca/display/MESH/Releases).

This study has both scientific and practical contributions as indicated above. the developed models can be used for efficient pothole storage dynamics simulation, inundation mapping, streamflow, and peak flow prediction in the prairies. The models can run in a wide spectrum of input/modelling purposes, ranging from limited data, conceptual-lumped-operational mode to a detailed physically based, research mode. The knowledge and outcome of this study contribute towards the success of the streamflow simulation, more accurate estimation of peak flows, the identification of the pothole flooding, and proper representation of earth system dynamics, which are valuable for research, management, and planning purposes.

5.3 Limitations

The proposed models showed potential to produce good flood simulations and pluvial-nival flooding extent maps. However, some investigations are needed to further understand the limitations of these models. HYPR is a lumped conceptual hydrologic model and consequently, some of its parameters represent a group of watershed properties and thus, it might be difficult to map them to actual observations. Since HYPR is a lumped model, the spatial variability of internal hydrological variables cannot be represented. Its applicability is limited to medium to small sized watersheds. However, if a large-scale watershed is of interest, it would be easy to model each sub-watershed independently and implement HYPR's routing algorithm to rout flows from each sub-watershed to the watershed outlet.

PRIMA needs to store the information (e.g., water ponding depth, travel time, soil moisture, accumulated snow) at each grid cell within the watershed, however, it is currently coded to support serial processing. Thus, with PRIMA's current setup, its applicability is limited to small to medium sized watershed. PRIMA uses simple vertical water budget calculations to account for infiltration and evaporation. Therefore, PRIMA as a stand-alone model might not be useful in conducting full hydrologic simulations, but MESH-PRIMA solves this problem. The limitation on the size of the basin (as indicated for PRIMA) also applies to MESH-PRIMA as PRIMA needs to rout the flows on the landscape, which is represented in PRIMA using a DEM. If PRIMA is recoded to support parallel processing or coded in a different programming language (e.g. agent-based modelling approach), its running time can be reduced significantly. Hence, the applicability of PRIMA and MESH-PRIMA can be extended to large-scale watersheds. Such computational improvements can make MESH-PRIMA applicable to the entire prairie pothole region.

5.4 Future Research

The results provided in this thesis are promising and the developed models and methodologies showed potential to contribute to solving the problem of flood prediction and the pluvial-nival flooding extent mapping in the Canadian prairie region. Accordingly, the developed models can be used in the future for investigating ideas or directions as follows.

It would be useful to test the predictive capabilities of the fully physically based MESH-PRIMA against the fully conceptual HYPR to understand the limitations and strengths of both models. The evaluation of both models should not be limited to streamflow simulation only; but it should include other important hydrologic variables (e.g., accumulated snow, evapotranspiration rates, soil moisture). This will provide better assessment of the range of applicability and suitability of both modeling approaches in the prairies. This comparison should be useful in understanding when and where each model fails/successes in predicting the hydrograph and can highlight areas for future model developments or improvements.

The PRIMA model needs to be recoded to support parallel processing, which can reduce its computational cost and running time significantly. This will facilitate further extensive testing of PRIMA on various watersheds of varying size, complexities, and DEM resolution. This will also help in extending the application of the physically based MESH-PRIMA model to large-scale watersheds and maybe to the entire prairie region. This can help in investigating the changes in the relationship between the contributing area and storage for different basins in the prairies using PRIMA. The different shapes of this relationship can help in assessing the complexities in different prairie basins. More importantly, this can help in the development/proposing of a more computationally efficient and possibly a conceptual algorithm that can replicate this relationship. This algorithm can be used as a new runoff generation algorithm that can accurately simulate the complexities of the prairie potholes and should improve the prairie streamflow prediction with a reduced computational cost compared to PRIMA.

It is important to assess the impacts of climate change, landuse change, artificial drainage of potholes on the response of prairie watersheds using MESH-PRIMA. These issues are of critical importance for the future of water resources and agriculture in the prairies. Such tasks have not been really feasible without such a model like MESH-PRIMA.

The non-contributing area map needs to be updated to be dynamic and changes based on the magnitude of the hydrologic event using MESH-PRIMA. The dynamic non-contributing area obtained from MESH-PRIMA would be valuable in re-evaluating the different basins in the prairie region under different storm conditions. This can help both researchers and practitioners in a quick estimation of the contributing area when full hydrologic modelling of the basin is not readily available.

Understanding and quantifying the different flood triggering mechanisms under different antecedent moisture conditions using the MESH-PRIMA model is needed. The magnitude of different components (corresponding to different return periods) controlling the generation of flow (inputs) can be manipulated to investigate which combination generates high or low flow (output). For example, a 100-year snowpack depth, 50-year soil moisture, 200-year water storage in depression, etc. can be used as initial conditions for MESH-PRIMA. Then, the model can predict the outflow of the basin. The outflow can then be related to a specific return period. The relation between the inputs and outputs can be investigated and a set of curves can be generated using regression analysis. The generated curves can be used to assess the situation of the basin and provide an estimation of the expected flow based on the current moisture conditions. Such information would help in further understanding of the complex prairie hydrology and flood/flow generation in the prairies using the proposed physically based model (MESH-PRIMA) in future studies. This also can help in a quick assessment of the possible flood magnitude, when detailed hydrologic modelling is not feasible, which can contribute to the management of the associated flood risks.

Appendix A: Permissions for reusing published articles in Chapters 2 and 3

A.1 Permission from ASCE for reproduction of Chapter 2

10/21/2020 Information for ASCE Authors: Reusing Your Own Material

ASCE | LIBRARY

MENU

- Guidelines for Permission Request
- ASCE Terms and Conditions for Permissions Requests
- Request Permission Online (Copyright Clearance Center)
- STM Permission Guidelines
- Reuse Author's Own Material
- Open Access Options and Rights

REUSE AUTHOR'S OWN MATERIAL

As the original author of an ASCE journal article or proceedings paper, you are permitted to reuse your own content for another ASCE or non-ASCE publication.

The following restrictions apply:

- Permission is denied if you request to republish an entire article in an ASCE or a non-ASCE publication.
- Permission is denied if the requested content constitutes more than 25% of your work in a new publication.
- **Internet posting of the** *published version* **of your article is strictly prohibited.**
- If the request is for an online coursepack, the site must be password-protected.
- If you wish to photocopy your content, the total number of copies cannot exceed 100. If you need more than 100 copies, please contact ASCE Permissions directly.

If the content has been prepared by an employee within the scope of employment, the employer shall enjoy the same rights as the authors.

If the content was prepared under a U.S. government contract, the federal government shall have the rights under the copyright law to the extent required by the contract.

POSTING YOUR ARTICLE OR PAPER ONLINE

Published Article
Authors may post a PDF of the ASCE-published version of their work on their employers' *Intranet* with password protection.

Draft Manuscript
Authors may post the final draft of their work on open, unrestricted Internet sites or deposit it in an institutional repository when the draft contains a link to the bibliographic record of the published version in the ASCE Library or Civil Engineering Database. "Final draft" means the version submitted to ASCE after peer review and prior to copyediting or other ASCE production activities; it does not include the copyedited version, the page proof, or a PDF of the published version.

When posting online, please add the statement: "This material may be downloaded for personal use only. Any other use requires prior permission of the American Society of Civil Engineers. This material may be found at [URL/link of abstract in the ASCE Library or Civil Engineering Database]."

ASCE
American Society of Civil Engineers

1801 Alexander Bell Drive
Reston, VA 20191-4400
703-295-6300 | 800-548-2723

ASCE LIBRARY

ASCE

https://ascelibrary.org/page/informationforasceauthorsreusingyourownmaterial 1/2

Ahmed, Mohamed

From:	em.jrnheeng.3788.6ec990.aa2ebd33@editorialmanager.com on behalf of Michele Esposito <em@editorialmanager.com>
Sent:	Wednesday, October 21, 2020 8:50 AM
To:	Ahmed, Mohamed
Subject:	ASCE HEENG-4746R2— - [EMID:96c2f54cbf59b10d]

CAUTION: External to USask. Verify sender and use caution with links and attachments. Forward suspicious emails to phishing@usask.ca

Date: 10/21/2020
Manuscript #: HEENG-4746R2
Manuscript Title: Towards Simple Modelling Practices in the Complex Canadian Prairie Watersheds
Authors: Mohamed Ismaiel, MSc; Amin Elshorbagy, PhD; Alain Pietroniro, PhD

Dear Mr. Ahmed,

As an original author of an ASCE journal article or proceedings paper, you are permitted to reuse your own content (including figures and tables) for another ASCE or non-ASCE publication, provided it does not account for more than 25% of the new work.

Please note that you may only use the **final draft** of your paper. "Final draft" means the version submitted to ASCE after peer review and prior to copyediting or other ASCE production activities; it does not include the copyedited version, the page proof, a PDF, or full-text HTML of the published version.

A full credit line must be added to the material being reprinted. Please note in your credit that you are using the pre-production version of your paper, with permission from ASCE, and include the DOI (noted below). For reuse in non-ASCE publications, add the words "With permission from ASCE" to your source citation. For Intranet posting, add the following additional notice: "This material may be downloaded for personal use only. Any other use requires prior permission of the American Society of Civil Engineers. This material may be found at [URL/link of abstract in the ASCE Library or Civil Engineering Database]."

Kind regards,

Michele Esposito
Production Editor

A.2 Permission from Elsevier for reproduction of Chapter 3

Copyright Clearance Center RightsLink® Home Help Email Support Sign in Create Account

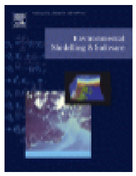

A novel model for storage dynamics simulation and inundation mapping in the prairies

Author: Mohamed Ismaiel Ahmed,Amin Elshorbagy,Alain Pietroniro
Publication: Environmental Modelling & Software
Publisher: Elsevier
Date: November 2020

Please note that, as the author of this Elsevier article, you retain the right to include it in a thesis or dissertation, provided it is not published commercially. Permission is not required, but please ensure that you reference the journal as the original source. For more information on this and on your other retained rights, please visit: https://www.elsevier.com/about/our-business/policies/copyright#Author-rights

BACK CLOSE WINDOW

Appendix B: Supplementary materials for Chapter 3

B.1 Pothole complexities and the non-contributing area map of the prairies

In the prairies, it is important to differentiate between runoff and streamflow (Shook *et al.*, 2015). Runoff in the prairies results in a mechanism known as "fill and spill", first identified in lakes in the Canadian shield (Spence and Woo, 2003) and later more formally characterized in the prairies (Shaw *et al.*, 2012), despite a long-term understating that this phenomenon existed. Each pothole traps surface runoff until it is filled. When a depression is filled, any further inputs of water release surface flows, which may eventually reach a stream channel, or contribute to another downstream pothole. Therefore, the majority of the prairies are designated as being non-contributing, as shown in Figure B.1, where they do not contribute flow to an outlet for events with a return period smaller than 2 years (Godwin and Martin, 1975).

The derivation of the non-contributing area map was quite subjective and based on a hydrologist understanding of the runoff and flow regime, which was derived from the visual interpretation of topographic contour maps. The government agencies in Canada and the USA used hard copy maps with coarse vertical resolution to identify depressions and their closed basins. The use of these maps leads to a high degree of uncertainty in identifying depressions and their contributing area. The uncertainty further increased when modelling a small-scale basin, in which these maps will not have sufficient vertical resolution to properly identify the depressions and their storage. Consequently, this leads to high degree of subjectivity, and the delineation of these maps can be different based on the individual assigned to each area, the scale of the basin, and the available data at that time. There is almost no standard method for contributing area delineation, which does not allow for objective delineation of the contributing area (Shaw *et al.*, 2013).

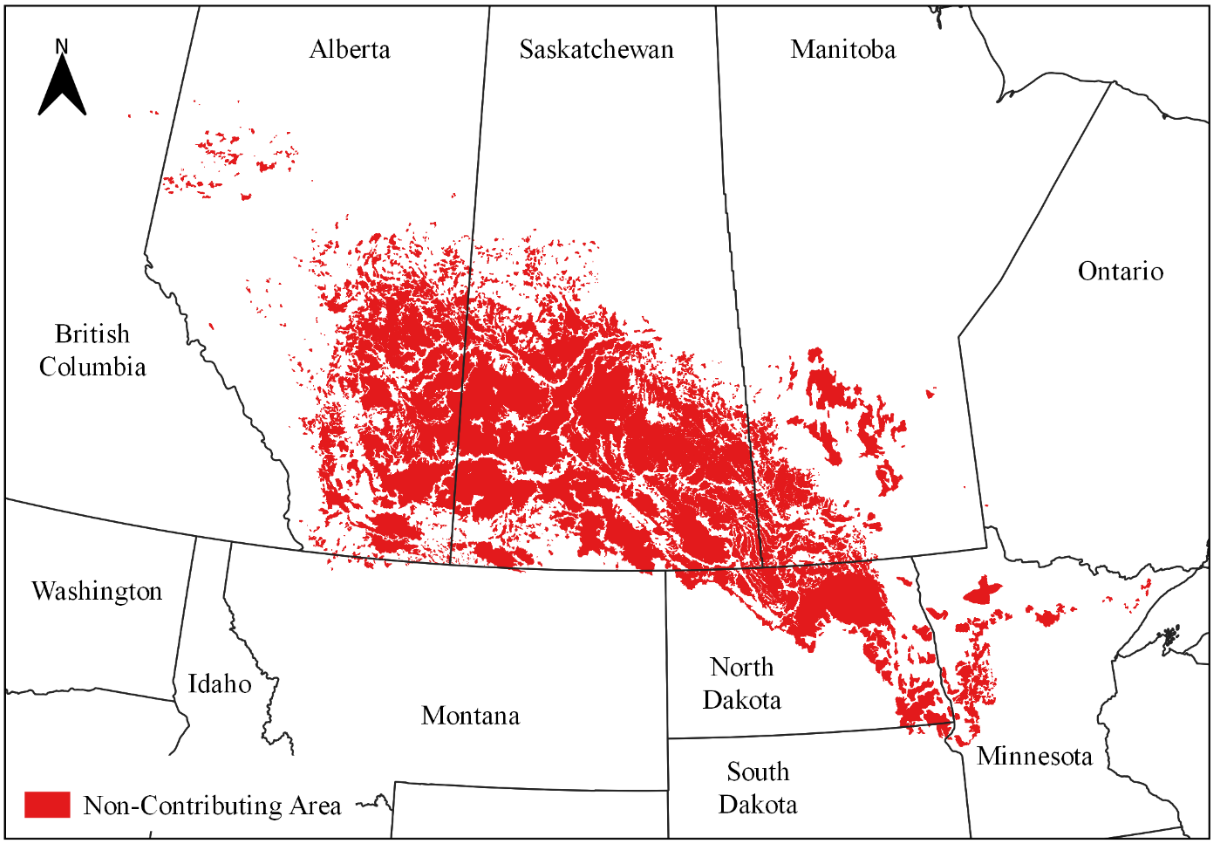

Figure B.1: A general layout of the extent of the non-contributing area in the prairies

B.2 A list of the implemented modification to develop PRIMA as an improved and computationally efficient CA-based hydrological routing model

Modification	PRIMA	CA approach	Reason
Cells involved in the water redistribution from the central cell.	Moore neighborhood rule (8 surrounding cells)	Von Neumann neighborhood rule (4 orthogonal surrounding cells)	For the CA approach, the water exchanges between the current (central) cell and the diagonal cells will require two additional iterations. Thus, we used the 8 surrounding cells to reduce the number of iterations required for convergence
The travel time calculations	The water velocity is calculated based on the fraction of water depth that is moving from cell to cell	Liu *et al.* (2015) used Manning's equation with the CA-method to calculate the velocity of water as a function of the full depth of water within a cell for an urban watershed	potholes trap most of the water and hence the water velocity calculations needed to be adjusted to account for the moving fraction of water depth
DEM cells order in solving	From highest elevation to lowest elevation	Based on their location in the provided DEM ascii file	PRIMA loops through the DEM cells from the highest to the lowest elevation to simulate the water movement from uplands to lowlands, and to reduce the required number of iterations

Modification	PRIMA	CA approach	Reason
Elevation and volume tolerance	Are implemented	N/A	This is introduced as an error measurement to terminate the run because the model may take thousands of iterations to make negligible changes in the water surface elevation
Drainage of water	From multiple cells on the main river.	From single-cell	Reduce the number of iterations because the water is removed from the system once it reaches the river. In this case, the model does not need to move the water along the stream to leave from the outlet. More details are provided in Section B.3.

B.3 A Novel Draining Approach within PRIMA

The computational efficiency of PRIMA in draining water was improved by a new method for specifying the outlet. The original draining of the excess water in PRIMA was done by removing the water through a single outlet cell or multiple cells near the outlet. The new draining approach drains the water from all of the river cells, i.e. the cells that lie within the stream channel. The river cells were identified as cells in DEM the were enclosed by the river polygon (that has an average 60 m width) identified from the available remote sensing data. Excess water is removed from the model once it reaches the river cells, which can reduce the number of iterations required for drainage, as the water does not have to be routed along the stream to leave from the outlet cell. The performance of the conventional and novel drain approaches of the PRIMA model was tested on the SCRB5 as it has a defined stream. The final water distribution after adding an arbitrary depth of water (100 mm) of water to the empty DEM of the SCRB5 with a tolerance of 1 mm was used to test the efficiency of the new drainage approach with 1 mm and 1 m^3 for the elevation and volume tolerance, respectively without using the losses component or the travel time calculations.

The number of iterations required to drain the excess water was decreased from 97,000 to 2,000 when the outlet cell was replaced by the river cells. The conventional drainage area is 25 m^2 (one cell), whereas the new drainage area was 0.85 km^2 (34,059 cells). The new drainage method increased the draining area by more than 34,000 times resulted in a reduction of the number of iterations by almost 48-fold.

The plots in Figure B.2 indicate that the spatial distributions of water depth were identical for both drainage methods, except for the region lying within the stream channel. The outflow cell approach was not able to effectively drain all the water in the stream. Using the original method, the upstream part of the river was not drained because water was being trapped upstream of a road that intersected the river and the DEM was not conditioned to represent the culvert. The use of the river outlet approach allowed the drainage of all water in the river and overcame the problem of existing culverts/bridges that would have to be manually burned into the DEM.

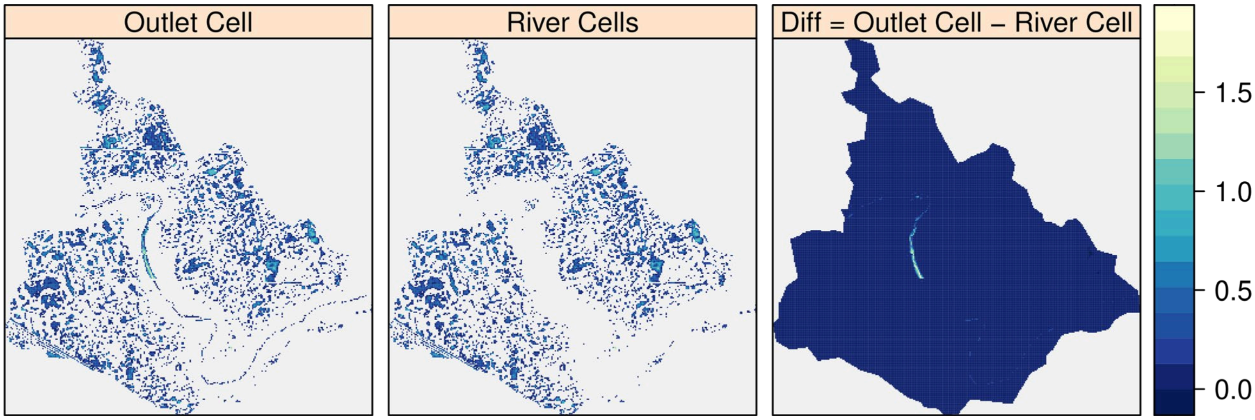

Figure B.2: The final water distribution of PRIMA after draining the excess water from adding 100 mm, using the traditional outlet cell and the new river cells approaches, and the difference between both cases.

The proposed drainage approach reduced the number of iterations dramatically for PRIMA. This made PRIMA computationally inexpensive, especially for areas with a defined stream network. Due to its efficiency, PRIMA can be used for inundation mapping purposes. More importantly, and given its ability to estimate the travel time of water, it has the potential to be implemented into hydrologic models, as a prairie runoff generation algorithm, for accurate simulation of the prairie spatiotemporal dynamics and connectivity.

B.4 Detailed comparison and discussion of PRIMA and WDPM Performance

B.4.1 Effect of elevation tolerance on the water distribution of PRIMA and WDPM models

The greater efficiency of PRIMA can be seen in the water extent plots in Figure B.3-a, especially for the area of the main river upstream of the outlet. Even for the very coarse elevation tolerances (100 to 1000 mm), PRIMA achieved good water distributions (i.e., close to the final solution). The water was not as effectively distributed by WDPM as there were minor creeks still connected to the main river in the basin, so they did not reach their equilibrium state. The use of different elevation tolerance had a significant effect on the water distribution in the main river, especially for WDPM, which needed a very fine tolerance to reach the solution. Figure B.3-b shows the differences between the water surfaces produced by PRIMA and WDPM. While most of the panels show small differences between the PRIMA and WDPM water depths, the panel for the 10 mm elevation tolerance's water extent difference was positive in the downstream and negative in the upstream part of the river, demonstrating that PRIMA moved more water downstream than did WDPM.

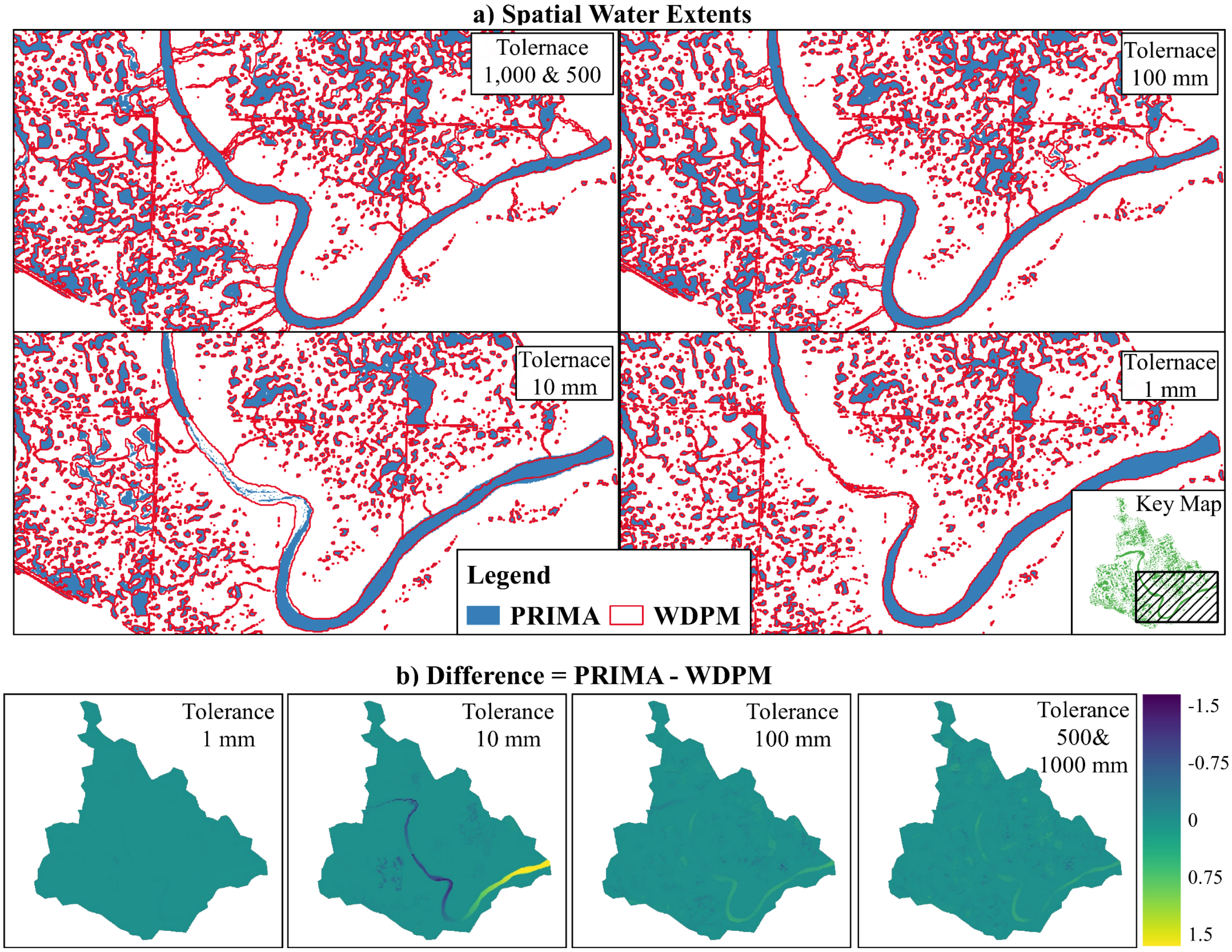

Figure B.3: (a) the spatial distribution of the water for the main river area upstream the outlet (hatched area in the keymap) at SCRB5 after adding 100 mm for different elevation tolerances for PRIMA and WDPM, as well as (b) the difference between water distributions resulting from both models. The color bar indicates the water depth in meters. The spatial distribution of water is identical for the coarse elevation tolerances (.>100 mm) for each model and hence the 1,000 mm tolerance was not plotted.

Figure B.4 shows the water depth change and the volume change (measured every 1,000 iterations) vs. the number of iterations for both models in the adding and draining tests using the 1 mm elevation tolerance, demonstrating how the models converge to their solutions. The top panel, representing the add test, shows that PRIMA initially converged more slowly, with greater depth change values than WDPM. After approximately 80,000 iterations, the PRIMA's depth change began to decrease quickly, and the model finished in one-third of the iterations required by WDPM.

The plot of the drain test (Figure B.4, middle panel) shows that, initially, the WDPM's depth change was slightly smaller than that of PRIMA, although both models showed very similar plots. At approximately 40,000 iterations, the PRIMA's depth change began to increase, until the model terminated suddenly at just under 100,000 iterations. The WDPM's depth change slowly increased after approximately 150,000 iterations, terminating at approximately 310,000 iterations; more than three times the number required by PRIMA. The changes in the drained volume for WDPM were smaller than that for PRIMA (Figure B.4, bottom panel), which also demonstrates the greater draining efficiency of PRIMA.

The use of different tolerance had a significant effect on the water extents of the WDPM model, especially for the main river. However, changing the tolerance had less effects on the water distribution over the pothole areas for both models. The WDPM model needed a very fine tolerance (1 mm) to move water efficiently near the SCRB5 outlet. However, PRIMA showed similar water extents for tolerances 10 and 1 mm, which proved its efficiency. This shows also that PRIMA can run without the need for a very fine tolerance, which can help in further reducing its computational cost.

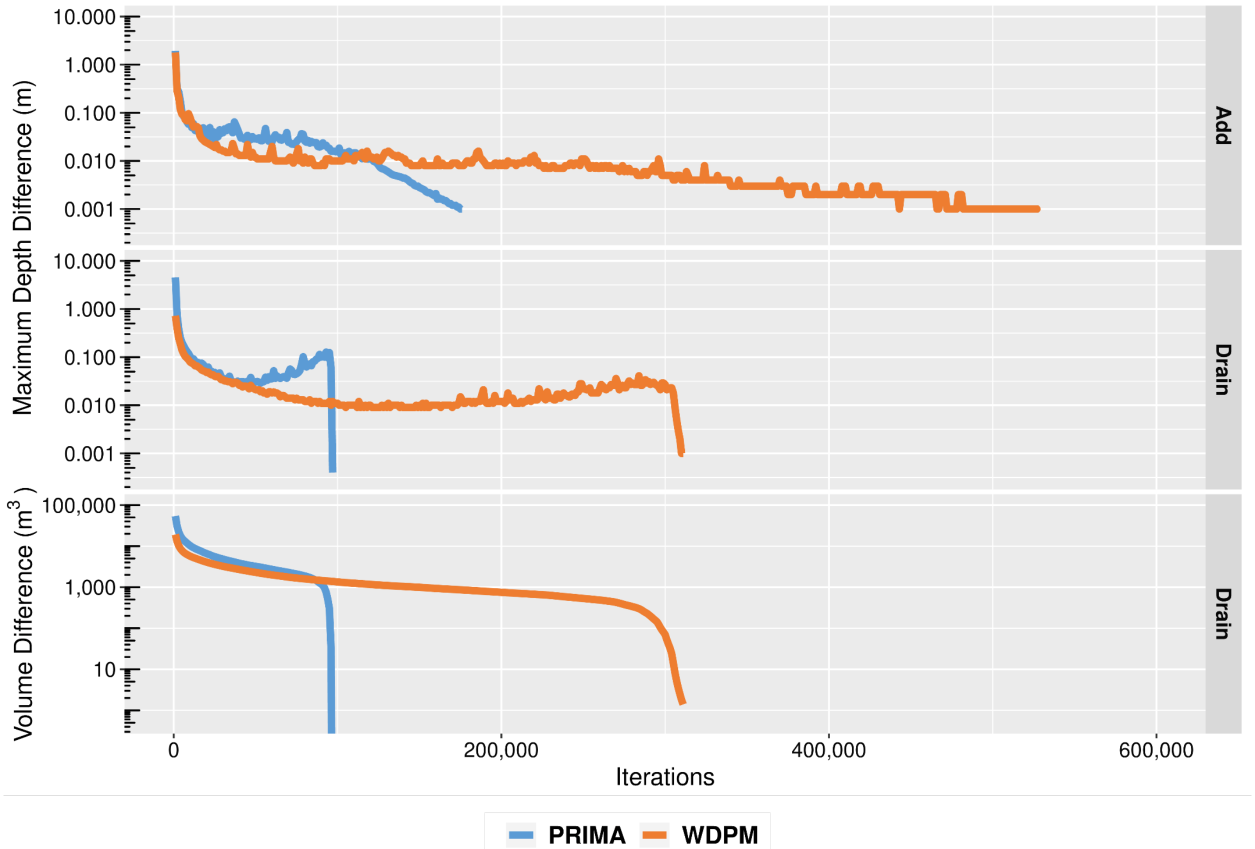

Figure B.4: Convergence of PRIMA and WDPM for SCRB5. The water depth change (m) for add and drain tests along with the change in the drained volume for the drainage test were used as an indication of the convergence of both models. Y-axes are logarithmic.

B.4.2 Why PRIMA Is More Computationally Efficient Than WDPM

It has been demonstrated that PRIMA is more computationally efficient than WDPM. An example from the SDNWA (Figure B.5) demonstrates why. The final water distributions after filling all potholes (adding 500 mm) and draining the excess water for both models were compared. For the add test, there were significant differences between the water distribution of both models with more water remaining upstream for WDPM. However, after draining the excess depth, the water distribution is almost identical for both models with a maximum difference of 0.7 mm. PRIMA efficiently moves water to the downstream part of the basin while running the add test with fewer iterations.

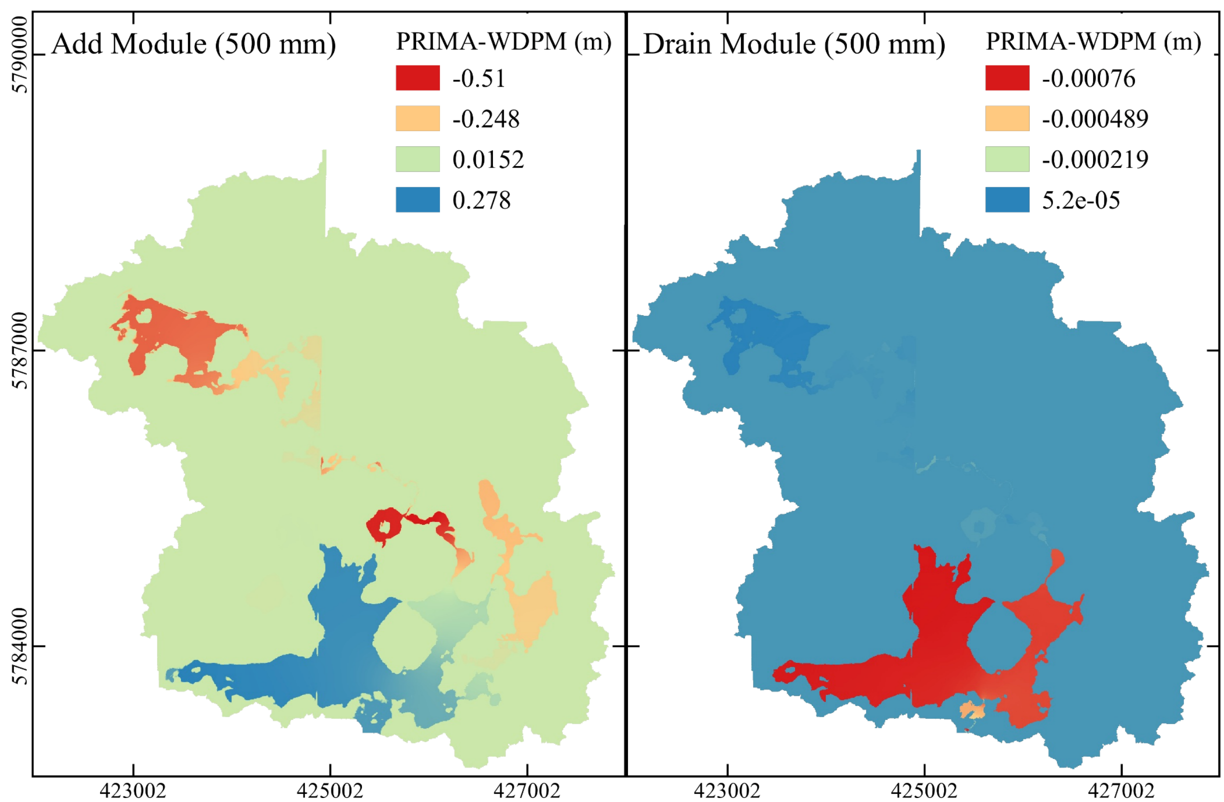

Figure B.5: Differences in the spatial water distributions of water depths between PRIMA and WDPM for adding 500 mm of water to the DEM (left) and draining the excess water from the outlet (right) for SDNWA. The projection is UTM-13.

A simple hypothetical example shown in Figure B.6 clearly demonstrates the efficiency of PRIMA. In this example, PRIMA needed one iteration to reach the final water distribution, where WDPM needed 26 iterations to arrive at the same conditions. Although there were only two surrounding cells containing water in the example, WDPM still distributed 1/8 of the difference to them, requiring WDPM to take many more iterations to reach the steady-state conditions.

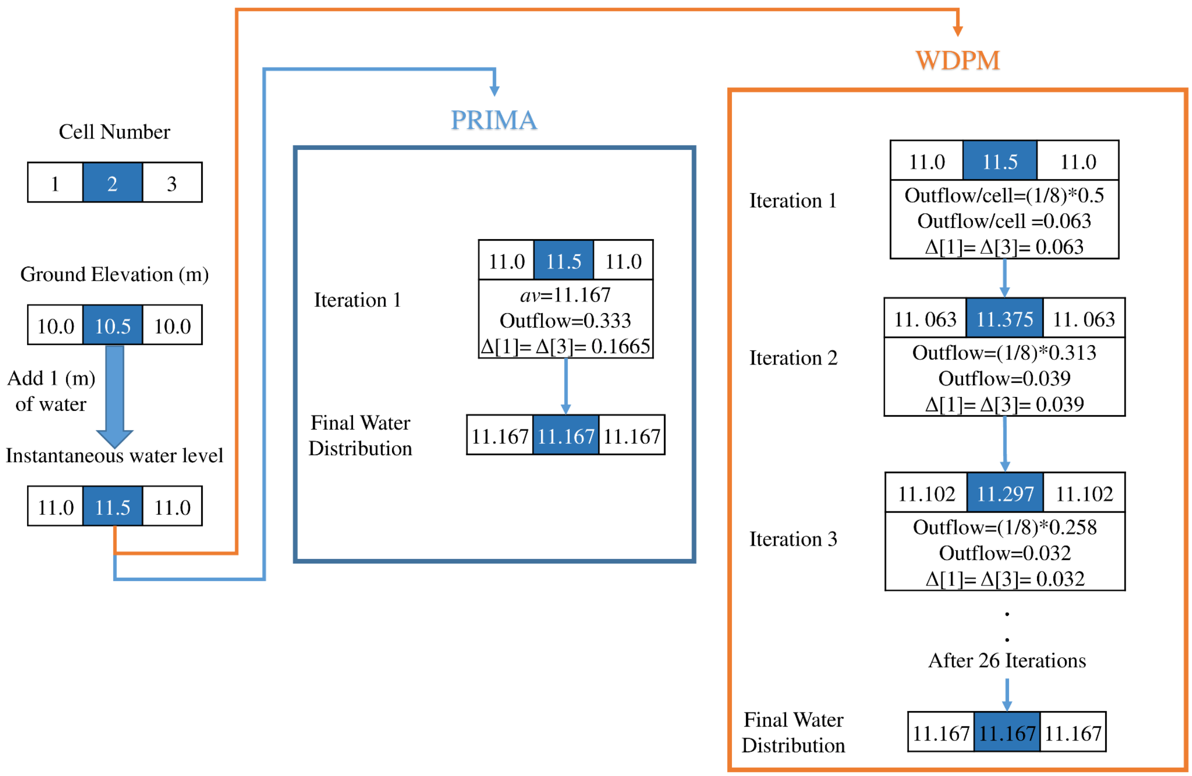

Figure B.6: A hypothetical example of the PRIMA and WDPM algorithms.

B.5 References

Godwin RB, Martin FRJ. 1975. Calculation of gross and effective drainage areas for the Prairie Provinces. In Canadian Hydrology Symposium - 1975 Proceedings, 11-14 August 1975, Winnipeg, Manitoba.Associate Committee on Hydrology, National Research Council of Canada; 219–223.

Liu L, Liu Y, Wang X, Yu D, Liu K, Huang H, Hu G. 2015. Developing an effective 2-D urban flood inundation model for city emergency management based on cellular automata. Natural Hazards and Earth System Sciences 15 (3): 381–391 DOI: 10.5194/nhess-15-381-2015

Shaw DA, Pietroniro A, Martz LW. 2013. Topographic analysis for the prairie pothole region of Western Canada. Hydrological Processes 27 (22): 3105–3114 DOI: 10.1002/hyp.9409

Shaw DA, Vanderkamp G, Conly FM, Pietroniro A, Martz L. 2012. The Fill-Spill Hydrology of Prairie Wetland Complexes during Drought and Deluge. Hydrological Processes 26 (20): 3147–3156 DOI: 10.1002/hyp.8390

Shook K, Pomeroy J, van der Kamp G. 2015. The transformation of frequency distributions of winter precipitation to spring streamflow probabilities in cold regions; case studies from the Canadian Prairies. Journal of Hydrology 521: 394–409 DOI: 10.1016/j.jhydrol.2014.12.014

Spence C, Woo MK. 2003. Hydrology of subarctic Canadian shield: Soil-filled valleys. Journal of Hydrology 279 (1–4): 151–166 DOI: 10.1016/S0022-1694(03)00175-6

Appendix C: Supplementary materials for Chapter 4

C.1 The connection between MESH and PRIMA

The following are the main steps conducted to calculate the streamflow in MESH-PRIMA for each time step:

1. CLASS calculates the vertical water and energy budget (e.g., snow ablation, infiltration to the soil, soil moisture, soil temperature, evapotranspiration, vegetation dynamics, etc.).
2. The lateral fluxes (i.e., surface runoff, interflow form the three soil layers, and baseflow from the bottom of the soil column) are calculated by WATROF.
3. Surface (ROFO) and interflow runoff from the first two soil layers ($ROFS_{1,2}$) are considered as input to the ponded water whereas infiltration and evaporation (calculated by MESH) are considered as losses from ponded depth.
4. The net water input to PRIMA is calculated as the difference between inputs and losses.
5. The net water input is passed to PRIMA and is added to the DEM.
6. PRIMA starts redistributing water from cell to cells over the DEM iteratively using the Water Redistribution and Routing (WRR) component. Each iteration of WRR (each loop over the DEM cells) includes the following (Ahmed et al., 2020b):
    a. The amount and direction of flow from cell to cell is obtained and the travel time is calculated based on the exchanged depth between neighboring cells based on the minimization algorithm and manning's equation from the WRR component.
    b. Any water reaching the stream network, identified in PRIMA as outlet cells on the main river, is removed from the system and stored as outflow.

c. The time step is calculated as the minimum travel time among all cells in the DEM.

d. PRIMA checks if the cumulative time step of PRIMA is greater than or equal to the current time step of MESH. If no, PRIMA re-iterates over the DEM to distribute water (start from step a) until the condition is met. If the condition is met (yes), then PRIMA stops redistributing water, and quantifies the net outflow depth as cumulative outflow/ number of DEM cells and the remaining average ponded depth over the basin (Σ water depth over all DEM cells/ number of DEM cell). The conversion from water depths over the DEM (ponded depth) to an average ponded depth (single value over the landscape, upscaling) is necessary to maintain mass balance and allow for communication between MESH and PRIMA (i.e., transfer of information from the micro scale grid of PRIMA to the meso scale grid MESH).

7. The average ponded depth from PRIMA is sent back to CLASS to be used for the next time steps in the calculations of the vertical water budget.
8. The net outflow depth from PRIMA and interflow runoff from the third soil column ($ROFS_3$) and baseflow runoff (ROFB) calculated by WATROF are passed to the routing component of MESH to be routed to the outlet and quantify the streamflow.

We assumed that $ROFS_3$ and ROFB will not change the storage in depressions because they occur on a relatively deep depth and most of the depressions have shallow depth. Even for deep depressions, we assumed that these runoff depths will not change storage inside the depressions as they will be treated as throughflow (Figure C.1).

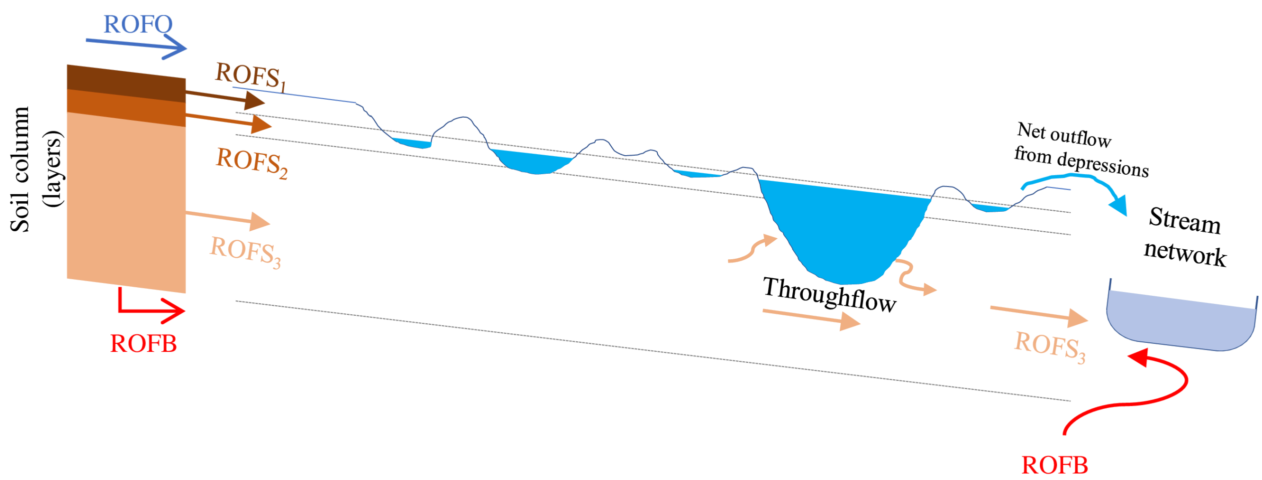

Figure C.1: Schematic representation of the interaction between lateral fluxes and depressions in MESH-PRIMA. The dashed lines represent the three soil layers.

C.2 Comparison of the observed and CaPA annual precipitation

The total annual precipitation from CaPA and the observation from the Langenburg station within SCRB are shown in Figure C.2. CaPA underestimated the precipitation of 2012 and 2016 with more than 100 mm. some underestimation was also found in 2017. The underestimated precipitation by CaPA caused MESH-PRIMA to underestimate and/or miss the flow events that correspond to these years. The rest of the years showed overestimation of the precipitation by CaPA (e.g., 2010 and 2014).

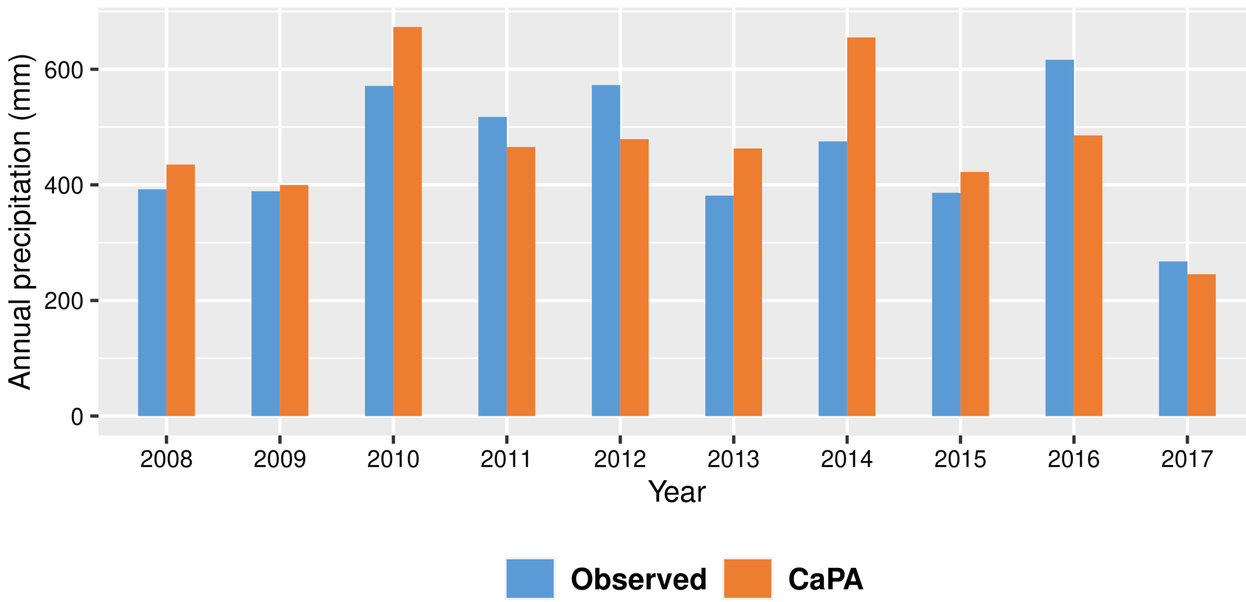

Figure C.2: The total annual precipitation from the Langenburg station (within the SCRB, ECCC station ID: 2941) and the CaPA field for each year in the simulation period. The Langenburg data were obtained from: https://climate.weather.gc.ca/historical_data/search_historic_data_e.html.

C.3 Flooding Extents of MESH-PRIMA in Dry and Wet Years

The flooding extents that correspond to the spring snowmelt peak of 2009 and 2014, which are a low flow (driest year in the simulation) and a flood year (wettest year in the simulation), respectively, are shown in Figure C.3. For the low flow year, the surface area of the depressions is small, and most depressions are isolated and did not reach their capacity. There was enough storage in the depressions to reduce the net outflow reaching the river network. For the 2014 flood year, both the surface area and stored water in depressions were significantly greater than that of the low flow year (Figure C.3). Most of the depressions are connected and formed larger depressions, especially in the central and norther parts of the basin (Figure C.3). In such a situation, any input to the basin will go directly to the river network as all depressions are full and there was no storage available to reduce the outflow. Further, the spatial distribution of water generated by MESH-PRIMA can be used as an indication of the pluvial/nival flood hazard in the basin. This information is useful as it can be used to develop flood risk management strategies in the basin.

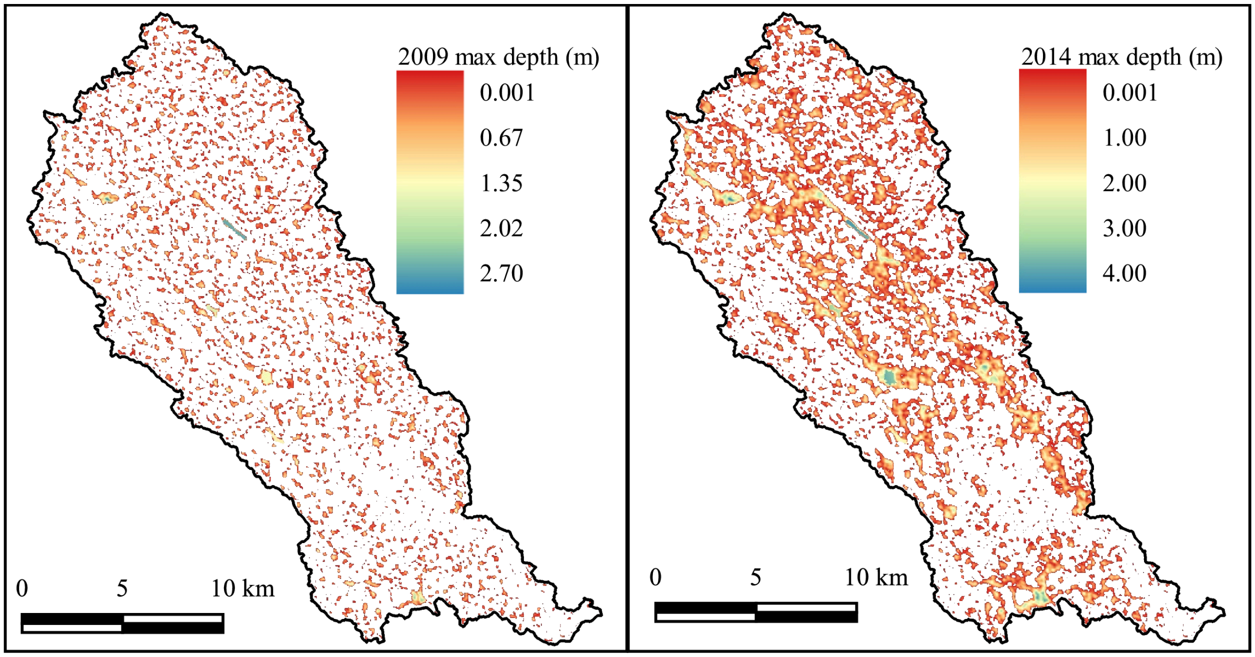

Figure C.3: The maximum flooding extents/depths that correspond to the spring snowmelt peak for a selected low flow year (2009, left panel) and a flood year (2014, right panel) generated by MESH-PRIMA for SCRB.

C.5 References

Ahmed MI, Elshorbagy A, Pietroniro A. 2020b. A novel model for storage dynamics simulation and inundation mapping in the prairies. Environmental Modelling & Software 133 (August): 104850 DOI: 10.1016/j.envsoft.2020.104850